Modeling and Optimization of CO_2 Fixation using Microalgae Cultivated in Oil Sands Process Water

by

Sepideh Kasiri

A thesis submitted in partial fulfillment of the requirements for the degree of

Doctor of Philosophy

in

Process Control

Department of Chemical and Materials Engineering

University of Alberta

Abstract

Biological fixation of CO_2 using microalgae is a potential CO_2 reduction strategy which can be applied to the oil sands operations in Alberta. These operations also produce large amounts of oil sands process water (OSPW), which can act as a growth medium for the microalgae. In this thesis, three different microalgae: *Botryococcus braunii*, *Chlorella pyrenoidosa* and *Chlorella kessleri* were investigated for their ability to grow in OSPW, and to uptake CO_2. Also, the effect of phosphate, nitrate, CO_2 concentrations and light intensity were studied using a fractional two-level and a full two-level factorial designs. These investigations eliminated *Botryococcus braunii* as it cannot grow in OSPW, and demonstrated that *Chlorella kessleri* has a higher CO_2 uptake rate than *Chlorella pyrenoidosa*. Moreover, CO_2 concentration, light intensity and phosphate concentration proved to have the strongest effects (in that order) on the growth and CO_2 uptake rate of *Chlorella kessleri*. To make biological fixation of CO_2 economically competitive compared to other CO_2 capture techniques, it is necessary to optimize CO_2 fixation rate and operate the algal culture at the optimal process conditions. Response surface methodology (RSM) was also used to develop statistical models for the CO_2 uptake rate and specific growth rate of *Chlorella kessleri*. The quadratic models developed were used to determine the optimal sets of CO_2 concentration, phosphate concentration and light intensity for CO_2 uptake rate and specific growth rate in batch operation. A multi-objective optimization technique was then used to maximize the CO_2 uptake rate and specific growth rate simul-

taneously. Moreover, to have a better understanding of microalgal dynamic behaviour, data generated using a central composite experimental design (CCD) with varying light intensity, CO_2 and phosphate concentration was used to develop a mathematical model that describes the kinetics of algal growth and CO_2, phosphate, nitrate and ammonium uptake rate of *Chlorella kessleri* cultivated in OSPW. This nonlinear dynamic model was used to determine the optimal CO_2 concentration, phosphate concentration and light intensity for CO_2 uptake and algal growth over a period of time in a batch culture using a multi-objective optimization technique to maximize CO_2 fixation and algal growth simultaneously. Finally, a lab-scale closed raceway photobioreactor was designed and assembled for cultivation of *Chlorella kessleri* in OSPW with the aim of combining CO_2 capture and algal production. A fed-batch model describing the dynamics of microalgae growth and CO_2, phosphate and ammonium uptake rate was developed based on the modification of a previously developed model for batch cultures, and was successfully validated against experimental data. The CO_2 uptake rate and algal growth can be maximized by properly manipulating the CO_2 and phosphate concentrations and availability and intensity of light. A model-based optimization method was used to calculate the optimal feeding strategies for CO_2, phosphate and light intensity.

Preface

The Materials presented in the current thesis are parts of the research project under supervision of Dr. Ania C. Ulrich and Dr. Vinay Prasad, which has been funded by Natural Sciences and Engineering Research Council (NSERC) of Canada and Oil Sands Tailings Research Facility (OSTRF).

Chapter 2 of this work is accepted as Kasiri, S., Prasad, V., Ulrich, A., 2014 "Strain and Factor Selection for Carbon Dioxide Fixation Using Microalgae Cultivated in Oil Sands Process Water", *Canadian Journal of Chemical Engineering* . Dr. Simmon Hofstetter helped in algal cell counting using BD FACSCalibur flow cytometer. Mrs. Lena Dlusskaya assisted with DNA extraction and DGGE analysis. Nitrate, nitrite and ammonium analysis was performed by Biogeochemical Analytical Service Laboratory (BASL) at the University of Alberta. Dr. Ania Ulrich was the supervisory author.

Chapter 3 of this work is submitted as Kasiri, S., Abdulsalam, S., Ulrich, A., Prasad, V., 2014 "Optimization of CO_2 Fixation by *Chlorella kessleri* using Response Surface Methodology", *Chemical Engineering Science*. Miss Shana Abdulsalam assisted with model development and data analysis. Phosphate, nitrate, nitrite and ammonium analysis was performed by Biogeochemical Analytical Service Laboratory (BASL) at the University of Alberta. Dr. Vinay Prasad was the supervisory author.

Chapter 4 of this work is in preparation for submission as Kasiri, S., Ulrich, A., Prasad, V., 2014 "Kinetic Modeling and Optimization of Carbon Dioxide Fixation Using

Microalgae Cultivated in Oil-Sands Process Water", to the journal of *Biotechnology and Bioengineering*. Phosphate, nitrate, nitrite and ammonium analysis was performed by Biogeochemical Analytical Service Laboratory (BASL) at the University of Alberta. Dr. Vinay Prasad was the supervisory author.

Chapter 5 of this work is in preparation for submission as Kasiri, S., Ulrich, A., Prasad, V., 2014 "Optimization of CO_2 Fixation by *Chlorella kessleri* in a Closed Raceway Photo-bioreactor", to the journal of *Biotechnology and Bioengineering*. The work in this chapter includes an automated raceway photobioreactor. I designed the photobioreactor. The body of the photobioreactor was built by Dr. Robert Lederer and modified by Mr. James McKinnon to install sensors for further analysis. Mr. Les Dean performed programming with the Labview software to communicate with the photobioreactor and assisted in proper operation of electrical parts. Mr. Walter Boddez helped with assembling an autosampler for the photobioreactor. Ammonium analysis was performed by Biogeochemical Analytical Service Laboratory (BASL) at the University of Alberta. Dr. Vinay Prasad was the supervisory author.

Dr. Ania Ulrich and Dr. Vinay Prasad provided the advice for conducting all the experimental designs, supervised the process of data collection and interpretation, and revised all publications.

It should be mentioned that the format of this thesis is paper-based and there might be some repetition, specially in the "Materials and Methods" of each chapter.

To my love and my parents, for their love, encouragement and support.

Acknowledgements

I am extremely grateful to my supervisors, Dr. Vinay Prasad and Dr. Ania Ulrich for their appreciable inspiration, support and patience throughout my PhD studies. Their invaluable kindness, guidance and comments allowed me to develop my personality and knowledge. It was a great pleasure to have the opportunity to work under their supervision.

I would like to express my special appreciation and thanks to Dr. Amos Ben-Zvi for his great inspiration, kindness and guidance. Also, I would like to thank Dr. Amit Kumar for his extensive discussions related to a part of my research.

I would like to acknowledge and thank Dr. William McCaffrey, Dr. Dominic Sauvageau and Dr. Yang Liu for their guidance and helpful suggestions. I would like to thank Dr. Arno de Klerk for his kindness to allow me to use the gas chromatograph (GC-TCD) in his lab and also Dr. Mingsheng Ma for his valuable suggestions and help.

I would like to express my gratitude to a number of technicians and research assistants for their valuable support, suggestions, and assistance aided the success of my experiments: Miss Emily Cao, Mrs. Elena Dlusskaya, Mrs. Maria Demeter, Mr. Walter Boddez, Mr. Les Dean, Mr. Clark Bicknell, Mr. Kevin Heidebrech, Mr. James McKinnon, Mrs. Chen Liang and Mrs. Shaofeng Yang.

I would especially like to thank Javad, Hamed, Simmon, Hector, Dena, Gouthami, Khushaal, Debanjan, Christina, Melissa, Jordan, Sara, Raymund, Fraser, Jess, Amy, Eve,

Lisa, Travis, Tim, Jeff, Matt and Huixin for their great help and encouragement.

I would like to gratefully acknowledge the Natural Sciences and Engineering Research Council (NSERC) of Canada and the Oil Sands Tailings Research Facility (OSTRF) for financial support. I would also like to thank Syncrude Canada Ltd. for providing tailings pond water samples.

Last but not least, I would like to express my gratitude to my husband and my parents for their continued, endless and unconditional support, patience, love and understanding throughout of my life. They always support my choices and dreams and encourage me to pursue them.

Contents

List of Tables

List of Figures

Chapter 1

Introduction

1.1 Introduction

The amount of atmospheric CO_2 has been increasing significantly in recent years, thus causing climate change. In 1997, 7.4 billion tons of CO_2 were released into the atmosphere from anthropogenic sources. By the year 2100, this number was estimated at 26 billion tons (Kane et al., 1999). Options for capturing and reducing CO_2 emissions include (1) utilizing carbon dioxide in value-added products such as plastics, paint, construction materials, solvents, cleaning compounds, and packaging (Lipinsky, 1992); (2) removing CO_2 from power plant flue gas using chemical absorbents (Stepan et al., 2002); (3) using alternative or renewable energy sources such as wind, solar, nuclear, and geothermal sources (Stepan et al., 2002); (4) converting CO_2 to chemicals (e.g., dry reforming with methane to produce syngas); and (5) biological fixation of carbon dioxide (Stepan et al., 2002). The first four options have high capital and/or operating costs; new waste streams requiring disposal, and/or minimum achievement of carbon dioxide offset versus energy input (Lipinsky, 1992; Stepan et al., 2002). However, biological fixation of CO_2 is an environmentally sustainable option because it puts carbon dioxide back into the natural carbon cycle through the photosynthetic process (Kumar et al., 2010; Stepan et al., 2002).

Photosynthesis is a slow reaction in larger plants since significant amounts of energy

must be expended to build their structure. However, smaller plants carry out photosynthesis at a higher efficiency, as they do not need to invest as much energy in building large structures. Single-celled algal organisms are the smallest and simplest forms of plants that can put nearly all of their energy into reproduction by not having to invest energy in growing roots, leaves and flowers (Freeman and Rhudy, 2007). In addition, microalgae have high proliferation rates, wide tolerance to extreme environments (Stepan et al., 2002), and the capability to assimilate CO_2 into other valuable materials such as carbohydrates and lipids (Murakami and Ikenouchi, 1997).

The tolerance of various microalgal strains to the concentration of CO_2 depends on the pH and the CO_2 concentration (Kumar et al., 2010). An early review on flue gas tolerance by microalgae showed that many microalgae can tolerate high levels of CO_2 and medium levels of SO_x and NO_x (up to 150 ppm) (Wang et al., 2008). Table 1.1, shows more than ten microalgae strains that have been studied for CO_2 fixation by Wang et al. (2008). de Morais and Costa (2007c) reported that *Scenedesmus obliquus* and *Chlorella kessleri* presented a good tolerance when exposed to 6%, 12% and 18% CO_2 (v/v). *Chlorella kessleri* showed maximum specific growth rates of 0.267 per day and biomass productivity of approximately 0.087 g/L per day when cultivated with 6% (v/v) and 12% (v/v) CO_2. Also, it grew well when the culture was exposed to 18% (v/v) CO_2 (Wang et al., 2008), which is a very high level for CO_2 streams from sources such as flue gases.

Murakami and Ikenouchi (1997) cultivated *Botryococcus braunii* SI-30 in a specific medium for hydrocarbon accumulation since it has high CO_2 fixation rates and hydrocarbon content. Sydney et al. (2010) then evaluated *Chlorella vulgaris* LEB-104, *Botryococcus braunii* SAG-30.81, *Spirulina platensis* LEB-52 and *Dunaliella tertiolecta* SAG-13.86 for CO_2 fixation. As shown in Table 1.2, *Botryococcus braunii* showed the highest CO_2 fixation rate and reached a biomass concentration of 3.11 g/L after 15 days cultivation.

Table 1.1: Selected microalgal strains studied for CO_2 bio-mitigation (Wang et al., 2008).

Microalgae	CO_2 %	P g/L.day	P_{CO_2} g/L.day	Notes
Chlorococcum littorale	40	N/A	1.0	
Chlorella kessleri	18	0.087	0.163*	
Chlorella sp. UK001	15	N/A	>1	
Chlorella vulgaris	15	N/A	0.624	Artificial wastewater
Chlorella vulgaris	Air	0.04	0.075*	Watanabe's Medium
Chlorella vulgaris	Air	0.024	0.045*	Low-N medium
Chlorella sp.	40	N/A	1.0	
Dunaliella	3	0.17	0.313*	High salinity, β-carotene
Haematococcus pluvialis	16-34	0.076	0.143	Commercial scale
Scenedesmus obliquus	Air	0.009	0.016	Wastewater, winter
Scenedesmus obliquus	Air	0.016	0.031	Wastewater, summer
Botryococcus braunii	-	1.1	>1.0	Accumulating hydrocarbon
Scenedesmus obliquus	18	0.14	0.26	

Note: En-dash not specified or not controlled.
CO_2% is the percentage of CO_2 (v/v) at the inlet.
P is biomass productivity and P_{CO_2} is CO_2 fixation rate.
*Calculated from the biomass productivity according to equation, P_{CO_2}=1.88×P, which is derived from the typical molecular formula of microalgal biomass, $C_{0.48}H_{1.83}N_{0.11}P_{0.01}$(Chisti, 2007).

However, it might be difficult to compare the various results in the literature, because of the different media and conditions under which the microalgae were grown. For example, Scragg et al. (2002) presented low biomass productivity in low nitrogen medium and did not use CO_2 enrichment. These conditions are different from those used in Sydney et al. (2010). On the other hand, Kishimoto et al. (1994) and de Morais and Costa (2007c) presented the CO_2 fixation rate of *Dunaliella tertiolecta* and *Spirulina platensis* grown in different conditions with the ones in Sydney et al. (2010). However, the results did not change significantly. Furthermore, Tang et al. (2011) investigated CO_2 fixation rates and lipids production of *Scenedesmus obliquus* SJTU-3 and *Chlorella pyrenoidosa* SJTU-2 grown with different CO_2 concentration from 0.03% to 50% (v/v). The maximum CO_2 biofixation rate and biomass concentration were found to be 10% CO_2 concentration for both microalgae. However, high CO_2 concentrations (30%-50%) were favorable for lipids accumulation.

Table 1.2: Comparison between carbon fixation rates indicated in Sydney et al. (2010) and other literature (modified from Sydney et al. (2010)

Microalgae	Literature mg_{CO_2}/L.day	Reference	Sydney et al. (2010) mg_{CO_2}/L.day
Chlorella vulgaris LEB-104	624	Yun and Park (2003)	252
Botryococcus braunii SAG-30.81	1100	Murakami and Ikenouchi (1997)	497
Spirulina platensis LEB-52	413*	de Morais and Costa (2007c)	318
Dunaliella tertiolecta SAG-13.86	313*	Kishimoto et al. (1994)	272

*Calculated from the biomass productivity (Wang et al., 2008).

Microalgal cultivation for CO_2 fixation can be integrated with wastewater treatment to reduce the cost of water and chemicals required for the growth medium (Yewalkar et al., 2011). Wastewater can be industrial wastewater from oil sands operations. The oil sands deposits in northern Alberta, Canada, are one of the largest sources of oil sands in the world. This makes Alberta one of the largest sources of oil sands process water (OSPW) since the steam assisted gravity drainage (SAGD) operation and the hot water extraction process (which separate bitumen from sand and clay), are processes that use water as a main constituent. The resulting process water contains a wide range of chemicals. OSPW is relatively hard with a pH of 8.0-8.4 and an alkalinity of approximately 800-1000 mg/L. OSPW contains a variety of inorganic compounds that are shown in Table 1.3 (Allen, 2008).

Since OSPW contains several nutrients, it may be suitable for growth of some microalgae (Yewalkar et al., 2011). Also, much of the OSPW is at moderate temperatures that are suitable for microalgal growth. Leung et al. (2001) identified several algae including *Botryococcus braunii*, *Gloeococcus schroeteri*, *Cosmarium depressum*, *Chrysococcus rufescens*, *Chromulina* spp., *Ochromonas* spp., and *Keratococcus* spp. in tailings ponds.

Furthermore, Yewalkar et al. (2011) investigated the potential for microalgae growth in OSPW with the aim of CO_2 fixation. *Chlorella pyrenoidosa*, obtained from the Canadian Centre for Culture of Microorganisms (CCCM), was cultivated in a medium con-

Table 1.3: Inorganic water chemistry of oil sands process waters (modified from Allen (2008)).

Variables (mg/L)	Syncrude MLSB (2003)	Suncor TPW (2000)
Total Dissolved Solids	2221	1887
Conductivity	2400	1113-1160
pH	8.2	8.4
Sodium	659	520
Calcium	17	25
Magnesium	8	12
Chloride	540	80
Bicarbonate	775	950
Sulphate	218	290
Ammonia	14	14

Note: MLSB, Mildred Lake Settling Basin and TPW, Tailings Pond Water.

taining 95% OSPW and different concentrations of Fe-ethylenediaminetetraacetic acid (EDTA), nitrate, and phosphate (Yewalkar et al., 2011).

Beside CO_2 fixation, the utilization of OSPW for microalgae cultivation has other benefits such as (1) the possibility of degrading unwanted dissolved contaminants, (2) reducing the use of water for algal cultivation, and (3) minimizing the use of algal nutrients such as metal ions and nitrogen (Sawayama et al., 1995; Wang et al., 2008).

1.2 Objective

The main objective of this research project is to maximize the CO_2 uptake rate and growth of microalgae cultivated in OSPW. The optimization of algal cultures is difficult due to the lack of appropriate mathematical models for many microalgal cultures. Therefore, identifying manipulating variables and developing a model of the algal system leads to a better understanding of the behavior of microalgae and eventually a method to find the optimal operation conditions. In order to achieve this goal, the following objectives have been established:

- Select the best microalgae strain based on its ability to grow in OSPW and capacity to uptake CO_2
- Identify the parameters that significantly affect CO_2 uptake and growth rate of the selected microalgae
- Develop statistical models of CO_2 uptake rate and growth rate of the selected microalgae by manipulating effective parameters and inputs and find the optimal initial conditions
- Develop a kinetic model of algal batch culture to describe algal growth, CO_2 and nutrient uptake rate and find the optimal initial conditions
- Modify the dynamic model for fed-batch culture and find the optimal feeding strategies to manipulate parameters

1.3 Research Questions

1.3.1 What is The Best Microalgal Strain for Our Purpose?

Three strains of *Botryococcus braunii*, *Chlorella pyrenoidosa* and *Chlorella kessleri* were investigated to find the best microalgal strain based on their ability to grow in OSPW and capacity to uptake CO_2. These strains were selected because 1) previous studies have demonstrated that *Botryococcus braunii* can grow in the presence of high concentrations of CO_2, and is capable of one of the highest CO_2 fixation rates reported in the literature, although no study has reported its cultivation in OSPW (Sydney et al., 2010); 2) *Chlorella pyrenoidosa* is not indigenous to OSPW but it has been cultivated in 95% OSPW by Yewalkar et al. (2011); and 3) *Chlorella kessleri* has been identified in OSPW by our research group (Mahdavi et al., 2012).

1.3.2 What are The Most Effective Parameters on CO_2 Uptake and Algal Growth?

The microalgal biomass production and CO_2 fixation are affected by a large number of factors. Therefore, different microalgae species have different ability of CO_2 fixation. Besides the inherent potential of algal species in CO_2 fixation, operating and cultivation conditions, such as light, availability of nutrient sources, pH, temperature, and mixing also influence algal growth and CO_2 fixation (Stepan et al., 2002; Chisti, 2007; Kumar et al., 2010; Singh and Dhar, 2011).

Light

The energy absorption by photosynthetic organisms depends on the chemical nature of their constitutive pigments. Chlorophylls, phycobilins, and carotenoids are the major pigment groups present in microalgae (Carvalho et al., 2011). Chlorophylls are the most important group amongst these, they absorb light and transfer that light energy to a specific chlorophyll pair in the reaction center of the photosystem. As shown in Figure 1.1, there are two photosystem units: photosystem I (with almost pure chlorophyll a) and photosystem II (with significant level of chlorophyll b). These two photosystems work together to transfer electrons from water to NADPH (Carvalho et al., 2011). Chlorophyll a is the most important molecule since the photosynthesis process starts when a photon impacts a chlorophyll a molecule. Chlorophyll b, chlorophyll c and carotenoids are accessory pigments. Since carotenoids are usually red, yellow or orange, they do not absorb light in those regions (Carvalho et al., 2011). The photosynthetic process has two main stages: light-dependent reactions, with adenosine triphosphate (ATP) and NADPH as intermediates, create energy and reduce power, respectively; and dark reactions, which compose the Calvin cycle, in which those intermediates react with CO_2 to

produce glucose as shown in Figure 1.2 (Carvalho et al., 2011).

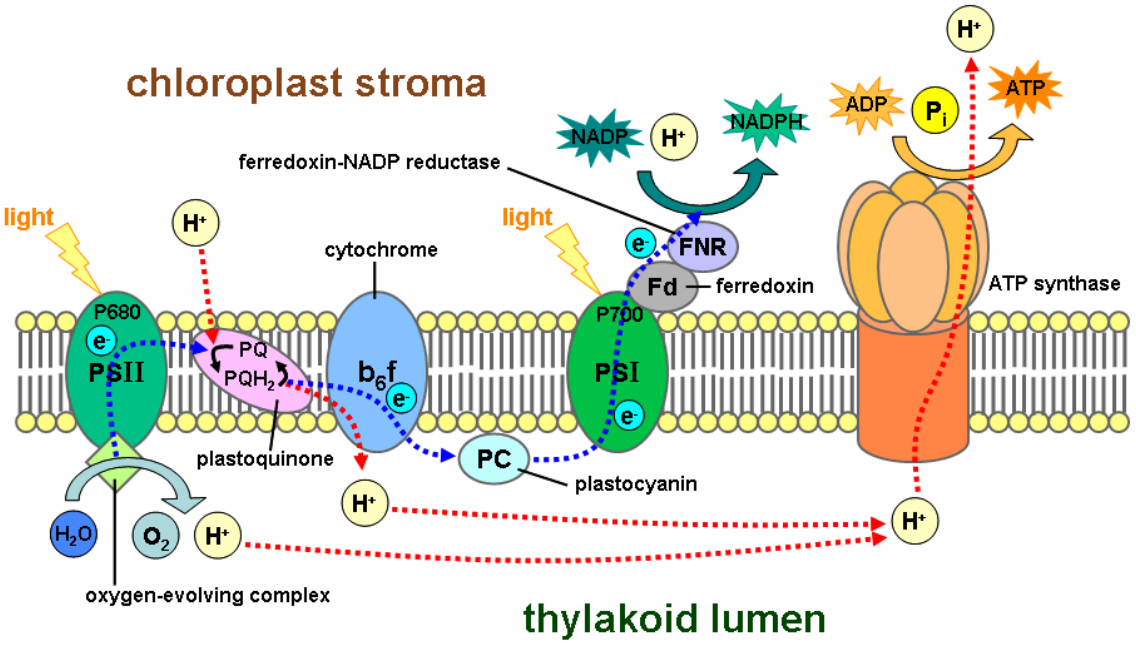

Figure 1.1: Light-dependent reactions of photosynthesis at the thylakoid membrane(CK-12 Foundation, 2014)

Therefore, light intensity is the most important factor in controlling photosynthetic growth in any algal system (Fan et al., 2007). The increase in the light intensity only corresponds to an increase in algal photosynthesis up to a certain value where the growth rate is the maximum attainable (saturation point). Increasing the light intensity beyond this point results in no increase and finally a reduction in the biomass productivity due to biochemical damage to the photosynthetic apparatus, as a result of excessive light (photoinhibition) (Camacho et al., 2003; Chisti, 2007; Fan et al., 2007; Lee, 1999; Richmond, 1996; Singh and Dhar, 2011; Zeng et al., 2011).

The light intensity available to microalgae is significantly attenuated in high-density cultures. Lee (1999) reported that saturated light can penetrate no more than 10 mm into dense algal liquid. Therefore, bioreactors should be designed with a high surface

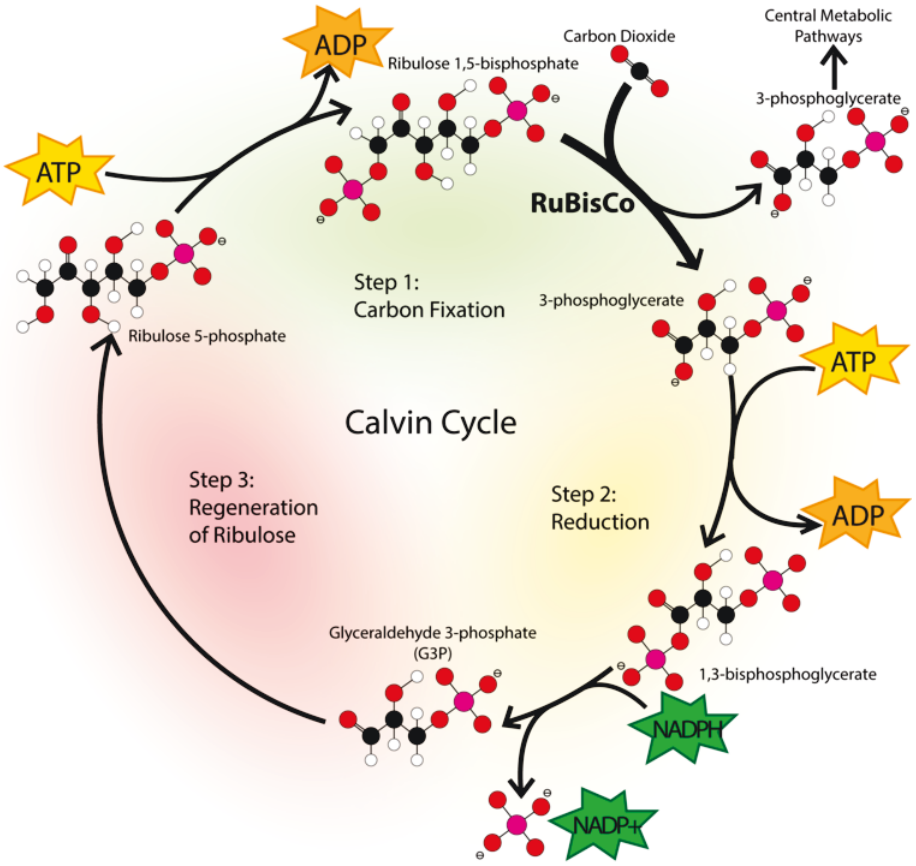

Figure 1.2: The Calvin cycle and carbon fixation (CK-12 Foundation, 2014)

area-to-volume ratio, as well as with a short light path (Kumar et al., 2010). At a given temperature, each type of microalga has a specific curve to correlate its growth rate to light intensity. Typically, the saturation light intensity increases with temperature (Carvalho et al., 2011). Usually, microalgal metabolic activity rates rise by increasing light intensity up to 400 μmol photons.m^{-2}.s^{-1}. For example, *Chlorella* and *Scenedesmus* sp. have a saturating light intensity of 200 μmol photons.m^{-2}.s^{-1}. The thermophilic *Chlorogleopsis* sp. shows high adaptability to light intensity; it grows well under both high light intensity (246.1 μmol photons.m^{-2}.s^{-1}) and low light intensity (36.9 μmol photons.m^{-2}.s^{-1}) (Zeng et al., 2011). Microalgae have an amazing capacity for photo-

acclimation in response to relatively quick and large changes in environmental light. The photo-acclimation process consists of a series of interrelated physical, biophysical, biochemical and physiological changes that help microalgal cells optimize their use of available light (Carvalho et al., 2011). Since microalgae are in the dark at night naturally, consideration of the dark period is essential. There is no agreement on what is the appropriate duration for a dark/light cycle. Long dark periods (e.g. several hours) cause biomass loss and drop in growth rates, because microalgae switch to respiration processes (Carvalho et al., 2011). Khoeyi et al. (2011) reported the biomass production of *Chlorella vulgaris* when it was cultivated under different light intensities (37.5, 62.5, and 100 μmol photons.m^{-2}.s^{-1}) and light/dark cycles (8:16, 12:12, and 16:8 h). They concluded that under different light intensities a light/dark cycle of 16:8h lead to increased specific growth rates. Also, the maximum growth rate was obtained at an irradiance of 100 μmol photons.m^{-2}.s^{-1} in 16:8 h light duration.

Carbon Dioxide

The photosynthetic characteristics of microalgal species are influenced by the ambient CO_2 concentration throughout growth (Sato et al., 2003). Generally, increasing CO_2 levels (up to the maximum levels that species can tolerate) increases photosynthesis in many species because more CO_2 from the external bulk medium diffuses to the active site of Rubisco; however, most of them have CO_2 concentrating mechanisms (CCMs) that facilitate CO_2 supply to Rubisco and most utilize HCO_3^- (Sato et al., 2003; Xu et al., 2010; Spalding, 2008). CCM consists of an active inorganic carbon (C_i; CO_2 and/or HCO_3^-) transport system for intracellular HCO_3^- accumulation and internal carbonic anhydrase (CA) to supply CO_2 to Rubisco by dehydration of the accumulated HCO_3^- (Colman et al., 2002; Sato et al., 2003; Spalding, 2008). CA is a zinc metalloprotein, often located in the periplasmic space of the cell, that catalyzes the interconversion of

CO_2 and HCO_3^- according to the following reactions (Moroney and Somanchi, 1999):

$$CO_2 + H_2O \rightleftharpoons H_2CO_3 \rightleftharpoons H^+ + HCO_3^-$$

Phosphorus

Phosphorus is another important nutrient that has a major effect on microalgal growth and metabolism. Since not all phosphorus compounds are bioavailable, they have to be supplied in excess as inorganic phosphorus (P_i; phosphate) (Kumar et al., 2010). High levels of phosphorus are necessary for the generation of ATP and phosphorylation of photosynthetic proteins and enzymes. It provides the energy requirement for active transport of C_i, and for synthesis of proteins involved in C_i utilization, and thus influences the capacity of algae to drive CCMs, which also costs energy (Geider et al., 1998a; Xu et al., 2010). It has been reported that increasing P_i supply results in microalgal growth enhancement. High P_i levels (i.e. 30 μM) increase the uptake rate of phosphorus, increase photosynthesis and raise the pigments content (Xu et al., 2010). Xu et al. (2010) reported that elevated CO_2 at high P_i levels improved the photosynthetic capability of *Gracilaria lemaneiformis*. Hence, enrichment of P_i may change the photosynthetic response of *Gracilaria lemaneiformis* to high CO_2 levels (i.e. 0.072%).

Nitrogen

Nitrogen is one of the most important nutrients required for microalgal growth and it is a component of both nucleic acids and proteins directly associated with the primary metabolism of microalgae. Variations in nitrogen supply cause changes in the partitioning of the reductant and photosynthate between synthesis of amino acids and carbohydrates. Nitrogen deficiency causes parallel reductions in the catalysts of photosynthetic electron transfer and carbon fixation in vascular plant chloroplasts because it leads to reductions

in the cellular content of chlorophyll a and increases in the content of non-photosynthetic carotenoids (Geider et al., 1998a; Kumar et al., 2010). Nitrate, ammonium, and urea (or combinations of them) are the most common nitrogen sources. It should be noted that ammonium is assimilated by microalgae in preference to other forms of nitrogen because unlike nitrate, it does not need reduction before being assimilated into amino acids (Molloy and Syrett, 1988; Wang et al., 2008). However, ammonium at high concentration has toxic effects on microalgal growth (Wang et al., 2008). OSPW contains high amounts of ammonia and to meet surface water guidelines, ammonia removal rates of 64%-93% would be required (Allen, 2008).

To achieve a high growth rate and CO_2 fixation rate, the maintenance of the exponential growth phase for a long period of time is essential (Jin et al., 2006). Jin et al. (2006) fed and controlled nitrogen intermittently into a fed-batch photobioreactor to describe the effect of the maintenance of nitrogen over the limiting level during carbon fixation. They then concluded that intermittent nitrate feeding methods might be a good option for increasing carbon fixation efficiency, and also prolonging the duration of carbon fixation in a given photobioreactor system. Lee and Lee (2002) studied nitrogen removal in wastewaters with low (approximately 0.015 to close to zero) carbon/nitrogen ratios, exploiting the photosynthetic ability of *Chlorella kessleri*. Therefore, *Chlorella kessleri* cultures removed excess nitrogen and utilized CO_2 from air or HCO_3^- ions. The results showed that *Chlorella kessleri* could successfully remove nitrogen from wastewater, as long as the mass transfer of CO_2 was not limited.

Oxygen

Algal growth and photosynthesis are affected by oxygen concentration. Inside the chloroplast, Rubisco (1,5-bisphosphate carboxylase oxygenase) can fix CO_2 and produce two molecules of 3-phosphoglycerate. Through a series of reactions, these two 3-carbon or-

ganic acids are synthetized as substrates for starch and oil production. Conversely, oxygen can compete with CO_2 to participate in the Calvin Cycle for Rubisco. Products of the oxygenase reaction are 3-phosphoglycerate and 2-phosphoglycolate. 2-Phosphoglycolate is consequently metabolized to glycine, which, when condensed with another glycine molecule to produce serine, causes the loss of CO_2. This carbon loss reduces the ability of the Calvin cycle to regenerate the 5-carbon sugar substrate (ribulose bisphosphate) required for the Calvin cycle by Rubisco, further decreasing the efficiency of photosynthesis. This overall process is called photorespiration, because it happens mainly in the presence of light. The photorespiration process decreases photosynthetic carbon fixation efficiency by 20-30%. To reduce the competitive inhibition of oxygen on the Calvin cycle by Rubisco, microalgae can actively pump and store sufficient CO_2 to elevate internal CO_2 concentrations above equilibrium levels with air (Zeng et al., 2011). Photosynthetic oxygen evolution of microalgae causes an increase of dissolved oxygen (DO) concentration in the culture medium, especially when the rate of photosynthesis is high. DO levels that are higher than air saturation values will cause formation of gas bubbles in the media, which can interfere with light absorption. Therefore, it is necessary to efficiently remove the photoinhibited effect of accumulative oversaturated DO on microalgal photosynthesis. In addition, excess oxygen combined with intense sunlight can cause photo-oxidative damage to the chlorophyll reaction centers of algal cells inhibiting photosynthesis and reducing productivity (Chisti, 2008; Singh and Dhar, 2011). An adequate degassing mechanism must be in place to readily rid the bioreactor of oxygen bubbles. However, the bubbles formed by aeration absorb DO which then moves to the surface and is subsequently exhausted out.

pH

pH is another factor that affects microalgal growth. Most microalgal species prefer neutral pH; however, some species have optimum growth under acidic or alkaline conditions. For example, the optimal pH of *Spirulina platensis* is 9 and the optimal pH of *Chlorococcum littorale* is 4 (Kumar et al., 2010; Zeng et al., 2011). There is a complex relationship between CO_2 concentration and pH in microalgal bioreactor systems, because of chemical equilibrium among chemical species such as CO_2, H_2CO_3, HCO_3^- and carbonate. First CO_2 combines H_2O to form H_2CO_3, which dissociates into HCO_3^- and H^+. HCO_3^- further dissociates into CO_2 or carbonate depending on the pH of the medium (de Morais and Costa, 2007b). CO_2 can enter into microalgal cells through active transport and then be biofixed. In open cultivation, the pH value quickly increases from 8.2 to 9.6 after a lag period of microalgal growth. In this case, the chemical equilibrium moves to the direction of consuming H^+ to carry out photosynthesis and growth. However, in closed cultivation, aeration of air containing CO_2 raises the H^+ concentration in the medium and decreases the pH value (Zhao et al., 2011). Increasing CO_2 concentrations leads to higher biomass productivity, but will also reduce pH (Kumar et al., 2010). A low pH value usually inhibits the microalgal growth, though different microalgae can tolerate different ranges of pH. For example, the microalga *Chlorella vulgaris* retained its maximum growth rate over a wide range of pH between 6.0 and 9.0, but started to be inhibited from pH 5.0. However, *Chlorella* strain KR-1 had a constant growth at pH 4.2 but was completely inhibited at pH 3.5 (Zhao et al., 2011). pH regulation is necessary to control CO_2 transfer in microalgal bioreactors. The most common system for controlling pH is the on-off type system in which CO_2 is injected into the culture when the pH exceeds a specific set point. Hence, CO_2 is used as a nutrient and also as a buffer for the medium (Kumar et al., 2010).

Temperature

Temperature is one of the main factors in microalgal growth. Temperature affects the growth rate by impacting the rate of enzyme-catalyzed reactions in the cell. Generally, an increase in temperature leads to exponential increase in algal growth due to increase in metabolic rates of microalgae until an optimum level is achieved, after which growth decreases (Singh and Dhar, 2011; Tansey and Brock, 1972); in addition increasing temperature decreases gas solubility in water (Stepan et al., 2002). The optimal temperature varies for different species, and is affected by other environmental parameters, such as light intensity. The optimal temperatures for many species have been reported as being between 25°C and 35°C. However, for some species, it has been reported to be between 15°C and 26°C (Kumar et al., 2010).

Mixing

A mixing system is required to maintain cells in suspension, to prevent thermal stratification, to disperse nutrients, and to ensure that the algal matter gets equal levels of light exposure. Also, mixing decreases the boundary layer around cells facilitating the uptake and excretion of metabolic products (Singh and Dhar, 2011). There are three options for mixing in microalgal bioreactors: pumping, mechanical stirring and gas injection. Pumping provides good mixing efficiency, but low gas transfer rates; the hydrodynamic stress increases with the rotation speed of the pumps, or the number of passes of the microalgal suspension through the pump units. Mechanical stirring provides good mixing efficiency and gas transfer; however, it may produce significant hydrodynamic stress. Gas injection (bubbling) provides reasonable mixing efficiency, and a good gas transfer rate while producing lower hydrodynamic stress; however, the gas sparging of culture increases cell damage as the biomass concentration increases (Kumar et al., 2010). Despite this, gas

injection is still the preferred option because sparging is a healthy method of supplying oxygen (Chisti, 2000).

It should be noted that the effects of CO_2 concentration, light intensity, phosphate and nitrate have been investigated in this study. These factors were selected because 1) it has been reported that phosphate and nitrate concentrations have significant effect on algal growth (de la Hoz Siegler, 2012; Yewalkar et al., 2011); 2) it has been reported that CO_2 concentration significantly affect algal growth and CO_2 uptake rate (Sydney et al., 2010; de Morais and Costa, 2007b); and 3) not many studies have evaluated the effect of light intensity on CO_2 uptake rate.

1.3.3 What are The Techniques to Optimize CO_2 Fixation and Algal Growth?

In order to make biological fixation of CO_2 economically competitive in comparison with carbon capture and storage (CCS) technologies, it is necessary to optimize CO_2 fixation rate and operate the algal culture at the optimal process conditions (de la Hoz Siegler et al., 2012). The optimization of algal cultures is difficult due to the lack of appropriate mathematical models for many microalgal cultures (de la Hoz Siegler et al., 2011). Therefore, developing a proper model of algal systems that describes the behavior of microalgal system can lead to estimated the optimal operation conditions. The statistical and mathematical approaches can be used to develop a model the algal systems and eventually find the optimal conditions.

Statistical Approach

Statistical approaches to optimal experimental designs are usually classified under response surface methodology (RSM). A few studies have been performed on optimal ex-

perimental designs to optimize algal growth and subsequently optimize the CO_2 fixation rate. Zheng et al. (2011) used RSM and the desirability function approach to vary the initial biomass concentration, the gas flow rate and different carbon dioxide concentrations to maximize the CO_2 fixation rate and intracellular starch productivity of *Tetraselmis subcordiformis* in a rectangular airlift photobioreactor. Ho et al. (2012) also used RSM to maximize the CO_2 fixation rate and specific growth rate of *Scenedesmus obliquus* CNW-N by manipulating the CO_2 concentration, CO_2 flow rate, magnesium concentration, and light intensity. In addition, Yewalkar et al. (2011) used RSM to find the optimum concentration of nitrate, phosphate, Fe-ethylenediaminetetraacetic acid (EDTA), and trace metal for *Chlorella pyrenoidosa* cultivated in 95% OSPW.

Mathematical Approach: Batch Mode

Several studies have been performed on mathematical modeling of algal systems in which the algal growth rate is considered to be a function of the nutrient concentration or a function of the cellular content (or quota) of the limiting nutrient using the Monod equation and nutrient uptake kinetics described by a Michaelis-Menten model (Droop, 1973; Morel, 1987; Zonneveld, 1996). The influence of light is explained by a number of equations including a modification of the Monod equation and a hyperbolic tangent (Jassby and Platt, 1976). However, the influences of different resources should be combined to better describe growth as a function of these multiple resources. Some studies have been performed on dynamic modeling of algal systems to describe the response of microalgal systems to light intensity as well as available nutrients (Bernard, 2011; Flynn, 2003; Geider et al., 1998b; de la Hoz Siegler et al., 2011; Packer et al., 2011). Geider et al. (1996) developed a new dynamic model to predict the chlorophyll a:carbon ratio and growth rate of phytoplankton at constant and varying irradiance. Later, they modified the model to predict the effects of irradiance, daylength, temperature and nutrient availability on

chlorophyll a:carbon ratio and growth rate (Geider et al., 1997). They also modified the former model to describe the nitrogen: carbon ratio in the algae (Geider et al., 1998b). Flynn (2003) developed mechanistic models to describe the growth of microalgae as functions of ammonium, nitrate, light, iron, silicon, phosphorus and temperature. A model was also developed by Packer et al. (2011) to describe the growth dynamics and neutral lipid production of microalgae when cultured in nitrogen-limited or high light conditions.

Mathematical Approach: Fed-Batch Mode

Furthermore, the choice of cultivation systems is an important aspect that significantly affects the efficiency and effectiveness of a microalgal production process (Singh and Dhar, 2011). Several studies have been done on different reactor configurations and cultivation modes to improve biomass growth with flue gas (Kumar et al., 2010; Schenk et al., 2008; Zhao et al., 2011). Generally, there are two environments used for the cultivation of microalgae: open raceway ponds and closed photobioreactors. Open ponds are easy and inexpensive to construct and operate, although they are limited in the ability to control of culture conditions and have a high risk of culture contamination. On the other hand, closed photobioreactors allow for better control of the cultivation conditions than open systems (Sanchez et al., 2011). For example, Zhao et al. (2011) reported that the specific growth rate and CO_2 fixation rate of *Chlorella* sp. in the aerated closed cultivation were 1.78 and 5.39 times of those in the open cultivation, respectively. Therefore, most of the modeling studies carried out so far have focused on the influence of culture conditions and nutrient avalability on biomass growth (Geider et al., 1998b; Flynn, 2003; Packer et al., 2011; Costache et al., 2013; Pruvost et al., 2011; Sforza et al., 2014). For example, Costache et al. (2013) developed an overall model that allows the simulation of the photosynthesis rate under different culture conditions (irradiance, temperature, pH, and dissolved oxygen). The model has then been validated

against experimental data obtained at different culture conditions. Sforza et al. (2014) developed a mathematical model to explain the biomass concentration and irradiation in a photobioreactor. Bernard and Remond (2012) also developed a model to describe the effect of temperature and light on microalgal growth, and predict productivity in outdoor photobioreactors or raceways. Using the bioprocess model, the states and inputs can be determined and used for optimization. He et al. (2012) developed a kinetic model for algal CO_2 utilization to describe the CO_2 uptake and algal growth as a function of CO_2 and light intensity in a fed-batch culture, and then determined the dynamic CO_2 inlet partial pressure using control vector parameterization to optimize the growth of algae fed by flue gases. A more complex model containing a set of six differential equations was proposed by de la Hoz Siegler et al. (2011) to model growth and oil production rates as a function of carbon and nitrogen sources in a photobioreactor. Later, de la Hoz Siegler et al. (2012) determined the optimal feeding strategies that maximize algal growth and experimentally compared the performance of the model-based optimization strategies against the performance of non-optimal fed-batch and batch cultures. Also, Abdollahi and Dubljevic (2012) established an optimal feeding strategy for lipid production using a state-of-the-art interior point optimizer (IPOPT) solver for the model developed by de la Hoz Siegler et al. (2011).

1.4 Thesis Outline

This thesis consists of 5 chapters focusing on answering the above questions. After the Introduction, in Chapter 2, fractional and full factorial designs were used as screening tools to select the best microalgal strain among *Botryococcus braunii*, *Chlorella pyrenoidosa* and *Chlorella kessleri* based on their ability to grow in OSPW and capacity to uptake CO_2 and also to select the factors which have significant effects on algal growth

and CO_2 fixation. This chapter focuses on answering the Question 1.3.1 and Question 1.3.2.

Chapter 3 focuses on development of quadratic regression models using a Box-Behenken response surface design and subsequently determining the optimum levels of the manipulated variables for CO_2 fixation and algal growth both individually and simultaneously, in response to Question 1.3.3. The details of response surface methodology (RSM) and multi-objective optimization techniques are also explained in this chapter.

Development of a kinetic model for describing the behavior of microalgae in batch mode and subsequently calculating the optimal operating conditions are presented in Chapter 4 to answer Question 1.3.3. The description of all possible kinetics and criteria for selection of the best model are detailed in this chapter. Also, particle swarm optimization (PSO) algorithm as a technique for parameter estimation and multi-objective optimization is comprehensively explained.

Chapter 5 focuses on modification of the previously developed batch model based on experimental data generated by a lab-scale raceway photobioreactor and subsequently calculation of the best feeding strategies, to answer Question 1.3.3. Also, the details of the photobioreactor design and experimental conditions are explained in this chapter.

Finally, Chapter 6 summarizes and concludes the thesis.

1.5 References

Abdollahi, J., Dubljevic, S., 2012. Lipid production optimization and optimal control of heterotrophic microalgae fed-batch bioreactor. Chemical Engineering Science 84, 619–627.

Allen, E.W., 2008. Process water treatment in Canada's oil sands industry: I. Target pollutants and treatment objectives. Journal of Environmental Engineering and Science 7, 123–138.

Bernard, O., 2011. Hurdles and challenges for modelling and control of microalgae for CO_2 mitigation and biofuel production. Journal of Process Control 21, 1378–1389.

Bernard, O., Remond, B., 2012. Validation of a simple model accounting for light and temperature effect on microalgal growth. Bioresource Technology 123, 520–527.

Camacho, F.R., Camacho, F.G., Sevilla, J.M.F., Chisti, Y., Grima, E.M., 2003. A mechanistic model of photosynthesis in microalgae. Biotechnology and Bioengineering 81, 459–473.

Carvalho, A.P., Silva, S.O., Baptista, J.M., Malcata, F.X., 2011. Light requirements in microalgal photobioreactors: An overview of biophotonic aspects. Applied Microbiology and Biotechnology 89, 1275–1288.

Chisti, Y., 2000. Marine biotechnology - A neglected resource. Biotechnology Advances 18, 547–548.

Chisti, Y., 2007. Biodiesel from microalgae. Biotechnology Advances 25, 294–306.

Chisti, Y., 2008. Biodiesel from microalgae beats bioethanol. Trends in Biotechnology 26, 126–131.

CK-12 Foundation, 2014. Photosynthesis: Sugar as food (http://www.ck12.org/book/ck-12-biology/r23/section/4.2).

Colman, B., Huertas, I.E., Bhatti, S., Dason, J.S., 2002. The diversity of inorganic carbon acquisition mechanisms in eukaryotic microalgae. Functional Plant Biology 29, 261–270.

Costache, T.A., Gabriel Acien Fernandez, F., Morales, M.M., Fernandez-Sevilla, J.M., Stamatin, I., Molina, E., 2013. Comprehensive model of microalgae photosynthesis rate as a function of culture conditions in photobioreactors. Applied Microbiology and Biotechnology 97, 7627–7637.

de la Hoz Siegler, H., 2012. Optimization of biomass and lipid production in heterotrophic microalgal cultures. Ph.D. thesis. University of Alberta, Canada.

de la Hoz Siegler, H., Ben-Zvi, A., Burrell, R.E., McCaffrey, W.C., 2011. The dynamics of heterotrophic algal cultures. Bioresource Technology 102, 5764–5774.

de la Hoz Siegler, H., McCaffrey, W.C., Burrell, R.E., Ben-Zvi, A., 2012. Optimization of microalgal productivity using an adaptive, non-linear model based strategy. Bioresource Technology 104, 537–546.

de Morais, M.G., Costa, J.A.V., 2007b. Isolation and selection of microalgae from coal fired thermoelectric power plant for biofixation of carbon dioxide. Energy Conversion and Management 48, 2169–2173.

de Morais, M.G., Costa, J.A.V., 2007c. Carbon dioxide fixation by *Chlorella kessleri*, *C. vulgaris*, *Scenedesmus obliquus* and *Spirulina* sp. cultivated in flasks and vertical tubular photobioreactors. Biotechnology Letters 29, 1349–1352.

Droop, M.R., 1973. Some thoughts on nutrient limitation in algae. Journal of Phycology 9, 264–272.

Fan, L., Zhang, Y., Cheng, L., Zhang, L., Tang, D., Chen, H., 2007. Optimization of carbon dioxide fixation by *Chlorella vulgaris* cultivated in a membrane-photobioreactor. Chemical Engineering and Technology 30, 1094–1099.

Flynn, K.J., 2003. Modelling multi-nutrient interactions in phytoplankton; balancing simplicity and realism. Progress in Oceanography 56, 249–279.

Freeman, B., Rhudy, R., 2007. Assessment of post-combustion capture technology developments. Technical Report. Electric Power Research Institute, Palo Alto, CA, USA.

Geider, R.J., Macintyre, H.L., Graziano, L.M., McKay, R.M.L., 1998a. Responses of the photosynthetic apparatus of *Dunaliella tertiolecta* (Chlorophyceae) to nitrogen and phosphorus limitation. European Journal of Phycology 33, 315–332.

Geider, R.J., MacIntyre, H.L., Kana, T.M., 1996. A dynamic model of photoadaptation in phytoplankton. Limnology and Oceanography 41, 1–15.

Geider, R.J., MacIntyre, H.L., Kana, T.M., 1997. Dynamic model of phytoplankton growth and acclimation: Responses of the balanced growth rate and the chlorophyll a:carbon ratio to light, nutrient-limitation and temperature. Marine Ecology Progress Series 148, 187–200.

Geider, R.J., MacIntyre, H.L., Kana, T.M., 1998b. A dynamic regulatory model of phytoplanktonic acclimation to light, nutrients, and temperature. Limnology and Oceanography 43, 679–694.

He, L., Subramanian, V.R., Tang, Y.J., 2012. Experimental analysis and model-based optimization of microalgae growth in photo-bioreactors using flue gas. Biomass and Bioenergy 41, 131–138.

Ho, S.H., Chen, C.Y., Chang, J.S., 2012. Effect of light intensity and nitrogen starvation on CO_2 fixation and lipid/carbohydrate production of an indigenous microalga *Scenedesmus obliquus* cnw-n. Bioresource Technology 113, 244–252.

Jassby, A.D., Platt, T., 1976. Mathematical formulation of the relationships between photosynthesis and light for phytoplankton. Limnology and Oceanography 21, 540–547.

Jin, H.F., Lim, B.R., Lee, K., 2006. Influence of nitrate feeding on carbon dioxide fixation by microalgae. Journal of Environmental Science and Health - Part A Toxic/Hazardous Substances and Environmental Engineering 41, 2813–2824.

Kane, B., Houghton, J., Reichle, D., Ekmann, J., Benson, S., Clarke, J., R., D., Hendrey, G., Herzog, H., Hunter-Cevera, J., Jacobs, G., Judkins, R., J., O., A., P., Socolow, R., Stringer, J., Surles, T., Wolsky, A., Woodward, N., York, M., 1999. Carbon sequestration: State of the science. Technical Report. Department of Energy, Washington, DC, USA: Office of Fossil Energy.

Khoeyi, Z.A., Seyfabadi, J., Ramezanpour, Z., 2011. Effect of light intensity and photoperiod on biomass and fatty acid composition of the microalgae, *Chlorella vulgaris*. Aquaculture International , 1–9.

Kishimoto, M., Okakura, T., Nagashima, H., Minowa, T., Yokoyama, S.Y., Yamaberi, K., 1994. CO_2 fixation and oil production using micro-algae. Journal of Fermentation and Bioengineering 78, 479–482.

Kumar, A., Ergas, S., Yuan, X., Sahu, A., Zhang, Q., Dewulf, J., Malcata, F.X., van Langenhove, H., 2010. Enhanced CO_2 fixation and biofuel production via microalgae: Recent developments and future directions. Trends in Biotechnology 28, 371–380.

Lee, C.G., 1999. Calculation of light penetration depth in photobioreactors. Biotechnology and Bioprocess Engineering 4, 78–81.

Lee, K., Lee, C.G., 2002. Nitrogen removal from wastewater by microalgae without consuming organic carbon sources. Journal of Microbiology and Biotechnology 12, 979–985.

Leung, S.S.C., MacKinnon, M.D., Smith, R.E.H., 2001. Aquatic reclamation in the Athabasca, Canada, oil sands: Naphthenate and salt effects on phytoplankton communities. Environmental Toxicology and Chemistry 20, 1532–1543.

Lipinsky, E.S., 1992. R&D status of technologies for utilization of carbon dioxide. Energy Conversion and Management 33, 505–512.

Mahdavi, H., Ulrich, A.C., Liu, Y., 2012. Metal removal from oil sands tailings pond water by indigenous micro-alga. Chemosphere 89, 350–354.

Molloy, C.J., Syrett, P.J., 1988. Effect of light and N deprivation on inhibition of nitrate uptake by urea in microalgae. Journal of Experimental Marine Biology and Ecology 118, 97–101.

Morel, F.M.M., 1987. Kinetics of uptake and growth in phytoplankton. Journal of Phycology 23, 137–150.

Moroney, J.V., Somanchi, A., 1999. How do algae concentrate CO_2 to increase the efficiency of photosynthetic carbon fixation? Plant Physiology 119, 9–16.

Murakami, M., Ikenouchi, M., 1997. The biological CO_2 fixation and utilization project by RITE (2): Screening and breeding of microalgae with high capability in fixing CO_2. Energy Conversion and Management 38, S493–S497.

Packer, A., Li, Y., Andersen, T., Hu, Q., Kuang, Y., Sommerfeld, M., 2011. Growth and neutral lipid synthesis in green microalgae: A mathematical model. Bioresource Technology 102, 111–117.

Pruvost, J., Van Vooren, G., Le Gouic, B., Couzinet-Mossion, A., Legrand, J., 2011. Systematic investigation of biomass and lipid productivity by microalgae in photobioreactors for biodiesel application. Bioresource Technology 102, 150–158.

Richmond, A., 1996. Efficient utilization of high irradiance for production of photoautotropic cell mass: A survey. Journal of Applied Phycology 8, 381–387.

Sanchez, A., Gonzalez, A., Maceiras, R., Cancela, A., Urrejola, S., 2011. Raceway pond design for microalgae culture for biodiesel. Chemical Engineering Transactions 25, 845–850.

Sato, N., Tsuzuki, M., Kawaguchi, A., 2003. Glycerolipid synthesis in *Chlorella kessleri* 11 h - II. effect of the CO_2 concentration during growth. Biochimica et Biophysica Acta - Molecular and Cell Biology of Lipids 1633, 35–42.

Sawayama, S., Inoue, S., Dote, Y., Yokoyama, S.Y., 1995. CO_2 fixation and oil production through microalga. Energy Conversion and Management 36, 729–731.

Schenk, P., Thomas-Hall, S., Stephens, E., Marx, U., Mussgnug, J., Posten, C., Kruse, O., Hankamer, B., 2008. Second generation biofuels: High-efficiency microalgae for biodiesel production. Bioenergy Research 1, 20–43.

Scragg, A.H., Illman, A.M., Carden, A., Shales, S.W., 2002. Growth of microalgae with increased calorific values in a tubular bioreactor. Biomass and Bioenergy 23, 67–73.

Sforza, E., Enzo, M., Bertucco, A., 2014. Design of microalgal biomass production in a continuous photobioreactor: An integrated experimental and modeling approach. Chemical Engineering Research and Design 92, 1153–1162.

Singh, N.K., Dhar, D.W., 2011. Microalgae as second generation biofuel. A review. Agronomy for Sustainable Development 31, 605–629.

Spalding, M.H., 2008. Microalgal carbon-dioxide-concentrating mechanisms: Chlamydomonas inorganic carbon transporters. Journal of Experimental Botany 59, 1463–1473.

Stepan, D., Shockey, R., Moe, T., Dorn, R., 2002. Subtask 2.3 - Carbon dioxide sequestering using microalgal systems. Technical Report. Department of Energy, Pittsburgh, PA, USA.

Sydney, E.B., Sturm, W., de Carvalho, J.C., Thomaz-Soccol, V., Larroche, C., Pandey, A., Soccol, C.R., 2010. Potential carbon dioxide fixation by industrially important microalgae. Bioresource Technology 101, 5892–5896.

Tang, D., Han, W., Li, P., Miao, X., Zhong, J., 2011. CO_2 biofixation and fatty acid composition of *Scenedesmus obliquus* and *Chlorella pyrenoidosa* in response to different CO_2 levels. Bioresource Technology 102, 3071–3076.

Tansey, M.R., Brock, T.D., 1972. The upper temperature limit for eukaryotic organisms. Proceedings of the National Academy of Sciences of the United States of America 69, 2426–2428.

Wang, B., Li, Y., Wu, N., Lan, C.Q., 2008. CO_2 bio-mitigation using microalgae. Applied Microbiology and Biotechnology 79, 707–718.

Xu, Z., Zou, D., Gao, K., 2010. Effects of elevated CO_2 and phosphorus supply on growth, photosynthesis and nutrient uptake in the marine macroalga *Gracilaria lemaneiformis* (rhodophyta). Botanica Marina 53, 123–129.

Yewalkar, S., Li, B., Posarac, D., Duff, S., 2011. Potential for CO_2 fixation by *Chlorella pyrenoidosa* grown in oil sands tailings water. Energy and Fuels 25, 1900–1905.

Yun, Y.S., Park, J.M., 2003. Kinetic modeling of the light-dependent photosynthetic activity of the green microalga *Chlorella vulgaris*. Biotechnology and Bioengineering 83, 303–311.

Zeng, X., Danquah, M.K., Chen, X.D., Lu, Y., 2011. Microalgae bioengineering: From CO_2 fixation to biofuel production. Renewable and Sustainable Energy Reviews 15, 3252–3260.

Zhao, B., Zhang, Y., Xiong, K., Zhang, Z., Hao, X., Liu, T., 2011. Effect of cultivation mode on microalgal growth and CO_2 fixation. Chemical Engineering Research and Design 89, 1758–1762.

Zheng, Y., Chen, Z., Lu, H., Zhang, W., 2011. Optimization of carbon dioxide fixation and starch accumulation by *Tetraselmis subcordiformis* in a rectangular airlift photobioreactor. African Journal of Biotechnology 10, 1888–1901.

Zonneveld, C., 1996. Modelling the kinetics of non-limiting nutrients in microalgae. Journal of Marine Systems 9, 121–136.

Chapter 2

Strain and Factor Selection for Carbon Dioxide Fixation Using Microalgae Cultivated in Oil Sands Process Water

2.1 Introduction

A review of the literature indicates that microalgae can grow in the presence of high concentrations of CO_2 (up to 40%) and medium concentrations of SO_x and NO_x (up to 150 ppm each) (Wang et al., 2008) while also exhibiting a range of CO_2 uptake rates (de Morais and Costa, 2007; Murakami and Ikenouchi, 1997; Sydney et al., 2010; Tang et al., 2011; Wang et al., 2008). These reported successes in using microalgae for CO_2 sequestration could be applied to Canada's oil sands industry, one of the largest oil sands operations in the world. These operations are one of the largest contributors to CO_2 emissions in Alberta (Yewalkar et al., 2011). In addition, these operations produce large amounts of oil sands process water (OSPW). OSPW is relatively hard (15-25 mg/L Ca^{2+}, 5-10 mg/L Mg^{2+}) with a pH of 8.0-8.4 and an alkalinity of approximately 800-1000 mg/L HCO_3^- (Allen, 2008). Additionally, OSPW contains a variety of organic (residual bitumen, naphthenic acids, etc.) and inorganic (sodium, calcium, magnesium, chloride,

sulphate, ammonia, etc.) compounds (Allen, 2008).

Extensive efforts have been dedicated to the development of high efficiency production and low-cost culturing systems for microalgae (Rosenberg et al., 2011; Wang and Lan, 2011). Along with CO_2 as a source of carbon, microalgal growth also requires the presence of essential nutrients and appropriate environmental conditions (e.g., light intensity, nitrogen, phosphorus, calcium, magnesium, potassium). For example, light intensity is the most important factor in controlling photosynthetic growth in any algal system, nitrogen is required for microalgal growth and is a component of nucleic acids and proteins directly associated with the primary metabolism of microalgae, and phosphorus has a major effect on microalgal growth and metabolism (Fan et al., 2007; Geider et al., 1998; Kumar et al., 2010).

Since OSPW contains several components necessary for microalgal growth, it can act as a growth medium for microalgae during CO_2 fixation. However, only a handful of microalgae have been found to survive in tailings ponds. For example, Leung et al. (2001) identified a few algal species in tailings ponds. Beside CO_2 fixation, the utilization of OSPW for microalgae cultivation has other benefits such as (1) the possibility of degrading unwanted dissolved contaminants, (2) reducing the use of water for algal cultivation, and (3) minimizing the use of algal nutrients such as metal ions and nitrogen (Sawayama et al., 1995; Wang et al., 2008).

The first objective of this study is to select the best microalgal strain among *Botryococcus braunii*, *Chlorella pyrenoidosa* and *Chlorella kessleri* based on their ability to grow in OSPW and capacity to uptake CO_2. These strains were selected because 1) previous studies have demonstrated that *Botryococcus braunii* can grow in the presence of high concentrations of CO_2, and is capable of one of the highest CO_2 fixation rates reported in the literature, although no study has been reported on its cultivation in OSPW (Sydney et al., 2010); 2) *Chlorella pyrenoidosa* is not indigenous to OSPW but it has

been cultivated in 95% OSPW by Yewalkar et al. (2011); and 3) *Chlorella kessleri* has been identified in OSPW by our research group (Mahdavi et al., 2012). To the best of our knowledge, no study has been performed on CO_2 fixation by native microalgae in OSPW.

The second objective of this study is to determine the manipulated variables that significantly affect the growth and the CO_2 uptake rate of the microalgae. The manipulated variables considered include CO_2 concentration, phosphorus concentration, nitrate concentration and light intensity. These key cultivation parameters can be manipulated to achieve higher growth and CO_2 uptake rate. Since modelling of biological systems is inherently complex, fractional and full factorial designs were used as screening tools in this study to identify the best strain for CO_2 uptake and which factors have significant effects on the response.

2.2 Materials and Methods

2.2.1 Strains and Culture Conditions

The *Botryococcus braunii* strain was obtained from UTEX, the culture collection of algae at the University of Texas (UTEX 2441, USA). The *Chlorella pyrenoidosa* strain was obtained from the Canadian Center for the Culture of Microorganisms (CCCM 7066, Department of Botany, University of British Columbia, Canada). *Chlorella kessleri* was obtained from our laboratory culture collection (Mahdavi et al., 2012).

2.2.2 Media Composition

The composition of modified bold 3N medium for *Botryococcus braunii* cultivation was $NaNO_3$ (750 mg/L), $CaCl_2.2H_2O$ (25 mg/L), $MgSO_4.7H2O$ (74 mg/L), K_2HPO_4 (75

mg/L), KH_2PO_4 (175.5 mg/L), NaCl (25 mg/L), $Na_2EDTA.2H_2O$ (4.5 mg/L), $FeCl_3.6H2O$ (0.582 mg/L), $MnCl_2.4H_2O$ (0.246 mg/L), $CoCl_2.6H_2O$ (0.012 mg/L), $Na_2MoO_4.2H_2O$ (24 μg/L), $ZnCl_2$ (0.03 mg/L), Vitamin B_{12} (0.135 mg/L), Biotin (25 μg/L), Thiamine (1.1 mg/L), and Soilwater (40 mL/L). The pH of the growth medium was adjusted to 6.2.

The composition of MES-Volvex medium for *Chlorella pyrenoidosa* cultivation was $Ca(NO_3)_2$ (118 mg/L), Na_2glycerophosphate.$5H_2O$ (60 mg/L), $MgSO_4.7H_2O$ (40 mg/L), KCl (50 mg/L), NH_4Cl (26.7 mg/L), $Na_2EDTA.2H_2O$ (4.5 mg/L), $FeCl_3.6H_2O$ (0.582 mg/L), $MnCl_2.4H_2O$ (0.246 mg/L), $ZnCl_2$ (0.03 mg/L), $Na_2MoO_4.2H_2O$ (0.024 mg/L), $CoCl_2.6H_2O$ (0.012 mg/L), Vitamin B12 (0.15 μg/L), Biotin (0.25 μg/L) and MES hydrate (1950 mg/L). The pH of the growth medium was adjusted to 6.7 using 1 N NaOH.

Chlorella kessleri is indigenous to OSPW; thus, it was maintained in this environment and no other medium was used. The OSPW media consist of 100% OSPW with different concentrations of phosphate (KH_2PO_4) and nitrate ($NaNO_3$). Since the concentration of phosphate and nitrate in OSPW is insufficient (about 1 and 3 mg/L, respectively), they were added to the media to provide these nutrients which are required for microalgal growth.

Also, the control media used in the experiments were OSPW autoclaved three times in three consecutive days with the same KH_2PO_4 and $NaNO_3$ concentrations as the OSPW media described above. No significant changes in cell counts, phosphate and nitrate concentration were observed in the control flasks.

All the experiments were conducted in 500 mL baffled Erlenmeyer flasks with 200 mL working volume. Flasks were incubated at 21$\pm$0.5°C, in a shaker at 150 rpm.

Experimental Design

In order to select an algal strain appropriate for fixing CO_2 while growing in OSPW, three experiments were performed. In the first experiment, two previously uncharacterized strains of interest (*Botryococcus braunii* and *Chlorella pyrenoidosa*) were screened for their ability to grow in OSPW. To accomplish this, the *Botryococcus braunii* and *Chlorella pyrenoidosa* were grown in modified bold 3N and MES-Volvex medium, respectively, as well as in OSPW medium (described above) with phosphate and nitrate concentrations of 1 mM each. They were exposed to a light intensity of 80 μmol photons.m^{-2}.s^{-1} for 15 days, at which time growth was measured.

In the second experiment, a factorial design was used to assess the effects of CO_2, light, and phosphate on the growth and CO_2 uptake of each strain. It is worth mentioning that while some studies have been performed on determining the effect of phosphate and nitrate on algal growth (de la Hoz Siegler et al., 2012; Yewalkar et al., 2011), not many studies have employed factorial designs to evaluate the effects of light intensity and CO_2 on algal growth and CO_2 uptake rate. Also, based on our preliminary experiments and studies from the literature (Yewalkar et al., 2011), phosphate was selected rather than nitrate in this design as it showed the potential to have a stronger effect on algal growth compared to nitrate.

A full factorial design for this system requires 8 (2^3) different treatments for each of *Chlorella kessleri*, *Chlorella pyrenoidosa* and the control; however, as presented in Table 2.1, a fractional two-level factorial design with 4 (2^{3-1}) treatments was employed in this experiment to have a manageable number of runs thus allowing for high quality data collection. Thus, with this design, the effect of the phosphate concentration was confounded by the interaction effects of the CO_2 concentration and light intensity. This design was used with varying phosphate concentration (P_L=1 mM and P_H=15 mM), CO_2

concentration (C_L=0.03% (CO_2 content in the air) and C_H=10%), and light intensity (I_L=20 and I_H=100 μmol photons.m^{-2}.s^{-1}) and nitrate concentration of 1 mM to evaluate the main effects on algal growth and CO_2 uptake. Air, enriched with 0 or 10% CO_2 with a flow-rate of 1 L/min, was bubbled into each flask for 3 min. The concentration of gas in the headspace was measured using a CO_2 gas sensor (Vernier CO_2 gas sensor, CO_2-BTA, Beaverton, Oregon ,USA). The flasks were then topped with a rubber stopper for 8 days, and the concentration of CO_2 was then measured again to estimate the uptake rate of CO_2.

Table 2.1: Fractional two-level factorial design to estimate the effects of CO_2 concentration, light intensity, and phosphate concentration on the growth and CO_2 uptake of each strain

Strain	Treatment						
	Symbol	$CO_2(x_1)$		Light(x_3)		Phosphate (x_2)	
		Coded	%	Coded	Photons	Coded	mM
Chlorella kessleri *Chlorella pyrenoidosa*	$C_H I_H P_H$	+1	10	+1	100	+1	15
Chlorella kessleri *Chlorella pyrenoidosa*	$C_L I_H P_L$	-1	Air	+1	100	-1	1
Chlorella kessleri *Chlorella pyrenoidosa*	$C_H I_L P_L$	+1	10	-1	20	-1	1
Chlorella kessleri *Chlorella pyrenoidosa*	$C_L I_L P_H$	-1	Air	-1	20	+1	15

A full factorial design with 4 (2^2) runs was employed in the third experiment, which investigated the effect of nitrate and phosphate concentration on the growth and CO_2 uptake of *Chlorella kessleri* and the control culture, as presented in Table 2.2. This design was used with varying phosphate concentration (P_L=1 mM and P_H=15 mM) and nitrate concentration (N_L=1 mM and N_H=20 mM). Air, enriched with 10% CO_2 with a flow-rate of 1 L/min was bubbled into each flask for 3 min. The concentration of gas in the headspace was measured using a CO_2 gas sensor. Then, the flasks were sealed and incubated for 8 days at light intensity of 70 μmol photons.m^{-2}.s^{-1}. The concentration of CO_2 was measured at the end of the experiment to estimate the uptake rate of CO_2.

Table 2.2: Full two-level factorial design to estimate the effects of nitrate and phosphate concentration on the growth and CO_2 uptake of *Chlorella kessleri*

Strain	Treatment				
	Symbol	Phosphate(x_2)		Nitrate(x_4)	
		Coded	mM	Coded	mM
Chlorella kessleri	P_HN_H	+1	15	+1	20
	P_LN_H	-1	1	+1	20
	P_HN_L	+1	15	-1	1
	P_LN_L	-1	1	-1	1

It should be noted that the levels of the independent variables, X_i, were coded as x_i according to Eq. 2.1 (Zheng et al., 2011):

$$x_i = \frac{X_i - X_0}{\triangle X_i}, i = 1, 2, \ldots, 4 \tag{2.1}$$

where X_0 is the value of an independent variable at the center point of its range and $\triangle X_i$ is the step change used in this design.

2.2.3 Analytical Methods

Growth Analysis: Algal biomass was determined using direct cell counts of 1 mL of the samples from each flask using a BD FACSCalibur flow cytometer (BD Biosciences, San Jose, California, USA). The number of algal cells at each condition was calculated as the average of three counts. In our preliminary experiments, the algal strains exhibited exponential growth with possibility of being linear after day 3. Therefore, the specific growth rate (SGR) was calculated based on the following equation (de la Hoz Siegler et al., 2011; Yewalkar et al., 2011):

$$\mathrm{SGR}\,[1/day] = \frac{\ln(N_2/N_1)}{(t_2 - t_1)} \tag{2.2}$$

where N_1 and N_2 are the number of cells at the initial time (t_1) and final time (t_2), respectively.

Carbon Dioxide Data Acquisition: At the inlet, the carbon dioxide and air flows were monitored using Dwyer Instruments variable area flowmeters (VFA-21, Michigan City, Indiana, USA). The percentage of CO_2 in the headspace of each flask was measured using a Vernier CO_2 gas sensor (CO_2-BTA, Beaverton, Oregon, USA) at the beginning and the end of the experiment. The CO_2 concentration in the headspace of control flasks changed approximately 1.5% and 10% for low and high initial CO_2 concentration treatments, respectively, due to leakage; thus, the final CO_2 concentration in the headspace of each flask containing algae was adjusted by adding an amount equal to the changes in the corresponding control flask.

Light Intensity: Two 40W fluorescent lamps were used to provide illumination to the culture. The photoperiod was 24 h to reach higher biomass productivity and CO_2 fixation (Jacob-Lopes et al., 2009). A high light intensity (100 μmol photons.m^{-2}.s^{-1}) and a low light intensity (20 μmol photons.m^{-2}.s^{-1}) was achieved by adjusting the distance of the flasks from the light source. The light intensity was measured using a Sper Scientific Light Meter LUX/FC model 840020 (Scottsdale, Arizona, USA).

Water Chemistry: Phosphorus was determined by taking a 2 mL sample from each culture and centrifuging it at relative centrifugal force (RCF) of 10000g for 10 min. The resulting supernatant was used to determine the amount of phosphorus, which was measured as orthophosphate (P-PO_4^{3-}) using the colorimetric method of 4500-P (Standard Methods for the Examination of Water and Wastewater (Eaton et al., 1999)) with the NanoDrop 2000C UV-Vis Spectrophotometer (Thermo Scientific, Wilmington, Delaware, USA). Alkalinity was determined by taking a 1 mL sample, centrifuging at RCF of 10000g for 10 min, and measuring the cell-free supernatant by titration with a 0.02 N H_2SO_4 solution using a Mettler Toledo DL53 titrator (Mississauga, Ontario, Canada). The amount

of nitrate, nitrite and ammonium of samples were measured using the colorimetric methods of 4500-NH_3 and 4500-NO_3 (Standard Methods for the Examination of Water and Wastewater (Eaton et al., 1999)) in the Biogeochemical Analytical Service Laboratory (BASL) at the University of Alberta.

2.3 Results and Discussion

2.3.1 Strain Selection

The best microalgae strain among *Botryococcus braunii*, *Chlorella pyrenoidosa* and *Chlorella kessleri* was selected based on its ability to grow in OSPW *and* its capacity to uptake CO_2.

A comparison of specific growth rates for *Botryococcus braunii*, *Chlorella pyrenoidosa* and *Chlorella kessleri* (already known to proliferate in OSPW) is presented in Table 2.3. The results indicate that after 15 days, no algal growth was observed for *Botryococcus braunii* cultivated in OSPW media, indicating that it is unable to grow in OSPW and is therefore not a suitable candidate for this study. For this reason, only *Chlorella pyrenoidosa* and *Chlorella kessleri* were investigated further. It should be noted that the culture purity was confirmed by extracting the DNA from each sample, completing denaturing gradient gel electrophoresis (DGGE) analysis and sequencing bands that confirmed *Chlorella pyrenoidosa* and *Chlorella kessleri* as the only algal species in their samples.

To narrow down our candidate strains further, their ability to uptake CO_2 was assessed, as was the influence of a variety of factors including CO_2, phosphate levels, and light intensity.

The specific growth rates of *Chlorella kessleri* and *Chlorella pyrenoidosa* in each treatment are calculated based on the algal cell density in day 0 and day 7 (Figure 2.1)

Table 2.3: The specific growth rate of strains in different media

Strain	Medium	SGR(1/day)
Botryococcus braunii	modified bold 3N medium	0.126
	OSPW pH=8.6	0.009
	OSPW pH=6.2	-0.014
	Autoclaved OSPW pH=9.7	-0.007
Chlorella pyrenoidosa	MES-Volvex Medium	0.145
	OSPW pH=8.6	0.114
	OSPW pH=6.7	0.119
Chlorella kessleri	OSPW pH=8.6	0.143

and presented in Table 2.4. *Chlorella kessleri* cultivated at a high CO_2 concentration, high light intensity and high phosphate concentration showed the highest specific growth rate of 0.205/day. In addition, a higher growth rate was observed for *Chlorella kessleri* in comparison with *Chlorella pyrenoidosa* cultivated in the same treatment, except when cultivated at a high CO_2 and a low phosphate concentration and exposed to low light intensity; for that condition, *Chlorella pyrenoidosa* showed a specific growth rate of 0.172/day, which is higher than the specific growth rate of *Chlorella kessleri* (0.127/day).

Table 2.4: The specific growth rate, CO_2 and phosphate uptake rates of strains at the different experimental treatments defined in Table 2.1. Values of CO_2 and phosphate uptake rates indicate mean ± standard deviation of ten and three measurements in each flask, respectively.

Treatment		Strain	SGR	CO_2 Uptake Rate	Phosphate Uptake Rate
			1/day	mg/L/day	mg/L/day
1	$C_H I_H P_H$	*Chlorella kessleri*	0.205	31.02 ± 0.12	2.52 ± 0.07
		Chlorella pyrenoidosa	0.154	29.64 ± 0.05	0.51 ± 0.03
2	$C_L I_H P_L$	*Chlorella kessleri*	0.120	7.07 ± 0.00	0.95 ± 0.02
		Chlorella pyrenoidosa	0.092	6.81 ± 0.00	0.17 ± 0.02
3	$C_H I_L P_L$	*Chlorella kessleri*	0.127	15.54 ± 0.14	0.90 ± 0.02
		Chlorella pyrenoidosa	0.172	15.43 ± 0.14	0.30 ± 0.04
4	$C_L I_L P_H$	*Chlorella kessleri*	0.053	4.25 ± 0.00	5.43 ± 0.06
		Chlorella pyrenoidosa	0.035	3.19 ± 0.00	1.12 ± 0.03

Generally, increasing CO_2 levels (up to the levels that species can tolerate) increases photosynthesis in many species because more CO_2 from the external bulk medium diffuses to the active site of the chloroplast where Rubisco (1,5-bisphosphate carboxylase oxyge-

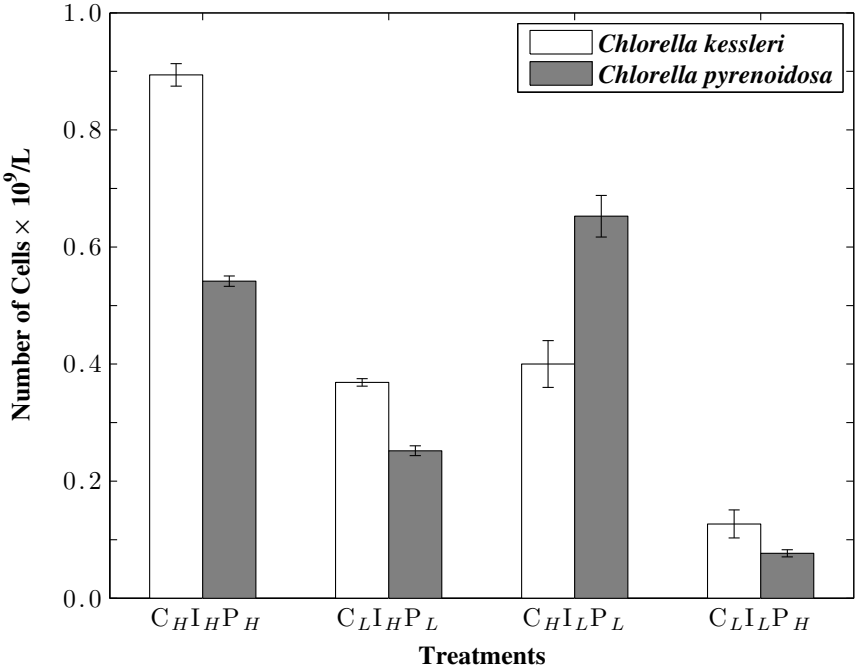

Figure 2.1: Change in cell density for *Chlorella kessleri* and *Chlorella pyrenoidosa* from day 0 to day 7. Data are means ± standard deviation of three measurements in each flask. Treatments were developed using the following parameters: C_H/C_L: high/low CO_2; I_H/I_L: high/low light intensity; P_H/P_L: high/low phosphate concentration.

nase) can fix CO_2 (Xu et al., 2010). The increase in the light intensity also corresponds to an increase in algal photosynthesis up to a certain value, after which a further increase in the light level results in no increase and finally a reduction in the biomass growth rate. Similarly, high phosphate levels increase algal growth up to a specific value after which a further increase in phosphate concentration causes growth inhibition. The mechanism can have several pathways, which includes inhibition of the phosphate transporter gene (TpPHO) transcription, the electron transport chain or the anti-oxidative defence system of the algal strain (Chefurka et al., 1976; Fu et al., 2013; Noctor and Foyer, 1998). The phosphate concentration that causes inhibition varies with different algae strains (Xu et al., 2010). The inhibition effect of phosphate on *Chlorella pyrenoidosa* growth rate

can be seen in this study where its specific growth rate in a low phosphate environment is higher than in a high phosphate environment. In contrast, phosphate has no inhibition effect on the growth of *Chlorella kessleri*, where the specific growth rate in a low phosphate environment is lower than in a high phosphate environment.

In general, *Chlorella kessleri* showed the highest SGR in comparison to *Chlorella pyrenoidosa*, which makes it a promising candidate for cultivation in OSPW.

The CO_2 uptake rate of each strain is presented in Table 2.4. It should be noted that the CO_2 uptake rate was calculated based on the change in the CO_2 concentration in the headspace of the each flask (Figure 2.2) and minimal change in alkalinity (Table 2.5) at the beginning and end of the experiments. Since the culture was pure, it was assumed that the changes in the CO_2 concentration are due to CO_2 consumption by each algal strain. As shown in Table 2.4, *Chlorella kessleri* exhibited the maximum CO_2 uptake rate of 31.02 mg/L/day when cultivated at high CO_2 and high phosphate concentration and high light intensity. Similar to the growth results described above, *Chlorella kessleri* cultured under the same treatments as *Chlorella pyrenoidosa* exhibited a higher CO_2 uptake rate in comparison. It can be seen that the CO_2 uptake rate of *Chlorella kessleri* and *Chlorella pyrenoidosa* cultivated at high CO_2 concentration were higher than those cultivated at low CO_2 concentration. This can be explained by luxury consumption of CO_2 that is in agreement with Droop (1973), Erifi and Turpin (1985) and Lai et al. (2011), who found that several algal strains store excess nutrients in intracellular pools to use during times of limited nutrient availability.

To summarize, *Chlorella kessleri* showed a higher CO_2 uptake rate and specific growth rate than *Chlorella pyrenoidosa*, and only *Chlorella kessleri* was investigated further.

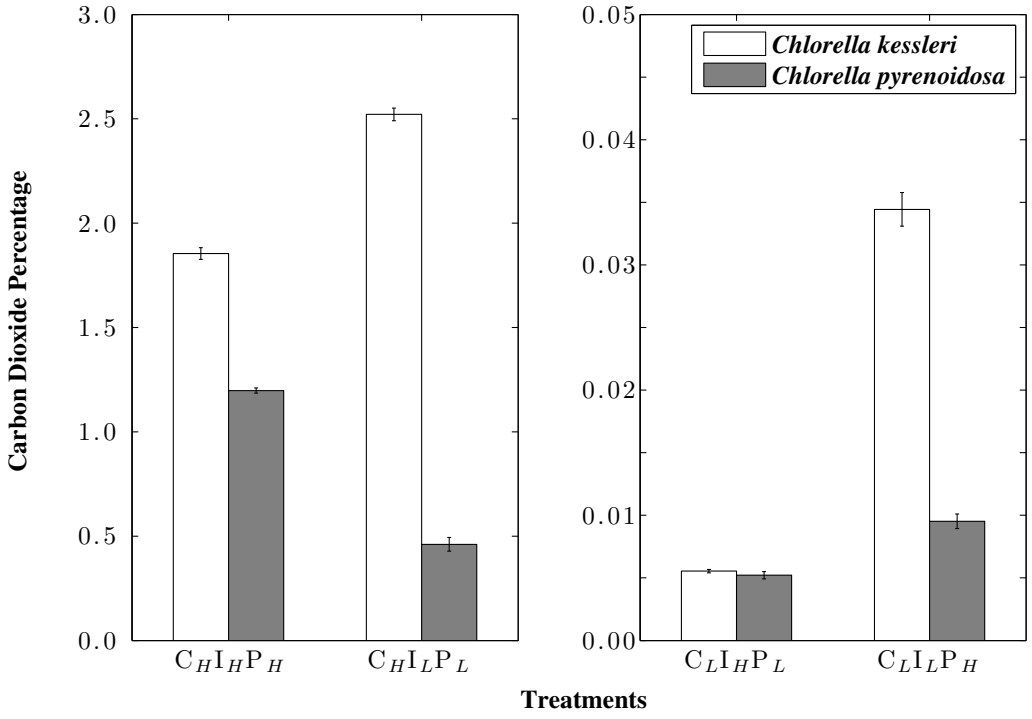

Figure 2.2: Change in CO_2 concentration in the headspace of *Chlorella kessleri* and *Chlorella pyrenoidosa* culture flasks from day 0 to day 7. Data are means ± standard deviation of ten measurements in each flask. Treatments were developed using the following parameters: C_H/C_L: high/low CO_2; I_H/I_L: high/low light intensity; P_H/P_L: high/low phosphate concentration.

Table 2.5: pH and alkalinity of *Chlorella kessleri* and *Chlorella pyrenoidosa* at day 0 and day 7

	Treatment	Strain	pH		Alkalinity (mmol/L)	
			Day 0	Day 7	Day 0	Day 7
1	$C_H I_H P_H$	*Chlorella kessleri*	7.17	6.98	13.1	13.7
		Chlorella pyrenoidosa	7.24	7.26	13.2	13.6
2	$C_H I_H P_H$	*Chlorella kessleri*	9.11	9.54	11.8	12.5
		Chlorella pyrenoidosa	9.15	9.68	11.9	12.8
3	$C_H I_H P_H$	*Chlorella kessleri*	8.94	8.12	11.8	12.2
		Chlorella pyrenoidosa	9.02	7.86	11.7	12.4
4	$C_H I_H P_H$	*Chlorella kessleri*	7.22	7.21	13.1	13.5
		Chlorella pyrenoidosa	7.21	7.17	13.0	13.4

2.3.2 Manipulated Variable Selection

Effects of Manipulated Variables on Algal Growth

Based on the results of SGR presented in Table 2.4, the main effects of light intensity, initial CO_2 and phosphate concentrations on the specific growth rate of *Chlorella kessleri* and *Chlorella pyrenoidosa* can be described by the following linear regression model, obtained by fitting the data obtained using the fractional factorial design:

$$\text{SGR of } \textit{Chlorella kessleri} = 0.126 + 0.039x_1 + 0.003x_2 + 0.036x_3 \tag{2.3}$$

$$\text{SGR of } \textit{Chlorella pyrenoidosa} = 0.113 + 0.050x_1 - 0.019x_2 + 0.010x_3 \tag{2.4}$$

where x_1, x_2 and x_3 are the coded values of the CO_2 concentration, phosphate concentration, and light intensity defined in Table 2.1 and calculated based on Eq. 2.1.

In this design, the effect of the phosphate concentration was confounded by the interaction effect of the CO_2 concentration and the light intensity. It was assumed that the main effects are larger than the two-factor interactions effects and that higher-order interactions are negligible.

Eq. 2.3 reveals that the initial CO_2 concentration had the strongest effect on the specific growth rate of *Chlorella kessleri*, followed by light intensity. As mentioned before, increasing CO_2 levels and light intensity (up to a certain level) increases photosynthesis in many species (Xu et al., 2010). These results are supported by Ruan et al. (2012), who reported that both CO_2 concentration and light intensity had a significant effect on *Chlorella kessleri* growth and nutrient removal from wastewater and by Li et al. (2012), who found that the light intensity had a significant effect on biomass accumulation for both *Chlorella kessleri* and *Chlorella protothecoide*. The initial CO_2 concentration also had the strongest effect on the specific growth rate of *Chlorella pyrenoidosa* (Eq. 2.4);

however, increasing phosphate concentration from 1 mM to 15 mM decreased the specific growth rate of *Chlorella pyrenoidosa* by 0.038 (1/day) likely due to phosphate inhibition.

The specific growth rates of *Chlorella kessleri* for each of the specific treatments are calculated based on the algal cell density in day 0 and day 7 (Figure 2.3) and presented in Table 2.7. *Chlorella kessleri* cultivated at a high phosphate concentration showed no difference in the maximum specific growth rate regardless of nitrate concentrations. In contrast, at low levels of phosphate, nitrate enrichment increased the specific growth rate of *Chlorella kessleri*.

The main and interaction effects of the phosphate and nitrate concentrations on the specific growth rate of *Chlorella kessleri* can be described by the following model:

$$\mathrm{SGR} = 0.161 + 0.011x_2 + 0.007x_4 - 0.005x_2x_4 \tag{2.5}$$

where x_2 and x_4 are the coded values of the phosphate and nitrate concentrations defined in Table 2.2 and calculated based on Eq. 2.1.

As illustrated in Eq. 2.5, phosphate concentration had a stronger effect on the specific growth rate of *Chlorella kessleri* than the nitrate concentration. A number of factors could have contributed to this effect, including 1) OSPW contains about 4 mg/L of ammonium (based on day 0 measurement), which is assimilated by microalgae in preference to nitrate or nitrite (Wang et al., 2008). The algal cells likely receive all the necessary nitrogen from the ammonium present in OSPW and do not require the additional nitrate. 2) Different algal strains have varying eco-physiological strategies in responding to nutrient limitation with regard to nitrogen and phosphorus. The literature shows that our understanding of the reason for these differences is incomplete; however, several researchers have observed different effects of phosphate and nitrate on algal growth. For example, Fried et al. (2003), Hu and Gao (2006) and Lai et al. (2011) found that nitrate

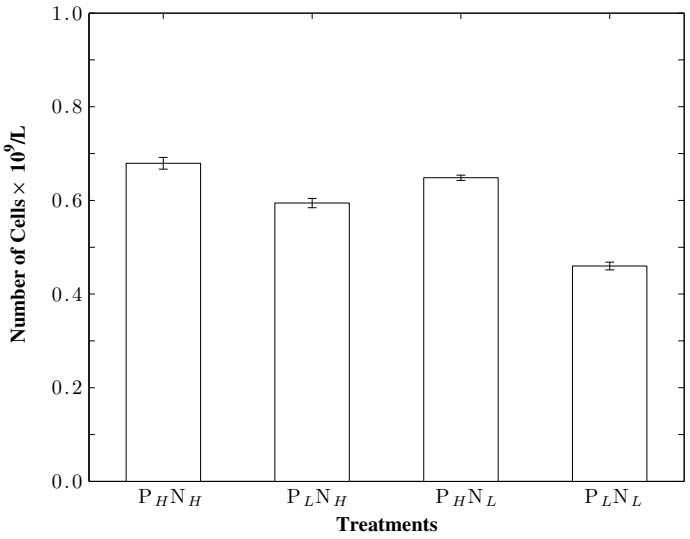

(a)

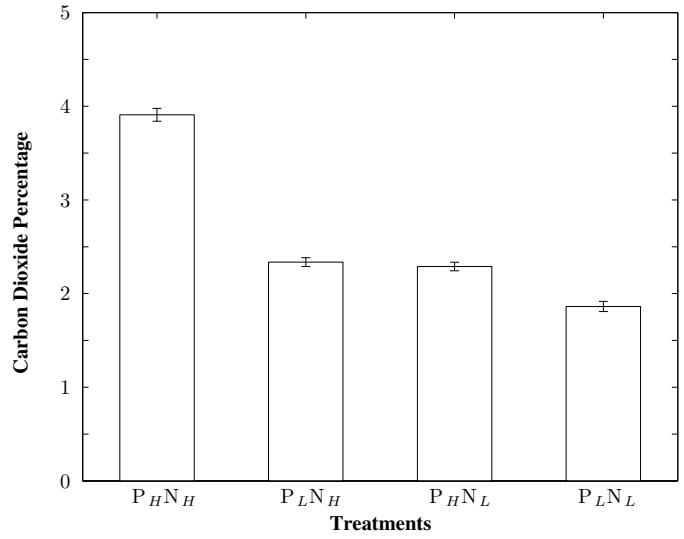

(b)

Figure 2.3: Change in (a) cell density and (b) CO_2 concentration in the headspace, for *Chlorella kessleri* from day 0 to day 7. Data are means ± standard deviation of three and ten measurements in each flask, respectively. Treatments were developed using the following parameters: P_H/P_L: high/low phosphate concentration; N_H/N_L: high/low nitrate concentration.

and phosphate levels have a significant effect on algal growth. These results are also contradicted by Tubea et al. (1981) and Zhang and Hong (2014), who found that phosphate levels had no significant effect on algal growth, and by Encarnacao et al. (2012), who found that nitrate levels had an inhibitory effect on algal growth.

Effects of Manipulated Variables on CO_2 Uptake

According to the results of the CO_2 uptake rate presented in Table 2.4, the main effects of CO_2, light intensity, and phosphate concentration on the CO_2 uptake rate for each culture can be described by the following empirical models:

$$CO_2 \text{ uptake rate of } \textit{Chlorella kessleri} = 14.48 + 8.81x_1 + 3.17x_2 + 4.57x_3 \quad (2.6)$$

$$CO_2 \text{ uptake rate of } \textit{Chlorella pyrenoidosa} = 13.77 + 8.76x_1 + 2.65x_2 + 4.46x_3 \quad (2.7)$$

As illustrated in Eqs. 2.6 and 2.7, it can be concluded that initial CO_2 concentration was the strongest factor affecting CO_2 uptake rate and growth rate of *Chlorella kessleri* and *Chlorella pyrenoidosa*, followed by light intensity and then phosphate concentration.

The CO_2 uptake rates for *Chlorella kessleri* with each treatment in the full factorial experiment are calculated based on the change in the CO_2 concentration in the headspace of the flask from day 0 to day 7 (Figure 2.3) and minimal change in the alkalinity (Table 2.6) and presented in Table 2.7. *Chlorella kessleri* exhibited the maximum CO_2 uptake rate of 43.73 mg/L/day when cultivated at high phosphate and high nitrate concentrations. CO_2 uptake rate of 24.58 mg/L/day was observed at high phosphate and low nitrate concentration, and this rate was slightly higher than the rate at low phosphate concentrations. These results showed that at low phosphate levels, nitrate enrichment decreased the CO_2 uptake rate of *Chlorella kessleri*; however, at high phosphate levels, it increased the CO_2 uptake rate.

Table 2.6: pH and Alkalinity of *Chlorella kessleri* at day 0 and day 7

	Treatment	Strain	pH		Alkalinity (mmol/L)	
			Day 0	Day 7	Day 0	Day 7
1	P_HN_H	*Chlorella kessleri*	6.52	7.49	13.8	15.1
2	P_LN_H	*Chlorella kessleri*	7.75	7.61	12.6	13.8
3	P_HN_L	*Chlorella kessleri*	6.53	7.15	13.3	13.9
4	P_LN_L	*Chlorella kessleri*	7.79	7.53	12.8	13.2

Table 2.7: The specific growth rate, CO_2 and phosphate uptake rates of *Chlorella kessleri* at the different experimental treatments defined in Table 2.2. Values of CO_2 and phosphate uptake rates indicate mean ± standard deviation of ten and three measurements in each flask, respectively.

Treatment		SGR	CO_2 Uptake Rate	Phosphate Uptake Rate	Total Nitrogen Uptake Rate
		1/day	mg/L/day	mg/L/day	mg/L/day
1	P_HN_H	0.175	43.73 ± 0.27	6.04 ± 0.05	12.0
2	P_LN_H	0.162	17.63 ± 0.28	0.85 ± 0.01	12.3
3	P_HN_L	0.170	24.58 ± 0.27	3.31 ± 0.03	1.0
4	P_LN_L	0.138	23.59 ± 0.26	0.74 ± 0.00	0.57

The main and interaction effects of the phosphate and nitrate concentrations on the CO_2 uptake rate can be described by the following equation:

$$CO_2 \text{ uptake rate} = 27.39 + 6.77x_2 + 3.30x_4 + 6.27x_2x_4 \tag{2.8}$$

Based on this equation, it can be seen that the phosphate concentration had a stronger effect on the CO_2 uptake rate of *Chlorella kessleri* compared to the nitrate concentration.; this can be explained by the fact that high levels of phosphorus are necessary for the generation of ATP and phosphorylation of photosynthetic proteins and enzymes (Kumar et al., 2010).

2.3.3 Nutrient Uptake

Phosphate Uptake

As shown in Table 2.4, the maximum phosphate uptake rate of 5.43 mg/L/day was observed for *Chlorella kessleri* when it was exposed to high phosphate, low CO_2 concentration and low light intensity. Also, it exhibited a higher phosphate uptake rate than *Chlorella pyrenoidosa* when they were exposed to the same treatments. It can be concluded that both microalgae cultivated at high phosphate levels had a faster uptake rate of phosphate than at low phosphate levels and can be explained by luxury consumption of phosphate in the excess of phosphate. Also, enhancement of CO_2 and light intensity increased the phosphate uptake rate significantly. At high phosphate and high nitrate concentrations, *Chlorella kessleri* showed the maximum phosphate uptake rate of 6.04 mg/L/day as presented in Table 2.7. It exhibited a phosphate uptake rate of 3.31 mg/L/day when cultivated at high phosphate and low nitrate concentrations. *Chlorella kessleri* cultivated at a high phosphate level also had a faster uptake rate of phosphate, and enhancement of the nitrate level increased the phosphate uptake rate significantly.

Nitrogen Uptake

As shown in Table 2.7, *Chlorella kessleri* exposed to a low phosphate and a high nitrate concentration showed the maximum nitrogen uptake rate of 12.3 mg/L/day. The total nitrogen uptake is the sum of ammonium uptake, nitrate uptake and nitrite excretion (Table 2.8). The uptake rate of nitrate increased about 10 times in media containing high levels of nitrate because of the luxury consumption of nitrate in the presence of high concentrations of nitrate. The nitrite uptake rate was negative, this observation appears to be widespread in microalgae and depends on nitrate uptake (Collos, 1998).

The ammonium uptake rate is almost the same for all treatments. The ammonium

analysis showed that all culture flasks were depleted in ammonium. This is because ammonium is preferentially assimilated by microalgae over other forms of nitrogen, and unlike nitrate, ammonium does not need reduction before being assimilated into amino acids (Molloy and Syrett, 1988; Wang et al., 2008). OSPW contains high amounts of ammonia and to meet surface water guidelines, ammonia removal rates of $64\% - 93\%$ would be required (Allen, 2008); based on these results, it seems that algal cultivation in OSPW is a promising option to reduce the amount of ammonia.

Table 2.8: Ammonium, nitrate and nitrite uptake rate of *Chlorella kessleri* at the different experimental treatments defined in Table 2.2

Treatment		Ammonium Uptake Rate	Nitrate Uptake Rate	Nitrite Uptake Rate
		mg/L/day	mg/L/day	mg/L/day
1	$P_H N_H$	0.39	11.6	-0.01
2	$P_L N_H$	0.27	12.0	-0.01
3	$P_H N_L$	0.26	0.75	0.00
4	$P_L N_L$	0.27	0.30	0.00

2.3.4 Comparison of Models

Based on the results of SGR and CO_2 uptake rates obtained from all factorial experiments, the following regression models can be developed to describe the SGR and CO_2 uptake rates of *Chlorella kessleri*. The first two models can be used to explain the SGR and CO_2 uptake rate of *Chlorella kessleri* by considering light intensity, CO_2, phosphate and nitrate concentrations as factors. Note that the interaction effects of CO_2 and light intensity and those of phosphate and nitrate were included in these models.

$$\text{SGR} = 0.125 + 0.036x_1 + 0.012x_2 + 0.035x_3 + 0.003x_4 - 0.016x_1x_3 - 0.006x_2x_4 \quad (2.9)$$

$$\text{CO}_2 \text{ uptake rate} = 17.46 + 8.66x_1 + 6.80x_2 + 4.54x_3 + 3.15x_4 + 2.58x_1x_3 + 6.24x_2x_4 \quad (2.10)$$

x_1, x_2, x_3 and x_4 are the coded values of the CO_2 concentration, phosphate concentration, light intensity, and nitrate concentration as defined in Table 2.1 and 2.2. Based on the values of the coefficient of determination of R^2_{SGR}=0.98 and $R^2_{CO_2}$=0.99 obtained from the regression models, it can be concluded that both the SGR and the CO_2 uptake rate can be described adequately by Eqs. 2.9 and 2.10 in the range of performed experiments, respectively. Also, nitrate showed the lowest main effect on the SGR and CO_2 uptake rate. Therefore, the effect of nitrate was excluded from further analysis to develop two new regression models to explain SGR and CO_2 uptake rate (Eqs. 2.11 and 2.12).

$$\text{SGR} = 0.123 + 0.036x_1 + 0.012x_2 + 0.035x_3 - 0.010x_1x_3 \tag{2.11}$$

$$CO_2 \text{ uptake rate} = 15.72 + 10.07x_1 + 6.51x_2 + 4.83x_3 - 3.10x_1x_3 \tag{2.12}$$

SGR can still be adequately described by Eq. 2.11 (R^2_{SGR}=0.97), while the CO_2 uptake rate cannot be described as well by Eq. 2.12 ($R^2_{CO_2}$=0.81).

The errors associated with including and excluding nitrate in the SGR and CO_2 uptake rate regression models, respectively, are presented in Table 2.9. The differences between the errors obtained from two models of SGR are relatively small and including nitrate does not improve the model significantly. However, Table 2.9 indicates that the errors in predicting CO_2 uptake obtained using Eq. 2.10 are lower than that of Eq. 2.12.

It should be noted that Eqs. 2.3 and 2.5 and also Eqs. 2.6 and 2.8 (original models) were used to predict the specific growth and CO_2 uptake rate of *Chlorella kessleri* for all factorial treatments, respectively. As shown in Table 2.10 the specific growth rate and the CO_2 uptake rate are well explained by the original models in some treatments; however, the error associated with some of the treatments that were excluded from model development is very high.

Given that we plan on exploring the use of response surface designs in the future to

Table 2.9: Model predictions and comparison with experimental data for the specific growth rate and CO_2 uptake rate of *Chlorella kessleri*

Treatment	SGR(1/day)					CO_2 Uptake Rate(mg/L/day)				
	Expt. data	Eq. 2.9		Eq. 2.11		Expt. data	Eq. 2.10		Eq. 2.12	
		Model	error(%)	Model	error(%)		Model	error(%)	Model	error(%)
$C_H I_H P_H$	0.205	0.195	4.6	0.197	3.8	31.02	30.65	1.2	34.03	9.7
$C_L I_H P_L$	0.120	0.120	0	0.120	0	7.07	7.07	0	7.07	0
$C_H I_L P_L$	0.127	0.120	4.9	0.122	4.1	15.54	15.29	1.6	17.55	12.9
$C_L I_L P_H$	0.053	0.053	0	0.053	0	4.25	4.25	0	4.25	0
$P_H N_H$	0.175	0.175	0	0.176	0.9	43.73	43.73	0	32.65	25.3
$P_L N_H$	0.162	0.162	0	0.152	5.7	17.63	17.66	0.2	19.62	11.3
$P_H N_L$	0.170	0.180	5.5	0.176	3.6	24.58	24.95	1.5	32.65	32.8
$P_L N_L$	0.138	0.144	4.5	0.152	10.5	23.59	23.84	1.0	19.62	16.8

Table 2.10: Model predictions and comparison with experimental data for the specific growth rate and CO_2 uptake rate of *Chlorella kessleri*

Treatment	SGR(1/day)					CO_2 Uptake Rate(mg/L/day)				
	Expt. data	Eq. 2.3		Eq. 2.5		Expt. data	Eq. 2.6		Eq. 2.8	
		Model	error(%)	Model	error(%)		Model	error(%)	Model	error(%)
$C_H I_H P_H$	0.205	0.205	0.0	0.170	17	31.02	31.02	0	24.58	20.8
$C_L I_H P_L$	0.120	0.120	0.0	0.138	15	7.07	7.07	0	23.59	233.7
$C_H I_L P_L$	0.127	0.127	0.0	0.138	15	15.54	15.54	0	23.59	51.8
$C_L I_L P_H$	0.053	0.053	0.0	0.170	220.7	4.25	4.25	0	24.58	478.3
$P_H N_H$	0.175	0.178	1.7	0.175	0	43.73	27.59	36.9	43.73	0.0
$P_L N_H$	0.162	0.172	6.1	0.162	0	17.63	21.26	20.6	17.63	0.0
$P_H N_L$	0.170	0.178	4.7	0.170	0	24.58	27.59	12.2	24.58	0.0
$P_L N_L$	0.138	0.172	24.6	0.138	0	23.59	21.26	9.9	23.59	0.0

optimize the SGR and CO_2 uptake, reducing the number of factors to be considered in these designs keeps the number of experiments to be performed at manageable levels, suggesting that we ignore the effect of nitrate in further investigations.

2.4 Conclusions

Our investigations indicate that *Chlorella kessleri* is the most promising of the three strains of microalgae considered for CO_2 uptake in OSPW, having a CO_2 uptake rate between $0.7 - 33\%$ higher than that of *Chlorella pyrenoidosa* at the same conditions. Also, its specific growth rate was significantly higher at most of the conditions explored. Further, an investigation into the factors that influence growth and CO_2 uptake rate revealed that CO_2 concentration, light intensity and phosphate concentration (in that order) had the strongest effects. To maximize the in situ CO_2 uptake rate of *Chlorella kessleri* the following modifications to OSPW are suggested: (1) increasing CO_2 levels by bubbling waste CO_2 from stacks, and (2) increasing phosphate levels by adding waste fertilizer or agricultural run-off. This study is part of a larger study which includes the development of statistical quadratic regression models and mechanistic models to better understanding the algal system and eventually find the optimal operation conditions (de la Hoz Siegler et al., 2011). Therefore, the optimization of algal growth and CO_2 uptake of *Chlorella kessleri* using response surface methodology is investigated in the next chapter.

2.5 References

Allen, E.W., 2008. Process water treatment in Canada's oil sands industry: I. Target pollutants and treatment objectives. Journal of Environmental Engineering and Science 7, 123–138.

Chefurka, W., Kashi, K.P., Bond, E.J., 1976. The effect of phosphine on electron transport in mitochondria. Pesticide Biochemistry and Physiology 6, 65–84.

Collos, Y., 1998. Nitrate uptake, nitrite release and uptake, and new production estimates. Marine Ecology Progress Series 171, 293–301.

Droop, M.R., 1973. Some thoughts on nutrient limitation in algae. Journal of Phycology 9, 264–272.

Eaton, A.D., Greenberg, A.E., Clesceri, L.S., 1999. Standard methods for the examination of water and wastewater. American Public Health Association Publications. 20^{th} edition.

Encarnacao, T., Burrows, H., Pais, A., Campos, M., Kremer, A., 2012. Effect of N and P on the uptake of magnesium and iron and on the production of carotenoids and chlorophyll by the microalgae *Nannochloropsis* sp. Journal of Agricultural Science and Technology 2, 824–832.

Erifi, I.R., Turpin, D.H., 1985. Steady state luxury consumption and the concept of optimum nutrient ratios: a study with phosphate and nitrate limited *Selenastrum minutum* (chlorophyta). Journal of Phycology 21, 592–602.

Fan, L., Zhang, Y., Cheng, L., Zhang, L., Tang, D., Chen, H., 2007. Optimization of carbon dioxide fixation by *Chlorella vulgaris* cultivated in a membrane-photobioreactor. Chemical Engineering and Technology 30, 1094–1099.

Fried, S., Mackie, B., Nothwehr, E., 2003. Nitrate and phosphate levels positively affect the growth of algae species found in perry pond. Tillers 4, 21–24.

Fu, M., Song, X., Yu, Z., Liu, Y., 2013. Responses of phosphate transporter gene and alkaline phosphatase in *Thalassiosira pseudonana* to phosphine. PLoS ONE 8.

Geider, R.J., Macintyre, H.L., Graziano, L.M., McKay, R.M.L., 1998. Responses of the photosynthetic apparatus of *Dunaliella tertiolecta* (Chlorophyceae) to nitrogen and phosphorus limitation. European Journal of Phycology 33, 315–332.

de la Hoz Siegler, H., Ben-Zvi, A., Burrell, R.E., McCaffrey, W.C., 2011. The dynamics of heterotrophic algal cultures. Bioresource Technology 102, 5764–5774.

de la Hoz Siegler, H., McCaffrey, W.C., Burrell, R.E., Ben-Zvi, A., 2012. Optimization of microalgal productivity using an adaptive, non-linear model based strategy. Bioresource Technology 104, 537–546.

Hu, H., Gao, K., 2006. Response of growth and fatty acid compositions of *Nannochloropsis* sp. to environmental factors under elevated CO_2 concentration. Biotechnology Letters 28, 987–992.

Jacob-Lopes, E., Scoparo, C.H.G., Lacerda, L.M.C.F., Franco, T.T., 2009. Effect of light cycles (night/day) on CO_2 fixation and biomass production by microalgae in photobioreactors. Chemical Engineering and Processing: Process Intensification 48, 306–310.

Kumar, A., Ergas, S., Yuan, X., Sahu, A., Zhang, Q., Dewulf, J., Malcata, F.X., van Langenhove, H., 2010. Enhanced CO_2 fixation and biofuel production via microalgae: Recent developments and future directions. Trends in Biotechnology 28, 371–380.

Lai, J., Yu, Z., Song, X., Cao, X., Han, X., 2011. Responses of the growth and biochemical composition of *Prorocentrum donghaiense* to different nitrogen and phosphorus concentrations. Journal of Experimental Marine Biology and Ecology 405, 6–17.

Leung, S.S.C., MacKinnon, M.D., Smith, R.E.H., 2001. Aquatic reclamation in the Athabasca, Canada, oil sands: Naphthenate and salt effects on phytoplankton communities. Environmental Toxicology and Chemistry 20, 1532–1543.

Li, Y., Zhou, W., Hu, B., Min, M., Chen, P., Ruan, R.R., 2012. Effect of light intensity on algal biomass accumulation and biodiesel production for mixotrophic strains *Chlorella kessleri* and *Chlorella protothecoide* cultivated in highly concentrated municipal wastewater. Biotechnology and Bioengineering 109, 2222–2229.

Mahdavi, H., Ulrich, A.C., Liu, Y., 2012. Metal removal from oil sands tailings pond water by indigenous micro-alga. Chemosphere 89, 350–354.

Molloy, C.J., Syrett, P.J., 1988. Effect of light and N deprivation on inhibition of nitrate uptake by urea in microalgae. Journal of Experimental Marine Biology and Ecology 118, 97–101.

de Morais, M.G., Costa, J.A.V., 2007. Isolation and selection of microalgae from coal fired thermoelectric power plant for biofixation of carbon dioxide. Energy Conversion and Management 48, 2169–2173.

Murakami, M., Ikenouchi, M., 1997. The biological CO_2 fixation and utilization project by RITE (2): Screening and breeding of microalgae with high capability in fixing CO_2. Energy Conversion and Management 38, S493–S497.

Noctor, G., Foyer, C.H., 1998. Ascorbate and glutathione: Keeping active oxygen under control. Annual Review of Plant Physiology and Plant Molecular Biology 49, 249–279.

Rosenberg, J.N., Mathias, A., Korth, K., Betenbaugh, M.J., Oyler, G.A., 2011. Microalgal biomass production and carbon dioxide sequestration from an integrated ethanol biorefinery in Iowa: A technical appraisal and economic feasibility evaluation. Biomass and Bioenergy 35, 3865–3876.

Ruan, M., Li, Y., Cheng, Y., 2012. Effect of exogenous CO_2 on algae growth and wastewater treatment under simulated natural light/dark cycle using municipal wastewater as feedstock. International Agricultural Engineering Journal 21, 1–8.

Sawayama, S., Inoue, S., Dote, Y., Yokoyama, S.Y., 1995. CO_2 fixation and oil production through microalga. Energy Conversion and Management 36, 729–731.

Sydney, E.B., Sturm, W., de Carvalho, J.C., Thomaz-Soccol, V., Larroche, C., Pandey, A., Soccol, C.R., 2010. Potential carbon dioxide fixation by industrially important microalgae. Bioresource Technology 101, 5892–5896.

Tang, D., Han, W., Li, P., Miao, X., Zhong, J., 2011. CO_2 biofixation and fatty acid composition of *Scenedesmus obliquus* and *Chlorella pyrenoidosa* in response to different CO_2 levels. Bioresource Technology 102, 3071–3076.

Tubea, B., Hawxby, K., Mehta, R., 1981. The effects of nutrient, ph and herbicide levels on algal growth. Hydrobiologia 79, 221–227.

Wang, B., Lan, C.Q., 2011. Biomass production and nitrogen and phosphorus removal by the green alga *Neochloris oleoabundans* in simulated wastewater and secondary municipal wastewater effluent. Bioresource Technology 102, 5639–5644.

Wang, B., Li, Y., Wu, N., Lan, C.Q., 2008. CO_2 bio-mitigation using microalgae. Applied Microbiology and Biotechnology 79, 707–718.

Xu, Z., Zou, D., Gao, K., 2010. Effects of elevated CO_2 and phosphorus supply on growth, photosynthesis and nutrient uptake in the marine macroalga *Gracilaria lemaneiformis* (rhodophyta). Botanica Marina 53, 123–129.

Yewalkar, S., Li, B., Posarac, D., Duff, S., 2011. Potential for CO_2 fixation by *Chlorella pyrenoidosa* grown in oil sands tailings water. Energy and Fuels 25, 1900–1905.

Zhang, Q., Hong, Y., 2014. Effects of stationary phase elongation and initial nitrogen and phosphorus concentrations on the growth and lipid-producing potential of *Chlorella* sp. HQ. Journal of Applied Phycology 26, 141–149.

Zheng, Y., Chen, Z., Lu, H., Zhang, W., 2011. Optimization of carbon dioxide fixation and starch accumulation by *Tetraselmis subcordiformis* in a rectangular airlift photobioreactor. African Journal of Biotechnology 10, 1888–1901.

Chapter 3

Optimization of CO_2 Fixation by *Chlorella kessleri* using Response Surface Methodology

3.1 Introduction

Several studies have been performed to optimize the CO_2 fixation rate in microalgae in an effort to make biological fixation competitive with carbon capture and storage technologies. Parameters that significantly affect the performance of CO_2 fixation by microalgae include the nutrients ratio, light intensity, temperature, pH, CO_2 concentration, flow rate, photobioreactor type and microalgae species (Cheng et al., 2013; Ho et al., 2012). Purba and Taharuddin (2010) optimized the CO_2 fixation of *Nannochloropsis oculata* and *Tetraselmis chuii* by manipulating CO_2 concentration (3, 6, and 9 %) and light intensity (360 and 1250 lumen). Also, the molar ratios of nitrogen to carbon, phosphorus to carbon, and magnesium to carbon in the culture as well as light intensity were optimized for *Chlorella PY-ZU1* (Cheng et al., 2013).

A few studies have also been performed on optimal experimental designs to optimize algal growth and subsequently optimize the CO_2 fixation rate (Ho et al., 2012; Yewalkar et al., 2011; Zheng et al., 2011). Statistical approaches to optimal experimen-

tal designs are usually classified under response surface methodology (RSM). Response surface methodology and the desirability function approach were used to vary the initial biomass concentration, the gas flow rate and different carbon dioxide concentrations to maximize the CO_2 fixation rate and intracellular starch productivity of *Tetraselmis subcordiformis* in a rectangular airlift photobioreactor (Zheng et al., 2011). Ho et al. (2012) employed RSM to maximize the CO_2 fixation rate and specific growth rate of *Scenedesmus obliquus CNW-N* by manipulating the CO_2 concentration, CO_2 flow rate, magnesium concentration, and light intensity. Yewalkar et al. (2011) also used RSM to find the optimum concentration of nitrate, phosphate, Fe-ethylenediaminetetraacetic acid (EDTA), and trace metals for *Chlorella pyrenoidosa* cultivated in 95% oil sands process water (OSPW).

Many previous studies related to CO_2 fixation by microalgae have focused on the cell growth rate and biomass productivity, since the CO_2 fixation rate of micoalgae is considered to be positively correlated to these parameters (Anjos et al., 2013; Cheng et al., 2013; Ho et al., 2012; Zheng et al., 2011). A few studies have also focused on direct evaluation of the CO_2 uptake rate in the system (Purba and Taharuddin, 2010). However, to the best of our knowledge, no study has been performed on optimal experimental design of native microalgae cultivated in OSPW to maximize the CO_2 uptake rate based on directly measured CO_2 concentrations; also, no studies have focused on simultaneous optimization of the CO_2 fixation rate and the specific growth rate.

In this chapter, a Box-Behnken response surface design varying the initial CO_2 concentration, the phosphate concentration and the light intensity was used to model the CO_2 uptake rate and the specific growth rate of *Chlorella kessleri*, a microalgal strain that is indigenous to OSPW, in batch operation. *Chlorella kessleri* exhibited the highest CO_2 fixation rate and specific growth rate among three strains, *Botryococcus braunii*, *Chlorella pyrenoidosa* and *Chlorella kessleri*, explained in the previous chapter (Kasiri

et al., 2014a). The quadratic regression models developed from the Box-Behnken design were validated against experimental data obtained by an alternate central composite design (CCD). The objectives of the study were to maximize the CO_2 uptake rate and the specific growth rate and determine the optimum levels of the manipulated variables based on multi-objective optimization.

3.2 Materials and Methods

3.2.1 Strains and Culture Conditions

Chlorella kessleri was obtained from our laboratory culture collection (Mahdavi et al., 2012). Since *Chlorella kessleri* is indigenous to OSPW, it is maintained in this environment and no other media is used. The OSPW media were made of 100% OSPW and nitrate ($NaNO_3$, 1mM) with different concentrations of phosphate (KH_2PO_4). Phosphate and nitrate were added as nutrients required for microalgal growth. All experiments were conducted in 500 mL baffled Erlenmeyer flasks with 250 mL working volume. Flasks were topped with septum DuoCAP® (TriForest labware, Irvine, USA) and then different concentrations of CO_2 were added to the sealed flasks. The flasks were then incubated at 21±0.5°C, in a shaker at 150 rpm for 8 days.

3.2.2 Analytical Methods

Growth Analysis: Biomass concentration was determined as total suspended solids (TSS) by centrifuging 2 mL of cell suspension with a relative centrifugal force (RCF) of 2500g for 15 min. Pellets were washed with Milli-Q water and recentrifuged. The final precipitate was dried at 105°C for 24 hours. In our preliminary experiments, *Chlorella kessleri* exhibited exponential growth; therefore, the specific growth rate (SGR) was

calculated based on:

$$\mu = \frac{\ln(N_2/N_1)}{t_2 - t_1} \tag{3.1}$$

where N_1 and N_2 are the biomass concentration at time t_1 and time t_2, respectively.

Carbon Dioxide Measurement: A 200 μL gas sample was taken and injected into an Agilent 7890A gas chromatograph with a thermal conductivity detector (GC-TCD) that was accompanied by a HayeSep R stainless steel column 80/100 (3.048 m×3.175 mm OD). Helium with a flow rate of 25 mL/min was used as the carrier gas. The oven was programmed to maintain a constant temperature of 140°C for 6 min. The CO_2 concentration was calculated using the CO_2 percentage and the headspace pressure measured by a Cecomp Electronics digital pressure gauge DPG1000B (Libertyville, Illinois, USA). It should be noted that the alkalinity (bicarbonate concentration) and pH are almost constant in each flask during the experiment. Therefore, it can be assumed with reasonable certainty that the changes in the CO_2 concentration at the headspace are due to the CO_2 consumption by *Chlorella kessleri*.

Water Chemistry: A 200 μL of clear supernatant from the centrifugation was used to determine the amount of phosphate and nitrate using Dionex DX600 Ion Chromatography (Dionex, Sunnyvale, CA, USA) in the Biogeochemical Analytical Service Laboratory (BASL) at the University of Alberta. The amount of nitrite and ammonium of samples were measured using the colorimetric methods of 4500-NH_3 and 4500-NO_3 (Eaton et al., 1999) in the Biogeochemical Analytical Service Laboratory (BASL) at the University of Alberta. The alkalinity of the cell-free supernatant was measured by titration with a 0.02 N H_2SO_4 solution using a Mettler Toledo DL53 titrator (Mississauga, Ontario, Canada).

Light Intensity: Four 40W fluorescent lamps were used to provide illumination to the culture. Different light intensity to the culture was achieved by adjusting the distance from the light sources. The light intensity was measured using a Sper Scientific Light

Meter LUX/FC model 840020 (Scottsdale, Arizona, USA).

3.2.3 Response Surface Methodology

Response Surface Methodology (RSM) is used to identify the relationship between the controllable input factors and the outputs, and to find the optimal set of inputs that maximize or minimize the response of the output. Typically, a second-order model of the form given in Eq. 3.2 is used in RSM (Aslan and Cebeci, 2007).

$$y = \beta_0 + \sum_{i=1}^{k} \beta_i x_i + \sum_{i=1}^{k-1} \sum_{j=i+1}^{k} \beta_{ij} x_i x_j + \sum_{i=1}^{k} \beta_{ii} x_i^2 \tag{3.2}$$

where x_1, x_2, ..., x_k are the coded value of input factors (independent variables) which influence the response y, and β_0, β_i,β_{ii} and β_{ij} are unknown parameters which are determined using least squares regression. The levels of the independent variables, X_i, were coded as x_i according to Eq. 3.3 (Zheng et al., 2011):

$$x_i = \frac{X_i - X_0}{\triangle X_i}, i = 1, 2, \ldots, k \tag{3.3}$$

where X_0 is the value of an independent variable at the center point of its range, and $\triangle X_i$ is the step change used in the RSM design.

The two most common RSM designs employed are Box-Behnken and central composite designs. While both methods employ quadratic models, the Box-Behnken designs place experimental points on the edge-centers of the bounding box of the range of input factors. In contrast, the most common version of the central composite design (CCD) places experimental points on the face centers of the bounding box (Ogunnaike, 2010). Box-Behnken designs are often used when corner points are infeasible or unimportant to explore.

In this study, a Box-Behnken experimental design (Table 3.1) was used to develop quadratic regression models for the CO_2 uptake rate and the specific growth rate of *Chlorella kessleri* and subsequently find the optimal levels of CO_2 and phosphate concentrations and light intensity. This design was used to vary the initial CO_2 concentration (C_L=5% and C_H=35%), phosphate concentration (P_L=1 mM and P_H=29 mM), and light intensity (I_L=10 and I_H=70 μmol photons.m^{-2}.s^{-1}), since these factors showed the most significant effects on CO_2 uptake and algal growth in our previous studies.

Table 3.1: Box-Behnken experimental design for optimizing CO_2 concentration, phosphate concentration and light intensity.

Experiment	$CO_2(x_1)$		Phosphate (x_2)		Light(x_3)	
Number	Coded	Actual(%)	Coded	Actual(mM)	Coded	Actual(Photons)
1	-	5	-	1	0	40
2	+	35	-	1	0	40
3	-	5	+	29	0	40
4	+	35	+	29	0	40
5	-	5	0	15	-	10
6	+	35	0	15	-	10
7	-	5	0	15	+	70
8	+	35	0	15	+	70
9	0	20	-	1	-	10
10	0	20	+	29	-	10
11	0	20	-	1	+	70
12	0	20	+	29	+	70
13	0	20	0	15	0	40
14	0	20	0	15	0	40
15	0	20	0	15	0	40

The central composite experimental design presented in Table 3.2 was also used to validate the quadratic regression models obtained from the Box-Behnken design. This design was used to vary the initial CO_2 concentration (C_L=8% and C_H=42%), phosphate concentration (P_L=1 mM and P_H=39 mM), and light intensity (I_L=7 and I_H=81 μmol photons.m^{-2}.s^{-1}). The central composite design always contains star points representing new extreme values (-α,α) for each factor in the design. The value of α depends on the number of experimental runs in the factorial portion of the central composite design (2^3); α=($2^{3/4}$)=1.68 in our case (Myers and Montgomery, 2002; Wang, 2006). Using the CCD

to validate the model developed using the Box-Behnken design provides a reasonable estimate of its accuracy over the entire range of possible experimental conditions.

Table 3.2: Central composite experimental design for optimizing CO_2 concentration, phosphate concentration and light intensity.

Experiment	$CO_2(x_1)$		Phosphate (x_2)		Light(x_3)	
Number	Coded	Actual(%)	Coded	Actual(mM)	Coded	Actual(Photons)
1	-	15	-	9	-	22
2	+	35	-	9	-	22
3	-	15	+	31	-	22
4	+	35	+	31	-	22
5	-	15	-	9	+	66
6	+	35	-	9	+	66
7	-	15	+	31	+	66
8	+	35	+	31	+	66
9	$-\alpha$	8	0	20	0	44
10	$+\alpha$	42	0	20	0	44
11	0	25	$-\alpha$	1	0	44
12	0	25	$+\alpha$	39	0	44
13	0	25	0	20	$-\alpha$	7
14	0	25	0	20	$+\alpha$	81
15	0	25	0	20	0	44
16	0	25	0	20	0	44
17	0	25	0	20	0	44
18	0	25	0	20	0	44
19	0	25	0	20	0	44
20	0	25	0	20	0	44

3.2.4 Multi-objective Optimization and Pareto Optimal Solutions

Pareto optimal solutions are invoked when the desired optimization involves multiple objectives that may conflict each other and thus involve trade-offs (Niu et al., 2013). The image or trajectory of all optimal solution sets is called the Pareto curve or surface; it indicates the nature of the trade-off between the different objective functions. The characteristic of the Pareto optimal set is that none of the objective functions can be improved in value without losing value in some of the other objective functions; thus, each of Pareto optimal solutions represents a particular choice of trade-off between the multiple objective functions.

A simple way to solve the multi-objective optimization problems is using weighted-sum or scalarization; this combines the multiple objectives into a single scalar objective function by assigning importance factors w_i>0 to each objective:

$$\begin{aligned} &\min_x \sum_{i=1}^{n} w_i f_i(x) \\ &\sum_{i=1}^{n} w_i = 1 \\ &x \in S \end{aligned} \tag{3.4}$$

where f_i, $(i = 1, \ldots, n)$ are the individual objective functions and S is the set of applicable equality and inequality constraints.

$$S = \{x| \in R^m : h(x) = 0, g(x) \geq 0\} \tag{3.5}$$

An alternate technique for multi-objective optimization is the ϵ-constraint method. In this method, one objective out of n is minimized and the remaining objectives are constrained to be less than or equal to specified target values.

$$\begin{aligned} &\min_x f_j(x) \\ &f_i(x) \leq \epsilon_i, \forall i \in \{1, \ldots, n\} \backslash \{j\} \\ &x \in S \end{aligned} \tag{3.6}$$

where $f_j(x)$ is the objective to be minimized and ϵ_i are the upper bounds of $f_i(x)$. The Pareto optimal set is generated by systematically varying the constraint values.

Several techniques exist to identify a single optimal solution from the members of the Pareto set. The most widely used method is to use the L_p norm. This technique

minimizes the distance from the Pareto set to an ideal solution (i.e. utopia point, f_i^*) based on (Kasprzak and Lewis, 2001):

$$\min \left(\sum_{i=1}^{n} (f_i(x) - f_i^*)^p \right)^{1/p} \tag{3.7}$$

In this study, the L_2 norm was used to determine the optimal Pareto set. The optimal compromise Pareto design is the member of the Pareto set which lies geometrically closest to the utopia point, calculated in terms of vector distance in the performance space. The utopia point has been generated by combining the maximum attainable CO_2 uptake rate and the maximum attainable specific growth rate.

3.3 Results and Discussion

The quadratic models developed based on the experiments conducted as described in Section 3.2.3 are presented in Section 3.3.1. The validation of the Box-Behnken models against central composite experimental data is presented in Section 3.3.2. Finally, the validation of the optimal sets of CO_2 and phosphate concentrations and light intensities are presented in Section 5.3.3.

3.3.1 Model Development

Table 3.3 presents the data for the CO_2 uptake rate and the specific growth rate of *Chlorella kessleri* obtained from the Box-Behnken experiments. Using the data, the following quadratic regression models are estimated to describe the CO_2 uptake rate and

the specific growth rate:

$$\begin{aligned} \text{CO}_2 \text{ uptake rate} = 48.35 + 13.89x_1 + 2.62x_2 + 9.40x_3 - 1.07x_1x_3 \\ + 11.37x_2x_3 - 6.66x_1^2 - 5.83x_2^2 - 9.18x_3^2 \end{aligned} \tag{3.8}$$

$$\begin{aligned} \text{Specific growth rate} = 0.232 - 0.014x_1 + 0.033x_2 + 0.028x_3 + 0.0.018x_1x_2 \\ - 0.002x_1x_3 + 0.012x_2x_3 - 0.008x_1^2 - 0.005x_2^2 + 0.010x_3^2 \end{aligned} \tag{3.9}$$

where x_1, x_2, and x_3 are the coded values of the initial CO_2 concentration, phosphate concentration and light intensity, as calculated based on Eq. 3.3 and defined in Table 3.1.

Table 3.3: CO_2 uptake rate and specific growth rate obtained in the Box-Behnken experiments (shown as mean value ± one standard deviation).

Experiment Number	CO_2 Uptake Rate (mg/L/day)	Specific Growth Rate (1/day)	Phosphate Uptake Rate (mg/L/day)	Nitrogen Uptake Rate (mg/L/day)
1	22.75±0.33	0.190±0.025	2.96	3.84
2	42.02±13.97	0.147±0.009	5.69	2.92
3	37.09±0.19	0.277±0.016	36.82	9.49
4	47.39±13.53	0.273±0.010	36.41	7.23
5	13.05±0.47	0.198±0.037	6.52	4.60
6	46.19±10.89	0.190±0.025	6.07	2.06
7	20.93±0.17	0.235±0.044	22.15	11.11
8	57.57±5.85	0.229±0.016	23.48	9.51
9	29.42±2.98	0.171±0.025	3.88	1.60
10	11.19±2.25	0.213±0.007	2.39	5.24
11	34.39±0.77	0.214±0.036	9.59	6.34
12	61.51±0.76	0.293±0.019	28.45	12.55
13	44.88±6.32	0.246±0.009	13.37	6.36
14	54.20±4.29	0.207±0.025	12.34	5.92
15	48.53±5.02	0.227±0.004	14.59	5.90

The coefficients of determination (R^2) of the regression equations for the CO_2 uptake rate and the specific growth rate were 0.87 and 0.90, respectively, indicating that the quadratic equations can adequately describe the relationship between the factors and responses. It should be noted that the term x_1x_2 is excluded in this regression model

because including this term decreases the R^2 of the regression equation for the CO_2 uptake rate. The adequacy of these models is also shown in Figure 3.1, which shows reasonably good agreement between the model predictions and the corresponding experimental data. There was no discernible trend or pattern in the variation in the residuals.

Tests of significance for the quadratic models for the CO_2 uptake rate and the specific growth rate were conducted using analysis of variance (ANOVA); the results are presented in Table 3.4 and 3.5, respectively. In this analysis, a model term is considered to be significant when the corresponding p-value is less than 0.05. As shown in Table 3.4, the CO_2 concentration (x_1, p= 0.0053) and the light intensity (x_3, p=0.0213) are significant factors for the CO_2 uptake rate, while the effect of phosphate concentration (x_2) on the CO_2 uptake rate is less than significant in the tested range. Furthermore, the interaction term between the phosphate concentration (x_2) and the light intensity (x_3) shows a significant effect on the CO_2 uptake rate. As shown in Table 3.5, when considering the specific growth rate as the response, the phosphate concentration (x_2, p= 0.0060) and the light intensity (x_3, p=0.0114) are the significant factors, while the initial CO_2 concentration (x_1) exhibited a less significant effect.

Table 3.4: Analysis of variance (ANOVA) for the CO_2 uptake rate from the Box-Behnken design.

Source	Coefficient (β)	Standard Error	t-Value	p-Value
Intercept	48.3492	4.9242	9.8187	0.0001*
x_1	13.8872	3.2576	4.2629	0.0053*
x_2	2.6209	3.0344	0.8637	0.4209
x_3	9.4023	3.0393	3.0936	0.0213*
x_1x_3	1.0747	4.6351	0.2319	0.8243
x_2x_3	11.3712	4.2817	2.6558	0.0377*
x_1^2	-6.6628	4.9873	-1.3360	0.2300
x_2^2	-5.8313	4.4414	-1.3129	0.2372
x_3^2	-9.1794	4.4659	-2.0554	0.0856

* Significant at p-Value <0.05

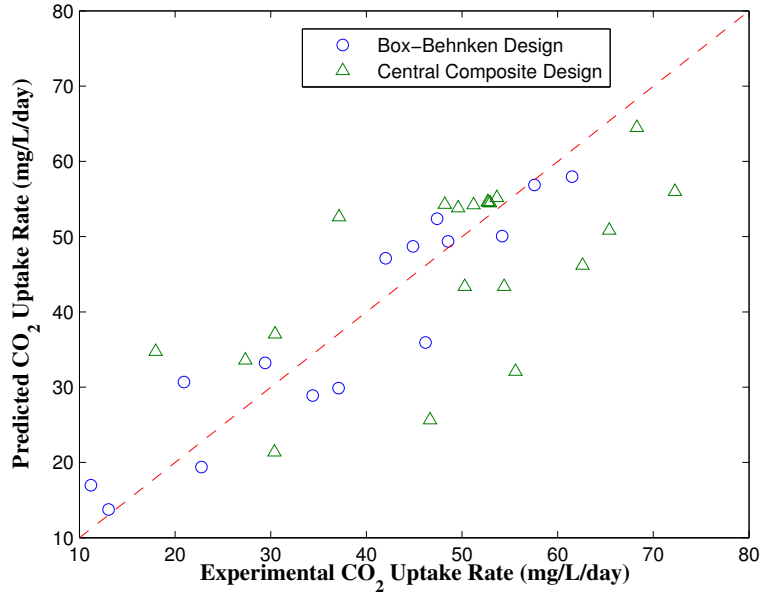

(a)

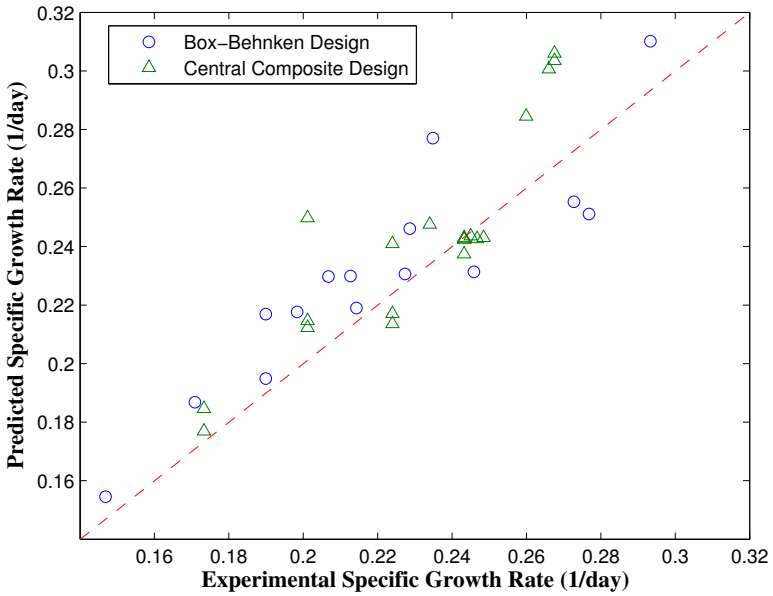

(b)

Figure 3.1: Model predictions, Box-Behnken and central composite design experimental data for (a) the CO_2 uptake rate and (b) the specific growth rate.

Table 3.5: Analysis of variance (ANOVA) for the specific growth rate from the Box-Behnken design.

Source	Coefficient (β)	Standard Error	t-Value	p-Value
Intercept	0.2317	0.0117	19.8469	<0.0001*
x_1	-0.0136	0.0077	-1.7531	0.1400
x_2	0.0330	0.0072	4.5657	0.0060*
x_3	0.0280	0.0072	3.8979	0.0114*
x_1x_2	0.0178	0.0107	1.6620	0.1574
x_1x_3	-0.0019	0.0110	-0.1748	0.8681
x_2x_3	0.0124	0.0101	1.2251	0.2751
x_1^2	-0.0081	0.0119	-0.6803	0.5265
x_2^2	-0.0051	0.0105	-0.4804	0.6512
x_3^2	0.0100	0.0106	0.9475	0.3869

* Significant at p-Value <0.05

Three-dimensional (3D) response surfaces and the 2D contour plot shown in Figure 3.2 and 3.3 were generated using Eqs. 3.8 and 3.9, respectively, to visualize the interaction effects on the CO_2 uptake rate and the specific growth rate. It should be noted that when the response surface for the effect of two factors was plotted, the other factor was set at level zero as described in Table 3.1. The blue stars in the 3D and 2D plots are the actual values obtained from Box-Behnken experiments.

Figure 3.2 (a) and (b) show the effects of CO_2 and phosphate concentrations on the CO_2 uptake rate. There is an increase in the CO_2 uptake rate with increased CO_2 concentration. This increase can be explained by the luxury consumption of CO_2 at high CO_2 concentrations. We hypothesize that the *Chlorella kessleri* attempts to store excess nutrients in intracellular pools for usage during times of nutrient limitation; this behaviour has been exhibited by many algal strains (Droop, 1973; Erifi and Turpin, 1985; Lai et al., 2011). The effects of CO_2 concentration and light intensity on the CO_2 uptake rate are shown in Figure 3.2 (c) and (d). The CO_2 uptake rate increases with increasing CO_2 concentration and light intensity; this is in agreement with Purba and Taharuddin (2010), who reported lower CO_2 amounts in the atmosphere (i.e., greater uptake) as the

CO_2 concentration and light intensity increase. Figure 3.2 (e) and (f) show the effects of phosphate concentration and light intensity on the CO_2 uptake rate when the CO_2 concentration is set to zero. At low light intensities, the CO_2 uptake rate is relatively constant at low phosphate concentrations; however, at higher phosphate concentrations, a decline in CO_2 uptake rate occurred, indicating an inhibitory response with respect to phosphate. However, this inhibitory response was not seen at higher light intensities; as shown in Figure 3.2 (f), the interaction effect of phosphate and light intensity significantly increases the CO_2 uptake rate.

As the CO_2 uptake rate is a function of algal growth, one might expect a similar response of the specific growth rate to increases in the CO_2 and phosphate concentrations and light intensity. However, this was not found to be the case. Figure 3.3 (a) and (b) show the effects of the CO_2 and phosphate concentrations on specific growth rate. The specific growth rate increases slightly as the phosphate concentration increases and decreases slightly as the CO_2 concentration increases at low phosphate concentrations. The tendency of the specific growth rate to increase slightly with increasing light intensity is shown in Figure 3.3 (c) and (d); this is in agreement with the ANOVA test. Figure 3.3 (e) and (f) show the effect of the phosphate concentration and light intensity on the specific growth rate. The specific growth rate increases when the phosphate concentration and light intensity are both high, even though the effect of light intensity is relatively insignificant by itself.

3.3.2 Model Validation

A set of central composite design experiments was performed to more comprehensively validate the models obtained by Box-Behnken design. The model predictions and data of the CO_2 uptake rate and specific growth rate for these validation experiments are pre-

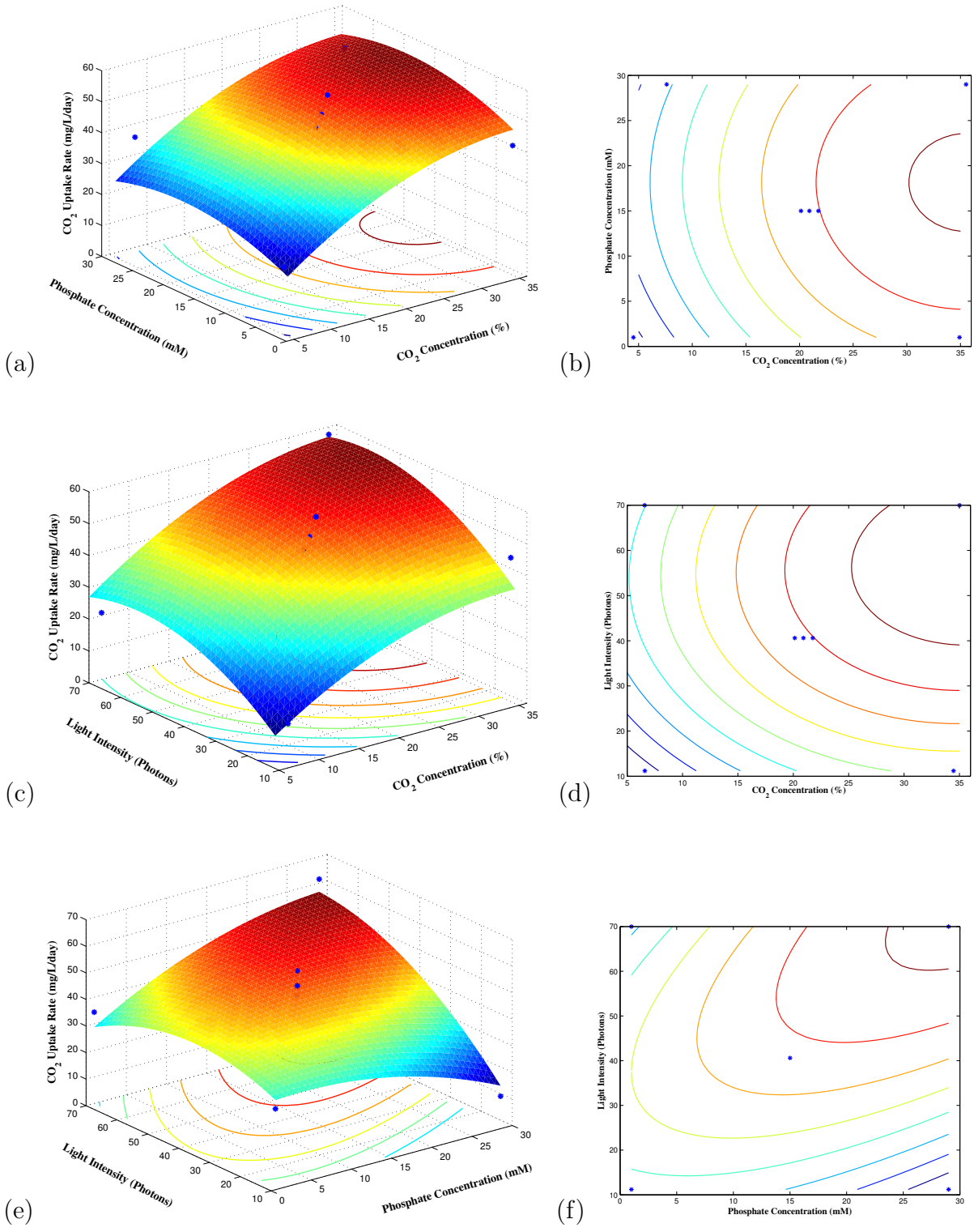

Figure 3.2: 3D response surface, the contour lines and the Box-Behnken experimental data ($*$) for the CO_2 uptake rate; (a)&(b) effects of CO_2 and phosphate concentrations, (c)&(d) effects of CO_2 concentration and light intensity, (e)&(f) effects of phosphate concentration and light intensity.

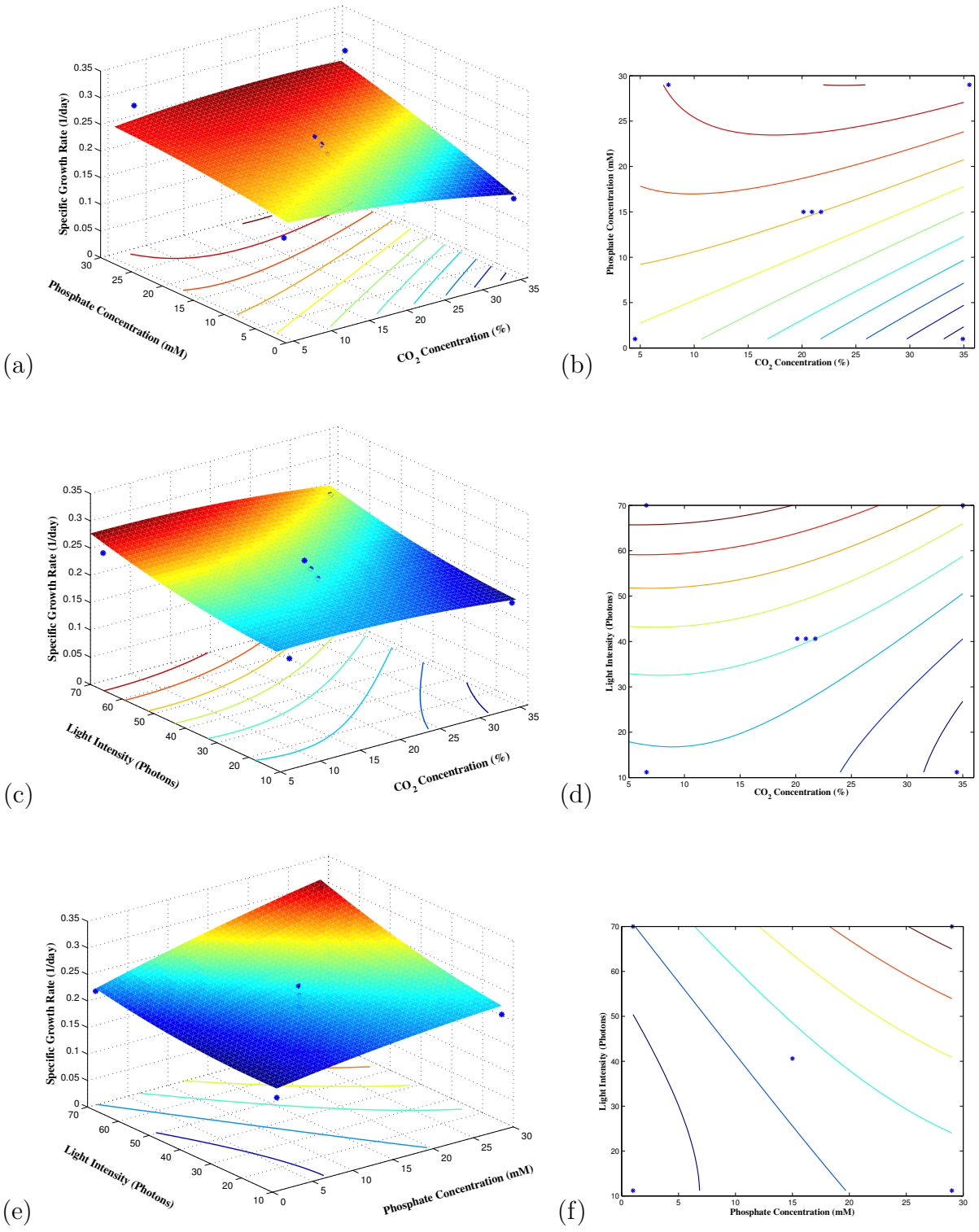

Figure 3.3: 3D response surface, the contour lines and the Box-Behnken experimental data ($*$) for the specific growth rate; (a)&(b) effects of CO_2 and phosphate concentrations, (c)&(d) effects of CO_2 concentration and light intensity, (e)&(f) effects of phosphate concentration and light intensity.

sented in Table 3.6. The CO_2 uptake rate model (Eq. 3.8) exhibits good agreement with the experimental data at the medium levels for all three factors (#15 to 20). However, it shows high error in the treatments that either have a very low concentration of CO_2 (8%, # 9) or very low light intensity (7 μmol photons.m^{-2}.s^{-1}, #13). It can be inferred that this model is unable to exhibit accurate prediction in very low treatments (-α). The adequacy of the models is also shown in Figure 3.1 (a), which shows good correlation between the model predictions of CO_2 uptake rate and the corresponding experimental data.

The specific growth rate model shows satisfactory agreement with experimental data for all treatments except in the combination of high light intensity and low CO_2 and phosphate concentrations (# 5). Similar to the CO_2 uptake rate model, this model shows high prediction accuracy in the medium level of all three factors (#15 to 20). As illustrated in Figure 3.1 (b), there is a good agreement between model predictions and experimental data.

It should be noted that the number of experiments performed was not large, which resulted in a relatively wide 95% confidence interval on the model predictions. The inclusion of more experimental data will decrease this interval.

Also, the models showed poor predictions in some treatments because these models are quadratic models and are perhaps unable to describe the dynamics of CO_2 fixation and algal growth in all kinetic regimes. Therefore, a mathematical model that describes the kinetics of algal growth and CO_2, phosphate, nitrate and ammonium uptake rate of *Chlorella kessleri* will be developed in the next chapter.

Table 3.6: The predicted CO_2 uptake rate and the specific growth rate for the central composite design (shown as mean value ± 95% confidence interval) and the corresponding experimental data.

	CO_2 Uptake Rate (mg/L/day)			Specific Growth Rate (1/day)		
Experiment Number	Model Prediction	Experimental Data	error %	Model Prediction	Experimental Data	error %
1	33.59±18.82	27.35	22.8	0.212±0.046	0.201	5.5
2	46.18±20.37	62.61	26.2	0.177±0.051	0.173	2.1
3	21.38±21.56	30.40	29.7	0.237±0.054	0.243	2.4
4	32.10±22.55	55.59	42.3	0.241±0.059	0.224	7.6
5	37.04±19.32	30.46	21.6	0.250±0.048	0.201	24.1
6	50.84±20.93	65.38	22.2	0.214±0.052	0.224	4.6
7	52.61±22.64	37.15	41.6	0.306±0.056	0.267	14.4
8	64.48±25.55	68.28	5.6	0.303±0.067	0.268	13.4
9	34.73±19.19	17.97	93.2	0.248±0.048	0.234	5.8
10	55.98±25.58	72.27	22.5	0.217±0.063	0.224	3.1
11	43.37±19.73	50.29	13.7	0.185±0.049	0.173	6.5
12	43.36±29.09	54.40	20.3	0.285±0.072	0.260	9.4
13	25.65±20.83	46.65	45.0	0.215±0.051	0.201	6.7
14	55.17±23.64	53.65	2.8	0.301±0.058	0.266	13.0
15	54.52±18.81	52.77	3.3	0.243±0.046	0.243	0.3
16	54.64±18.80	52.70	3.7	0.242±0.046	0.243	0.3
17	54.47±18.81	52.95	2.9	0.243±0.046	0.247	1.6
18	54.28±18.83	48.20	12.6	0.243±0.046	0.243	0.1
19	54.22±18.83	51.21	5.9	0.243±0.046	0.248	2.2
20	53.81±18.86	49.59	8.5	0.244±0.046	0.245	0.6

3.3.3 Optimization

Optimization of the CO_2 Uptake Rate

The quadratic model presented in Eq. 3.8 can be used to find the optimal set of experimental parameters in the range considered that maximize the CO_2 uptake rate. The maximum CO_2 uptake rate is predicted to be 65.03 mg/L/day and the optimal CO_2 and phosphate concentrations and the light intensity are estimated to be 35%, 29 mM and 70 μmol photons.m^{-2}.s^{-1}, respectively.

Specific Growth Rate Optimization

Similarly, the maximum specific growth rate of 0.310 per day is calculated by optimization of the model described by Eq. 3.9. The optimal CO_2, phosphate concentration and initial light intensity are estimated to be 22%, 29 mM and 70 μmol photons.m^{-2}.s^{-1},

respectively.

Generally, an increase in the light intensity corresponds to an increase in algal photosynthesis (Chisti, 2007; Fan et al., 2007); also, high phosphate levels increase the uptake rate of phosphorus, increase photosynthesis and raise the pigment content and eventually increase algal growth (Xu et al., 2010). Therefore, the maximum specific growth rate was obtained at high phosphate concentrations (29 mM) and light intensity (70 μmol photons.m^{-2}.s^{-1}).

Similarly, increasing CO_2 levels increase algal growth because more CO_2 from the external bulk medium diffuses to the active site of Rubisco; however, beyond a specific level (that varies with different algal strains), a further increase in the CO_2 concentration causes inhibition in algal growth due to a reduction in the efficiency of the CO_2 concentrating mechanisms (CCMs) that facilitate CO_2 supply to Rubisco by dehydration of the accumulated bicarbonate (Spalding, 2008; Wang et al., 2008; Xu et al., 2010). Moreover, microalgal cells in response to nutrient availability undergo a series of metabolic acclimations that regulate the growth of algal cells and their reproduction, and a trade-off exists between algal growth and nutrient storage (Bender et al., 2014; Lai et al., 2011). It would seem that CO_2 injection at a concentration higher than 22% should inhibit the reproduction of algal cells and decrease the cell number. However, the cells exploit high concentrations of CO_2 by luxury consumption of CO_2 and storage in intracellular pools, which results in the maximum CO_2 uptake rate occurring at 35% CO_2.

Multi-objective Optimization

The scalarization method described in Section 4.2.7 was used to maximize the CO_2 uptake rate and the specific growth rate simultaneously. The Pareto curve, the utopia point and the optimal Pareto set (*) are shown in Figure 3.4 (a). To emphasize that this is, indeed, the closest point, a circle centered on the utopia point with the radius of the vector is

drawn. Since no other points on the Pareto set appear within this circle, this point is the closest to the utopia point.

The optimal Pareto set is found to occur at a CO_2 uptake rate of 62.98 mg/L/day and a specific growth rate of 0.309 per day. The x^* is estimated to be 28% initial CO_2, 29 mM phosphate concentration and 70 μmol photons.m^{-2}.s^{-1} light intensity.

These results are in adequate agreement with de Morais and Costa (2007c) who reported that *Chlorella kessleri* showed maximum specific growth rates of 0.267 per day and maximum CO_2 fixation of 163 mg/L/day when cultivated with 6% (v/v) and 12% (v/v) CO_2. It should be noted that de Morais and Costa (2007c) calculated the CO_2 fixation from the biomass productivity according to equation, CO_2 fixation=1.88×biomass productivity, which is derived from the typical molecular formula of microalgal biomass, $C_{0.48}H_{1.83}N_{0.11}P_{0.01}$ (Chisti, 2007). However, it might be difficult to compare the various results in the literature, because of the different media and conditions under which the *Chlorella kessleri* was grown.

Validation of Optimal Points

These optimum treatments were applied to duplicate experiments to validate the optimal model predictions of the CO_2 uptake rate and specific growth rate as well as the Pareto optimal point.

The experimental CO_2 uptake rate and model predictions of all three optimal points are presented in Table 3.7. The model exhibits its highest prediction error of 5.0% for the CO_2 uptake rate at the Pareto optimal point. The specific growth rate and model predictions of all three optimal points are also presented in Table 3.7. The maximum prediction error of 8.8% in the specific growth rate is also obtained at the Pareto optimal point. It can also be seen that the 95% confidence intervals (CI) of the predictions of the CO_2 uptake rate and specific growth rate models encompass the experimental data at the

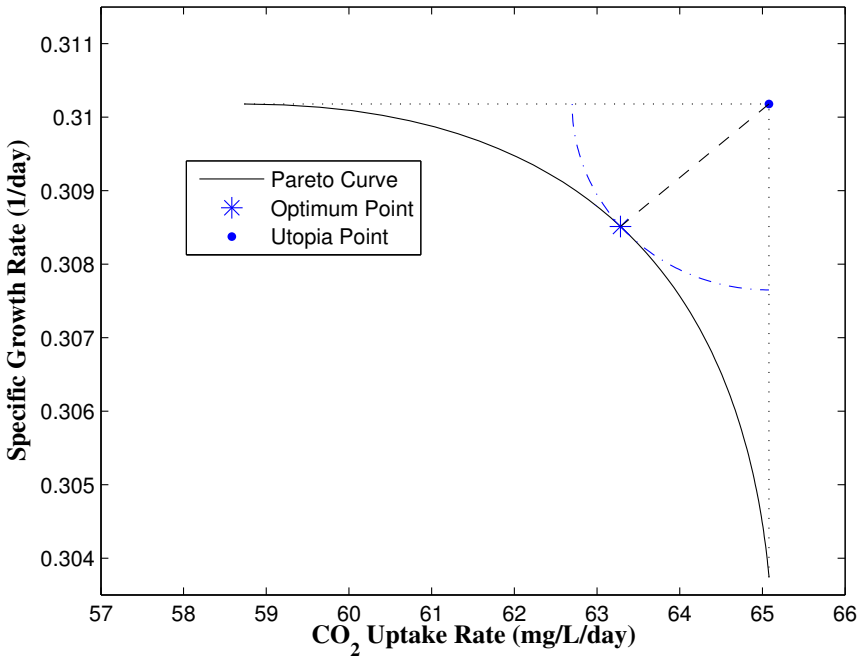

(a)

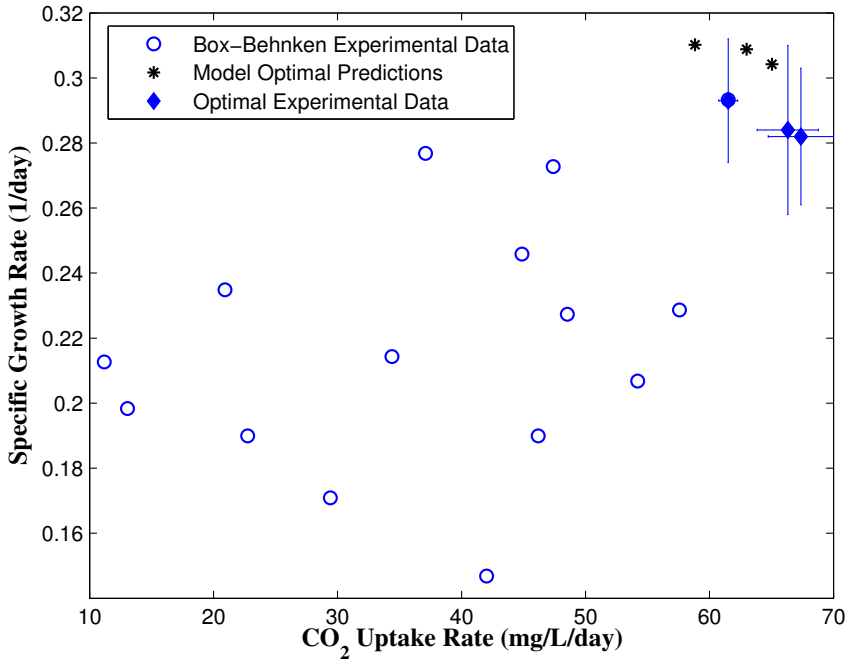

(b)

Figure 3.4: (a) Pareto curve based on the scalarization method, the Pareto optimal set and the utopia point, (b) The Box-Behnken experiments, the model-predicted and the experimentally determined optima (shown as mean value ± one standard deviation).

Table 3.7: The predicted CO_2 uptake rate and specific growth rate of the optimal points (shown as mean value ± 95% confidence interval) and corresponding experimental data (shown as mean value ± one standard deviation).

Objective Function	Optimal Condition			CO_2 Uptake Rate (mg/L/day)			Specific Growth Rate (1/day)		
	CO_2 (%)	Phosphate (mM)	Light Intensity (Photons)	Model Prediction	Experimental Data	error %	Model Prediction	Experimental Data	error %
CO_2 Uptake Rate	35	29	70	65.03±24.22	67.37±2.63	3.5	0.304±0.062	0.282±0.021	7.8
Specific Growth Rate	22	29	70	58.83 ±21.71	61.51±0.76	4.4	0.310±0.054	0.293±0.019	5.8
Multiobjective Optimization	28	29	70	62.98±24.22	66.32±2.47	5.0	0.309±0.062	0.284±0.026	8.8

optimal points, and the prediction errors of both models are relatively low. Figure 3.4 (b) shows the CO_2 uptake rate and the specific growth rate for the predicted optimal points and the experimental optima along with the Box-Behnken experimental data. It can be concluded that there is good agreement between model predictions and experimental data, and the models can adequately describe the CO_2 uptake rate and specific growth rate of *Chlorella kessleri*.

3.4 Conclusions

The CO_2 uptake rate and the specific growth rate of *Chlorella kessleri* can be adequately described by quadratic models developed using Box-Behnken experimental designs. Model validation using experimental data generated with a central composite design demonstrated that there is good agreement between model predictions and experimental data. 35% CO_2 concentration, 29 mM phosphate concentration and 70 μmol photons.m^{-2}.s^{-1} light intensity maximized CO_2 uptake rate to 65.03 mg/L/day. Also, 22% CO_2 concentration, 29 mM phosphate concentration and 70 μmol photons.m^{-2}.s^{-1} light intensity maximized specific growth rate to 0.310 per day. Multi-objective Pareto optimization resulted in a CO_2 uptake rate of 62.98 mg/L/day and a specific growth rate of 0.309 per day at 28% CO_2 concentration, 29 mM phosphate concentration and 70 μmol photons.m^{-2}.s^{-1} light intensity. The results from this study formed the basis for the investigations on the dynamics and kinetics of CO_2 uptake and algal growth explained in the next chapter.

3.5 References

Anjos, M., Fernandes, B.D., Vicente, A.A., Teixeira, J.A., Dragone, G., 2013. Optimization of CO_2 bio-mitigation by *Chlorella vulgaris*. Bioresource Technology 139, 149–154.

Aslan, N., Cebeci, Y., 2007. Application of Box-Behnken design and response surface methodology for modeling of some Turkish coals. Fuel 86, 90–97.

Bender, D., Diaz-Pulido, G., Dove, S., 2014. The impact of CO_2 emission scenarios and nutrient enrichment on a common coral reef macroalga is modified by temporal effects. Journal of Phycology 50, 203–215.

Cheng, J., Huang, Y., Feng, J., Sun, J., Zhou, J., Cen, K., 2013. Improving CO_2 fixation efficiency by optimizing *Chlorella* PY-ZU1 culture conditions in sequential bioreactors. Bioresource Technology 144, 321–327.

Chisti, Y., 2007. Biodiesel from microalgae. Biotechnology Advances 25, 294–306.

de Morais, M.G., Costa, J.A.V., 2007c. Carbon dioxide fixation by *Chlorella kessleri*, *C. vulgaris*, *Scenedesmus obliquus* and *Spirulina* sp. cultivated in flasks and vertical tubular photobioreactors. Biotechnology Letters 29, 1349–1352.

Droop, M.R., 1973. Some thoughts on nutrient limitation in algae. Journal of Phycology 9, 264–272.

Eaton, A.D., Greenberg, A.E., Clesceri, L.S., 1999. Standard methods for the examination of water and wastewater. American Public Health Association Publications. 20^{th} edition.

Erifi, I.R., Turpin, D.H., 1985. Steady state luxury consumption and the concept of optimum nutrient ratios: a study with phosphate and nitrate limited *Selenastrum minutum* (chlorophyta). Journal of Phycology 21, 592–602.

Fan, L., Zhang, Y., Cheng, L., Zhang, L., Tang, D., Chen, H., 2007. Optimization of carbon dioxide fixation by *Chlorella vulgaris* cultivated in a membrane-photobioreactor. Chemical Engineering and Technology 30, 1094–1099.

Ho, S.H., Chen, C.Y., Chang, J.S., 2012. Effect of light intensity and nitrogen starvation on CO_2 fixation and lipid/carbohydrate production of an indigenous microalga *Scenedesmus obliquus* cnw-n. Bioresource Technology 113, 244–252.

Kasiri, S., Prasad, V., Ulrich, A., 2014a. Strain and factor selection for carbon dioxide fixation using microalgae cultivated in oil sands process water. Canadian Journal of Chemical Engineering, *in press* (DOI: 10.1002/cjce.22055) .

Kasprzak, E.M., Lewis, K.E., 2001. Pareto analysis in multiobjective optimization using the colinearity theorem and scaling method. Structural and Multidisciplinary Optimization 22, 208–218.

Lai, J., Yu, Z., Song, X., Cao, X., Han, X., 2011. Responses of the growth and biochemical composition of *Prorocentrum donghaiense* to different nitrogen and phosphorus concentrations. Journal of Experimental Marine Biology and Ecology 405, 6–17.

Mahdavi, H., Ulrich, A.C., Liu, Y., 2012. Metal removal from oil sands tailings pond water by indigenous micro-alga. Chemosphere 89, 350–354.

Myers, R., Montgomery, D., 2002. Response surface methodology: Product and process optimization using designed experiments. John Wiley and Sons, New York. 2^{nd} edition.

Niu, B., Wang, H., Wang, J., Tan, L., 2013. Multi-objective bacterial foraging optimization. Neurocomputing 116, 336–345.

Ogunnaike, B.A., 2010. Random phenomena: Fundamentals of probability and statistics for engineers. CRC Press.

Purba, E., Taharuddin, 2010. CO_2 reduction and production of algal oil using microalgae *Nannochloropsis oculata* and *Tetraselmis chuii*. Chemical Engineering Transactions 21, 397–402.

Spalding, M.H., 2008. Microalgal carbon-dioxide-concentrating mechanisms: Chlamydomonas inorganic carbon transporters. Journal of Experimental Botany 59, 1463–1473.

Wang, B., Li, Y., Wu, N., Lan, C.Q., 2008. CO_2 bio-mitigation using microalgae. Applied Microbiology and Biotechnology 79, 707–718.

Wang, L., 2006. Recommendations for Design Parameters for Central Composite Designs with Restricted Randomization. Ph.D. thesis. Virginia Polytechnic Institute and State University, USA.

Xu, Z., Zou, D., Gao, K., 2010. Effects of elevated CO_2 and phosphorus supply on growth, photosynthesis and nutrient uptake in the marine macroalga *Gracilaria lemaneiformis* (rhodophyta). Botanica Marina 53, 123–129.

Yewalkar, S., Li, B., Posarac, D., Duff, S., 2011. Potential for CO_2 fixation by *Chlorella pyrenoidosa* grown in oil sands tailings water. Energy and Fuels 25, 1900–1905.

Zheng, Y., Chen, Z., Lu, H., Zhang, W., 2011. Optimization of carbon dioxide fixation and starch accumulation by *Tetraselmis subcordiformis* in a rectangular airlift photobioreactor. African Journal of Biotechnology 10, 1888–1901.

Chapter 4

Kinetic Modeling and Optimization of Carbon Dioxide Fixation Using Microalgae Cultivated in Oil-Sands Process Water

4.1 Introduction

Developing a dynamic model of algal systems can lead to a better understanding of the behavior of microalgae and eventually to find the optimal operation conditions. Thus, several studies have been performed on mathematical modeling of algal systems. For example, Jassby and Platt (1976) explained the effect of light using a number of equations including a modification of the Monod equation and a hyperbolic tangent. Also Bernard (2011); Flynn (2001); Geider et al. (1998); de la Hoz Siegler et al. (2011); Packer et al. (2011) combined the effects of different resources to better describe growth as a function of these multiple resources. A new dynamic model was developed by Geider et al. (1996) to predict the chlorophyll a:carbon ratio and growth rate of phytoplankton at constant and varying irradiance. Later, Geider et al. (1997) modified the model to predict the effects of irradiance, daylength, temperature and nutrient availability on chlorophyll a:carbon ratio and growth rate. They also modified the former model to describe the nitrogen:

carbon ratio in the algae (Geider et al., 1998). A mechanistic model for describing the growth of microalgae as functions of ammonium, nitrate, light, iron, silicon, phosphorus and temperature was developed by Flynn (2001). Also, Packer et al. (2011) developed a model to describe the growth dynamics and neutral lipid production of microalgae when cultured in nitrogen-limited or high light conditions. However, to the best of our knowledge, no mathematical model has been developed to describe algal growth, CO_2 uptake, phosphate uptake, nitrate and ammonium uptake rates of *Chlorella kessleri* that is indigenous to oil sands process water (OSPW).

In this study, a central composite experimental design with varying initial CO_2 concentration, phosphate concentration and light intensity was used to develop a nonlinear dynamic model that describes algal growth and CO_2, phosphate, nitrate and ammonium uptake rates of *Chlorella kessleri* cultivated in OSPW. The changes in algal growth, medium composition (phosphate, nitrate, ammonium and nitrite concentrations, pH and alkalinity) and gas content (CO_2 concentration) were monitored in batch cultures over a period of 21 days. The model parameters were estimated by minimizing the weighted sum of squared errors between model predictions and experimental data. The model then was validated against independent experimental data. Finally, the model was used to find the initial CO_2 concentration, phosphate concentration and light intensity that maximized CO_2 fixation and algal growth both individually and simultaneously.

4.2 Materials and Methods

4.2.1 Strain and Culture Conditions

Chlorella kessleri was obtained from our laboratory culture collection (Mahdavi et al., 2012). Since *Chlorella kessleri* is indigenous to OSPW, it is maintained in this envi-

ronment and no other media is used. The OSPW media was made of 100% OSPW and nitrate ($NaNO_3$, 1mM) with different concentrations of phosphate (KH_2PO_4). Phosphate and nitrate were added to provide phosphorus and nitrogen, the most important nutrients required for microalgal growth. All experiments were conducted in 500 mL baffled Erlenmeyer flasks with 250 mL working volume. Flasks were topped with septum DuoCAP® (TriForest labware, Irvine, USA) and then incubated at 21±0.5°C in a shaker at 150 rpm for 21 days.

4.2.2 Central Composite Experimental Design

In this study, a central composite experimental design (CCD, Table 4.1) was used to generate data to develop and validate a set of differential equations to describe algal growth and CO_2, phosphate, nitrate and ammonium uptake rates of *Chlorella kessleri* at different conditions. This design was used with varying initial CO_2 concentrations (C_L=8% and C_H=42%), phosphate concentrations (P_L=1mM and P_H=39 mM), and light intensity (I_L=7 and I_H=81 μmol photons.m^{-2}.s^{-1}), since these factors showed the most significant effects on CO_2 uptake and algal growth in our previous studies (Kasiri et al., 2014b,a) explained in Chapters 2 and 3. The central composite design always contains star points representing new extreme values (-α,α) for each factor in the design. The value of α depends on the number of experimental runs in the factorial portion of the central composite design (2^3); α=($2^{3/4}$)=1.68 in our case (Myers and Montgomery, 2002; Wang, 2006).

4.2.3 Analytical Methods

Growth Analysis: Biomass concentration was determined as total suspended solids (TSS) by centrifuging 2 mL of cell suspension with a relative centrifugal force (RCF) of

Table 4.1: Central composite experimental design with varying CO_2 concentration, phosphate concentration and light intensity. α=1.68 in this design.

Flask	CO_2		Phosphate		Light	
Number	Coded	Actual(%)	Coded	Actual(mM)	Coded	Actual(Photons)
1	-	15	-	9	-	22
2	+	35	-	9	-	22
3	-	15	+	31	-	22
4	+	35	+	31	-	22
5	-	15	-	9	+	66
6	+	35	-	9	+	66
7	-	15	+	31	+	66
8	+	35	+	31	+	66
9	$-\alpha$	8	0	20	0	44
10	$+\alpha$	42	0	20	0	44
11	0	25	$-\alpha$	1	0	44
12	0	25	$+\alpha$	39	0	44
13	0	25	0	20	$-\alpha$	7
14	0	25	0	20	$+\alpha$	81
15	0	25	0	20	0	44
16	0	25	0	20	0	44
17	0	25	0	20	0	44
18	0	25	0	20	0	44
19	0	25	0	20	0	44
20	0	25	0	20	0	44

2500g for 15 min. Pellets were washed with autoclaved Milli-Q water and recentrifuged. The final precipitate was dried at 105°C for 24 hours and then weighed using a Mettler Toledo XP205 microbalance (Mississauga, Ontario, Canada).

Carbon Dioxide Measurement: A 200 μL gas sample was taken and injected into an Agilent 7890A gas chromatograph with a thermal conductivity detector (GC-TCD) that was accompanied by a HayeSep R stainless steel column 80/100 (3.048 m×3.175 mm OD). Helium with a flow rate of 25 mL/min was used as the carrier gas. The oven temperature was programmed to be constant at 140°C for 6 min. The CO_2 concentration was calculated using the CO_2 percentage and the headspace pressure measured using a Cecomp Electronics digital pressure gauge DPG1000B (Libertyville, Illinois, USA).

Water Chemistry: A 200 μL sample of clear supernatant from the centrifugation was used to determine the amount of phosphate and nitrate using Dionex DX600 Ion Chromatography (Dionex, Sunnyvale, CA, USA) in the Biogeochemical Analytical Service

Laboratory (BASL) at the University of Alberta. The amount of nitrite and ammonium of the sample was measured using the colorimetric methods of 4500-NH_3 and 4500-NO_3 (Eaton et al., 1999) in the Biogeochemical Analytical Service Laboratory (BASL) at the University of Alberta. The alkalinity of the cell-free supernatant was measured by titration with a 0.02 N H_2SO_4 solution using a Mettler Toledo DL53 titrator (Mississauga, Ontario, Canada).

Light Intensity: Four 40W fluorescent lamps were used to provide illumination to the culture to mimic natural light conditions. Different light intensities to the culture were obtained by adjusting the distance from the light sources. The light intensity was measured using a Sper Scientific Light Meter LUX/FC model 840020 (Scottsdale, Arizona, USA).

4.2.4 Kinetic Models

In order to develop a kinetic model for the algal system, the effect of significant factors and nutrients on the algal growth and the uptake rate of these nutrients should be modeled.

Algal Growth

The algal growth rate can be calculated from:

$$\frac{dX}{dt} = \mu X - k_d X \tag{4.1}$$

where X is the biomass concentration, μ is the specific growth rate and k_d is the decay coefficient. There are some parameters that significantly affect the specific growth rate of microalgae including nutrient concentrations, light intensity, temperature and pH (Cheng et al., 2013; Ho et al., 2012). Therefore, the specific growth rate is commonly expressed by the multiplication of rate expressions for each of the influencing factors (Bastin and

Dochain, 1990).

$$\mu(t) = \mu(S_1).\mu(S_2).\mu(I).\mu(T).\mu(pH).... \tag{4.2}$$

where S_1 and S_2 are the substrates, I is the light intensity and T is the temperature. Several models have been proposed to describe the specific growth rate. The most common specific growth rate model is the Michaelis-Menten model (1949), that is also called the Monod model (Bastin and Dochain, 1990).

$$\mu = \mu_m \frac{S}{K_S + S} \tag{4.3}$$

where μ_m is the maximum growth rate, S is the substrate concentration and K_S is the half-substrate saturation constant. A downside of the Monod model is that it displays monotonic behavior and it does not consider any possible inhibition at high substrate concentrations (Bastin and Dochain, 1990). The Haldane-like model is non-monotonic and describes inhibition at high substrate concentrations (Pic-Marco et al., 2006):

$$\mu = \mu_m \frac{S}{K_S + S + S^2/K_I} \tag{4.4}$$

where K_I is the inhibition parameter.

Substrate Uptake Rate

The substrate uptake rate by microalgae can be expressed using several models to uncouple the uptake of nutrients from growth. The model used most commonly was proposed by Droop (1973), in which the substrate uptake is described by conventional Michaelis-

Menten type kinetics.

$$\rho = \rho_m \frac{S}{K_\rho + S} \tag{4.5}$$

where ρ is the substrate uptake rate, ρ_m is the maximum uptake rate and K_ρ is the uptake half-saturation constant. Also, Caperon and Meyer (1972) observed that the uptake rate of some nutrients fall to zero at a specific concentration, S_0. Therefore, they introduced a parameter S_0 in the kinetic expression and proposed the following model (the so-called Caperon-Meyer Model):

$$\rho = \rho_m \frac{S - S_0}{K_\rho + S - S_0} \tag{4.6}$$

4.2.5 Parameter Estimation

Parameters involved in the models were estimated by minimizing the weighted sum of squared errors (WSSE) of the states of the model, i.e., biomass, CO_2, phosphate, nitrate and ammonium concentrations. The WSSE for a set of model parameters (P) can be calculated as (de la Hoz Siegler et al., 2011):

$$WSSE(P) = \sum_{i=1}^{M} \sum_{j=1}^{N} \left(Y_{ij} - \hat{Y}_{ij}\right)^T W_i^{-1} \left(Y_{ij} - \hat{Y}_{ij}\right) \tag{4.7}$$

where N is the number of experimental data points used to estimate the model, M is the number of measurable states, Y_{ij} is the measured value of state i at time j and $\hat{Y}_{ij}$ is the value of state i at time j as predicted by the model and W_i is the weight factor of state i equal to the variance of the experimental data.

4.2.6 Model Selection

Several models can often explain the same data; therefore, objective criteria are needed to choose among these models. The criteria to select a model should consider the trade-off between increased information and cost. The parsimony principle says that out of two or more competing models that explain the data well, the model with the smallest number of independent parameters should be chosen (de la Hoz Siegler et al., 2011). Two model discrimination criteria were considered in this study. The first criterion is the Akaike information criterion (AIC), which can be calculated as (de la Hoz Siegler et al., 2011):

$$AIC = 2n_P + N\left\{ln\left(\frac{2\pi WSSE(\hat{P})}{N}\right) + 1\right\} \tag{4.8}$$

where n_P is the number of estimated parameters. The second criterion is the Bayesian information criterion (BIC), which can be calculated from (de la Hoz Siegler et al., 2011):

$$BIC = N\left\{ln\left(\frac{2\pi WSSE(\hat{P})}{N}\right)\right\} + n_P ln(N) \tag{4.9}$$

The best model was chosen based on the lowest AIC and BIC calculated for the same data-set. It should be noted that the difference between these two criteria is that free parameters are more strongly penalized in the BIC than in the AIC.

4.2.7 Optimization

A wide variety of evolutionary algorithms (EAs) have been used to solve different types of optimization problems. Particle swarm optimization (PSO) algorithm, one of the major evolutionary global optimization algorithms, was used to minimize the objective function (f) since it has shown a high convergence rate in multivariable problems (Cabrera and

Coello, 2007; Chu et al., 2011; Zhang et al., 2004).

$$\min_x f(x) \tag{4.10}$$
$$x \in S \subset \mathbb{R}^n$$

The PSO algorithm, first proposed by Kennedy and Eberhart (1995), starts with a randomly selected initial population and then successively evolves the individuals in a swarm:

$$x_i = x_{i-1} + v_i \tag{4.11}$$
$$v_i = c_0 v_{i-1} + c_1 r_1 \otimes (\hat{x}_i - x_{i-1}) + c_2 r_2 \otimes (\hat{g} - x_{i-1})$$

where x is the position of an individual particle, v is the velocity that determines the displacement of the particle, i is the index for current iteration, c_0 is the inertia weight, c_1 and c_2 are the acceleration constants that control the influence of each of the velocity components, r_1 and r_2 are random vectors with the dimensionality of the search space, $\hat{x}$ is the particle's best-ever position, $\hat{g}$ is the swarm's best-ever position and $\otimes$ stands for element-by-element vector multiplication. In other words, the position of an individual particle is updated by a displacement that depends on the particle's velocity of previous iteration, the best previous location of the particle (*pbest*) and the best-ever location of the particle among all particles (*gbest*) (Chu et al., 2011; Zhang et al., 2004).

However, the particles tend to move outside of the feasible boundary in the first few iterations (Chu et al., 2011). Therefore, handling boundary constraints is required to achieve the best performance with PSO. Several methods for handling boundary constraints including random, reflecting and absorbing methods have been proposed in the literature (Chu et al., 2011). In this study, we have bounds on the values of the estimated

parameters (they should be greater than zero). In order to handle these bounds, a new method was proposed. In this method, when the particle flies outside of the boundary, the calculated displacement is divided by a factor, b, which is dynamically modified until the particle lies inside of the boundary based on the following equation:

$$x_i = x_{i-1} + v_i/b_{ij} \tag{4.12}$$
$$b_{ij} = \lambda b_{ij-1}$$

where λ is a constant value and is problem dependent.

Evolutionary algorithms also require an additional mechanism to account for constraints that are not simple bounds, such as linear or nonlinear inequality constraints (Cabrera and Coello, 2007).

$$g_i(x) \leq 0, \quad i = 1, \ldots, m \tag{4.13}$$

Penalty functions are the most commonly used techniques used with evolutionary optimization, and they solve the constrained optimization problem via a sequence of unconstrained optimization problems. Penalty functions can be stationary or non-stationary. Stationary penalty functions use fixed penalty values throughout the minimization; however, the penalty values are dynamically modified in non-stationary penalty functions. The results obtained by non-stationary penalty functions are almost always superior to those obtained through stationary functions (Parsopoulos and Vrahatis, 2002), and we employed this technique in our work. Parsopoulos and Vrahatis (2002) proposed a non-stationary multi-stage assignment penalty function technique to transform a constrained problem to an unconstrained one. They defined a penalty function of the form

(Parsopoulos and Vrahatis, 2002):

$$F(x) = f(x) + h(k)H(x) \tag{4.14}$$

where $f(x)$ is the original objective function of the constrained optimization problem in Eq. 4.10, $h(k)$ is a dynamically modified penalty value, where k is the algorithm's current iteration number and $H(x)$ is a penalty factor, defined as:

$$H(x) = \sum_{i=1}^{m} \theta\left(q_i(x)\right) q_i(x)^{\gamma(q_i(x))} \tag{4.15}$$

where $q_i(x) = \max\{0; g_i(x)\}$, $i = 1, \ldots, m$. $\theta\left(q_i(x)\right)$ is a multistage assignment function; $\gamma\left(q_i(x)\right)$ is the power of the penalty function; and $g_i(x)$ are the constraints (Eq. 4.13). The functions $h(\cdot)$, $\theta(\cdot)$ and $\gamma(\cdot)$ are problem dependent. Details of the penalty function used in this study are presented in Section 4.3.3.

Multi-objective Optimization and the Pareto-optimal Solution

Sometimes, optimization problems involve multiple, conflicting objective functions and the optimal decisions involve trade-offs between two or more conflicting objectives. In that case, there exist (a possibly infinite number of) Pareto optimal solutions that satisfy the different objectives (Niu et al., 2013). The image of all optimal solution sets is called Pareto curve or surface that indicates the nature of the trade-offs between the different objective functions. The goal is to find a set of optimal trade-off, the so-called Pareto-optimal set.

A simple way to solve the multi-objective optimization problem is the ϵ-constraints method. In this method, one objective out of n is minimized and the remaining objectives

are constrained to be less than or equal to given target values.

$$\begin{aligned} &\min_x f_j(x) \\ &f_i(x) \leq \epsilon_i, \forall i \in \{1, \ldots, n\} \backslash \{j\} \\ &x \in S \subset \mathbb{R}^n \end{aligned} \tag{4.16}$$

where $f_j(x)$ is the objective to be minimized and ϵ_i are the upper bounds of $f_i(x)$.

Several techniques exist to determine which member of the Pareto set is the optimal solution. The most widely used method employs L_p norms. This technique minimizes the distance from the Pareto set to an ideal solution (i.e. the utopia point, f_i^*) to find the optimal solution based on the following equation (Kasprzak and Lewis, 2000):

$$\min \left(\sum_{i=1}^{n} (f_i(x) - f_i^*)^p \right)^{1/p} \tag{4.17}$$

Typical applications of the L_p norm are the L_1, L_2 and L_∞ norms where p = 1, 2 and ∞, respectively. In this study, the L_2 norm was used to determine the optimal Pareto set. According to the L_2 norm method, the optimal compromise Pareto design is the member of the Pareto set which lies geometrically closest to the utopia point, calculated in terms of vector distance in the performance space.

4.3 Results and Discussion

4.3.1 Model Formulation

The data obtained from the CCD experiment was divided into two parts: estimation and validation data, because once a model is built based on data, validation of the model

is necessary. In this study, the data of 14 flasks was used for model formulation and parameter estimation and the rest (flasks 4, 5, 7, 9, 12, 18) were used for validation of the model. The estimation and validation sets were chosen such that each included sufficient variation in the levels of each factor to provide enough variability in the data for accurate modeling.

Several models were examined to describe the algal growth and CO_2, phosphate, nitrate and ammonium uptake rates of *Chlorella kessleri*. The best model was then selected based on the lowest AIC and BIC, and the results are presented in Table 4.2.

Table 4.2: Comparison between competing kinetic expressions to model the algal growth rate and nutrient (CO_2, phosphate, nitrate and ammonium) uptake rate. WSSE, AIC and BIC are calculated based on Eq. 4.7, Eq. 4.8 and Eq. 4.9, respectively.

		Kinetic Model	WEES$\times 10^4$	AIC$\times 10^3$	BIC$\times 10^3$
Algal Growth Rate	μ_{CO_2}	Monod (Eq. 4.3)	5.01	6.18	5.35
		Haldane-like (Eq. 4.4)	5.00	6.18	5.35
		Haldane-like &Caperon-Meyer (Eq. 4.19)	2.19	5.44	4.61
	$\mu_{PO_4^{-3}}$	Monod (Eq. 4.3)	2.51	5.55	4.73
		Haldane-like (Eq. 4.4)	2.19	5.44	4.61
	μ_I	Monod (Eq. 4.3)	2.19	5.44	4.61
		Haldane-like (Eq. 4.4)	2.76	5.64	4.82
Nutrient Uptake Rate	ρ_{CO_2}	Droop (Eq. 4.5)	6.01	6.34	5.52
		Caperon-Meyer (Eq. 4.6)	2.19	5.44	4.61
	$\rho_{PO_4^{-3}}$	Droop (Eq. 4.5)	2.79	5.65	4.83
		Caperon-Meyer (Eq. 4.6)	2.19	5.44	4.61
	$\rho_{NO_3^-}$	Droop (Eq. 4.5)	4.26	6.03	5.21
		Caperon-Meyer (Eq. 4.6)	2.19	5.44	4.61
	$\rho_{NH_4^+}$	Droop (Eq. 4.5)	2.19	5.44	4.61
		Caperon-Meyer (Eq. 4.6)	2.69	5.62	4.80

Algal Growth

As mentioned in Section 4.2.4, the specific growth rate can be expressed in terms of the multiplication of the influencing factors. In this study, pH and temperature are constant; therefore, the specific growth rate can be written as:

$$\mu(t) = \mu_m.\mu_{CO_2}.\mu_{PO_4^{-3}}.\mu_I \tag{4.18}$$

where μ_{CO_2}, $\mu_{PO_4^{-3}}$ and μ_I are the growth rates influenced by the CO_2 concentration, phosphate concentration and the light intensity, respectively.

Influence of CO_2 Concentration: As presented in Table 4.2, Monod and Haldane-like models were found to be unsuitable to explain the influence of CO_2 concentration on the growth of *Chlorella kessleri*. Therefore, a new model combining Haldane-like and Caperon-Meyer models was proposed to consider only the influence of the effective CO_2 concentration ($[CO_2]$-$[CO_2]_0$):

$$\mu_{CO_2} = \frac{[CO_2] - [CO_2]_0}{K_{S_{CO_2}} + [CO_2] - [CO_2]_0 + [CO_2]^2 / K_{I_{CO_2}}} \tag{4.19}$$

where $[CO_2]$ is the concentration of CO_2 (mg/L) in the headspace, $[CO_2]_0$ is the minimum concentration of CO_2 in the headspace below which no CO_2 can be taken up by the microalgae, $K_{S_{CO_2}}$ is the half-substrate saturation constant and $K_{I_{CO_2}}$ is an inhibition parameter.

Influence of Phosphate Concentration: The influence of phosphate concentration can be adequately explained by both Monod and Haldane-like models; however, the Haldane-like model showed a slightly lower AIC and BIC than the Monod model (Table 4.2):

$$\mu_{PO_4^{-3}} = \frac{\left[PO_4^{-3}\right]}{K_{S_{PO_4^{-3}}} + \left[PO_4^{-3}\right] + \left[PO_4^{-3}\right]^2 / K_{I_{PO_4^{-3}}}} \tag{4.20}$$

where $\left[PO_4^{-3}\right]$ is the concentration of PO_4^{-3} (mg/L) at the culture, $K_{S_{PO_4^{-3}}}$ is the half-substrate saturation constant and $K_{I_{PO_4^{-3}}}$ is the inhibition parameter.

Influence of Light Intensity: In several studies (Bechet et al., 2013; Bordel et al., 2009; Post et al., 1985), the algal specific growth rate was adequately explained by a Monod model based on the average light intensity; however, Haario et al. (2009) and

Bernard (2011) used Monod and Haldane-like models, respectively, to express the influence of incident light intensity on the algal specific growth rate. In this study, as presented in Table 4.2, the Monod model was found to be suitable enough to capture the effect of incident light intensity on the growth of *Chlorella kessleri*.

$$\mu_I = \frac{I}{K_{S_I} + I} \tag{4.21}$$

where I is the light intensity (μmol photons.m^{-2}.s^{-1}).

Nutrient Uptake Rate

CO_2 Uptake Rate: The CO_2 in the gas phase and liquid phase are in equilibrium with each other in this closed batch experiment:

$$CO_{2_{(gas)}} \rightleftharpoons CO_{2_{(aq)}} \tag{4.22}$$

and based on Henry's law:

$$\frac{[dCO_2]}{[CO_2]} = k_{H_{cc}} \tag{4.23}$$

where $[CO_2]$ is CO_2 concentration in gas phase, $[dCO_2]$ is dissolved CO_2 concentration in liquid phase and $k_{H_{cc}}$ is the dimensionless Henry's constant.

Also, the dissolved CO_2 is in chemical equilibrium with carbonic acid:

$$CO_{2_{(aq)}} + H_2O \rightleftharpoons H_2CO_3 \tag{4.24}$$

with

$$\frac{[dCO_2]}{[H_2CO_3]} = K_D \tag{4.25}$$

However, the hydration equilibrium constant (K_D) ranges between 350 and 990 (Kern, 1960). Therefore, only a small fraction of aqueous CO_2 is converted into carbonic acid; also, the conversion of aqueous CO_2 to carbonic acid is slow and can be written as:

$$CO_{2_{(aq)}} + H_2O \rightarrow H_2CO_3 \tag{4.26}$$

In this experiment, the pH and alkalinity (as bicarbonate concentration) are almost constant in each flask. Moreover, the dissociation of carbonic acid to bicarbonate is instantaneous at pH<8. Therefore, the changes in aqueous CO_2 can be written as:

$$\frac{d\,[dCO_2]}{dt} = K_L a \left([CO_2]_{(saturation)} - [dCO_2] \right) - \rho_{dCO_2} X \tag{4.27}$$

where $K_L a$ is the volumetric CO_2 mass transfer coefficient, $[CO_2]_{(saturation)}$ is the dissolved CO_2 saturation concentration in the liquid phase, and ρ_{dCO_2} is the microalgal CO_2 uptake rate. Since the system is in equilibrium, $[CO_2]_{(saturation)}$ is equal to $[dCO_2]$ at each time and the first term on the right hand side of Eq. 4.27 is equal to zero. This simplifies the dissolved CO_2 dynamics to:

$$\frac{d\,[dCO_2]}{dt} = -\rho_{dCO_2} X \tag{4.28}$$

The Caperon-Meyer model (Eq. 4.6) estimates the CO_2 uptake rate as:

$$\rho_{dCO_2} = \rho_{m_{dCO_2}} \frac{[dCO_2] - [dCO_2]_0}{K_{\rho_{dCO_2}} + [dCO_2] - [dCO_2]_0} \tag{4.29}$$

where ρ_{dCO_2} is the uptake rate of dissolved CO_2, $\rho_{m_{dCO_2}}$ is the maximum uptake rate of dissolved CO_2, $K_{\rho_{dCO_2}}$ is the uptake half-saturation constant of dissolved CO_2 and $[dCO_2]_0$ is the dissolved CO_2 concentration at which the uptake rate is zero.

Based on Eq. 4.23, Eq. 4.29 can be rearranged by substituting $[dCO_2]$ with $[CO_2]$ as follows:

$$\rho_{CO_2} = \rho_{m_{dCO_2}} k_{H_{cc}} \frac{[CO_2] - [CO_2]_0}{K_{\rho_{dCO_2}}/k_{H_{cc}} + [CO_2] - [CO_2]_0} \tag{4.30}$$

Also, $\rho_{m_{dCO_2}} k_{H_{cc}}$ and $K_{\rho_{dCO_2}}/k_{H_{cc}}$ can be reparameterized to:

$$\rho_{CO_2} = \rho_{m_{CO_2}} \frac{[CO_2] - [CO_2]_0}{K_{\rho_{CO_2}} + [CO_2] - [CO_2]_0} \tag{4.31}$$

where ρ_{CO_2} is the uptake rate of CO_2, $\rho_{m_{CO_2}}$ is the maximum uptake rate of CO_2, $K_{\rho_{CO_2}}$ is the uptake half-saturation constant of CO_2 and $[CO_2]_0$ is the CO_2 concentration at which the uptake rate is zero. As presented in Table 4.2, the Droop model could not adequately explain CO_2 uptake rate; thus, the Caperon-Meyer model (Eq. 4.6) was used to estimated the CO_2 uptake rate.

Phosphate Uptake Rate: The Droop and Caperon-Meyer models were compared to describe the phosphate uptake rate. As shown in Table 4.2, Caperon-Meyer model showed better performance in describing the experimental data (Eq. 4.5):

$$\rho_{PO_4^{-3}} = \rho_{m_{PO_4^{-3}}} \frac{\left[PO_4^{-3}\right] - \left[PO_4^{-3}\right]_0}{K_{\rho_{PO_4^{-3}}} + \left[PO_4^{-3}\right] - \left[PO_4^{-3}\right]_0} \tag{4.32}$$

where $\rho_{PO_4^{-3}}$ is the uptake rate of phosphate, $\rho_{m_{PO_4^{-3}}}$ is the maximum uptake rate of phosphate and $K_{\rho_{PO_4^{-3}}}$ is the uptake half-saturation constant of phosphate and $\left[PO_4^{-3}\right]_0$ is the phosphate concentration at which the uptake rate is zero.

Nitrogen Uptake Rate: The dynamics of nitrate concentration were better described

by the Caperon-Meyer model; however, the Droop model (Eq. 4.5) was found to be adequate to estimate the ammonium uptake rate (Table 4.2):

$$\rho_{NO_3^-} = \rho_{m_{NO_3^-}} \frac{\left[NO_3^-\right] - \left[NO_3^-\right]_0}{K_{\rho_{NO_3^-}} + \left[NO_3^-\right] - \left[NO_3^-\right]_0} \tag{4.33}$$

$$\rho_{NH_4^+} = \rho_{m_{NH_4^+}} \frac{\left[NH_4^+\right]}{K_{\rho_{NH_4^+}} + \left[NH_4^+\right]} \tag{4.34}$$

where $\rho_{NO_3^-}$ is the uptake rate of nitrate, $\rho_{m_{NO_3^-}}$ is the maximum uptake rate of nitrate, $K_{\rho_{NO_3^-}}$ is the uptake half-saturation constant of nitrate, $\left[NO_3^-\right]_0$ is the nitrate concentration at which the uptake rate is zero, $\rho_{NH_4^+}$ is the uptake rate of ammonium, $\rho_{m_{NH_4^+}}$ is the maximum uptake rate of ammonium and $K_{\rho_{NH_4^+}}$ is the uptake half-saturation constant of ammonium.

Overally, the dynamics of the system can be described by a set of following differential equations:

$$\frac{dX}{dt} = \mu_m \frac{[CO_2] - [CO_2]_0}{K_{S_{CO_2}} + [CO_2] - [CO_2]_0 + [CO_2]^2 / K_{I_{CO_2}}} \frac{\left[PO_4^{-3}\right]}{K_{S_{PO_4^{-3}}} + \left[PO_4^{-3}\right] + \left[PO_4^{-3}\right]^2 / K_{I_{PO_4^{-3}}}} \frac{I}{K_{S_I} + I} X - k_d X \tag{4.35}$$

$$\frac{d\left[CO_2\right]}{dt} = -\rho_{m_{CO_2}} \frac{[CO_2] - [CO_2]_0}{K_{\rho_{CO_2}} + [CO_2] - [CO_2]_0} X \tag{4.36}$$

$$\frac{d\left[PO_4^{-3}\right]}{dt} = -\rho_{m_{PO_4^{-3}}} \frac{\left[PO_4^{-3}\right] - \left[PO_4^{-3}\right]_0}{K_{\rho_{PO_4^{-3}}} + \left[PO_4^{-3}\right] - \left[PO_4^{-3}\right]_0} X \tag{4.37}$$

$$\frac{d\left[NO_3^-\right]}{dt} = -\rho_{m_{NO_3^-}} \frac{\left[NO_3^-\right] - \left[NO_3^-\right]_0}{K_{\rho_{NO_3^-}} + \left[NO_3^-\right] - \left[NO_3^-\right]_0} X \tag{4.38}$$

$$\frac{d\left[NH_4^+\right]}{dt} = -\rho_{m_{NH_4^+}} \frac{\left[NH_4^+\right]}{K_{\rho_{NH_4^+}} + \left[NH_4^+\right]} X \tag{4.39}$$

The model parameters were estimated by minimizing the WSSE using PSO with 20 particles (λ=10), and they are presented in Table 4.3. It should be noted that all the parameters were subjected to a lower boundary constraint (P>0) which was handled using Eq. 4.12.

Table 4.3: The estimated values of model parameters (Eqs. 4.35 to 4.39) based on data from flasks 1, 2, 3, 6, 8, 10, 11, 13-17, 19 and 20.

Parameter	Estimated Value	Unit	Parameter	Estimated Value	Unit
μ_m	3.01×10^{-2}	1/h	k_d	2.32×10^{-5}	1/h
$K_{S_{CO_2}}$	10.2	mg_{CO_2}/L	$K_{I_{CO_2}}$	1.41×10^{3}	mg_{CO_2}/L
$K_{S_{PO_4^{-3}}}$	760	$mg_{PO_4^{-3}}$/L	$K_{I_{PO_4^{-3}}}$	9.92×10^{3}	$mg_{PO_4^{-3}}$/L
K_{S_I}	6.70	μmol photons.m^{-2}.s^{-1}			
$\rho_{m_{CO_2}}$	0.175	mg_{CO_2}/($mg_{Biomass}$.h)	$K_{\rho_{CO_2}}$	2.58×10^{3}	mg_{CO_2}/L
$\rho_{m_{PO_4^{-3}}}$	8.62×10^{-2}	$mg_{PO_4^{-3}}$/($mg_{Biomass}$.h)	$K_{\rho_{PO_4^{-3}}}$	233	$mg_{PO_4^{-3}}$/L
$\rho_{m_{NO_3^-}}$	4.64×10^{-3}	$mg_{NO_3^-}$/($mg_{Biomass}$.h)	$K_{\rho_{NO_3^-}}$	930	$mg_{NO_3^-}$/L
$\rho_{m_{NH_4^+}}$	1.39×10^{-2}	$mg_{NH_4^+}$/($mg_{Biomass}$.h)	$K_{\rho_{NH_4^+}}$	127	$mg_{NH_4^+}$/L

4.3.2 Model Validation

It is necessary to validate the model against experimental data obtained under different conditions. Therefore, data obtained from flasks 4, 5, 7, 9, 12, 18 was used to validate the developed model. The WSSE of each state for these flasks was calculated and is presented in Table 4.4. In flask 4, the model showed the best fit for biomass and nitrate against experimental data; however, it represented the worst fit for ammonium concentration. The model demonstrated the best fit for CO_2 and phosphate in flask 7 and flask 5,

respectively. It can be concluded that the model can satisfactorily predict the dynamics of CO_2 and phosphate concentration when their initial concentrations are low. However, the model demonstrated the best fit for ammonium in flask 5 as well. Totally, the model showed the best fit against experimental data for flask 18 as expected because of multiple runs in the center point. Model predictions and experimental data for flasks 4, 5, 7, 9, 12 and 18 are also shown in Figures 4.1-4.6 to demonstrate the accuracy of the model. Overall, in the validation, the best accuracy of model predictions was achieved for CO_2, phosphate and ammonium, and reasonable accuracy was achieved for biomass and nitrate. Based on this, we concluded that the accuracy of the model was sufficient for use in optimization studies.

Table 4.4: The WSSE for each state in the model and the total WSSE calculated based on Eq. 4.7 for the validation flasks

Flask	WSSE$\times 10^2$					
Number	Biomass	Carbon Dioxide	Phosphate	Nitrate	Ammonium	Total
4	1.45	1.35	0.901	1.38	5.48	10.6
5	16.1	0.163	0.065	8.12	0.739	25.1
7	3.81	0.049	0.335	22.5	3.94	30.6
9	13.0	0.118	0.122	6.10	1.83	21.2
12	15.1	0.256	0.958	46.1	2.56	65.0
18	4.75	0.524	0.361	2.69	1.02	9.35

4.3.3 Optimization

The validated dynamic model of microalgal culture presented in Eqs. 4.35 to 4.39 can be used to find optimal initial conditions, $\xi(t_0)^*$, to maximize the objective function.

$$\xi(t_0)^* = \underset{\xi(t_0)}{\operatorname{argmax}} J\left(\xi(t_0); t_f\right) \tag{4.40}$$

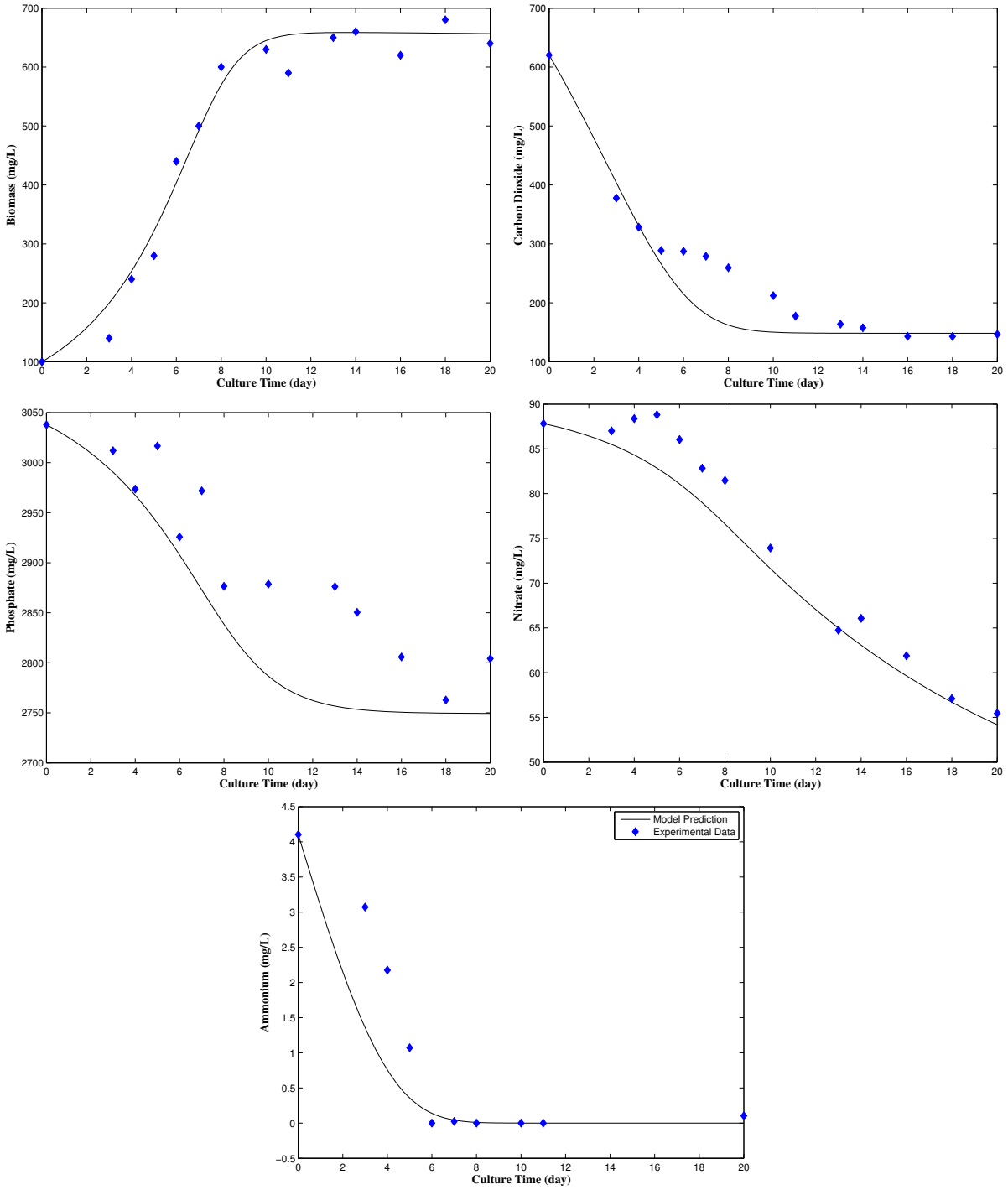

Figure 4.1: Validation of the model in flask 4 (conditions of high CO_2 concentration, high phosphate concentration and low light intensity)

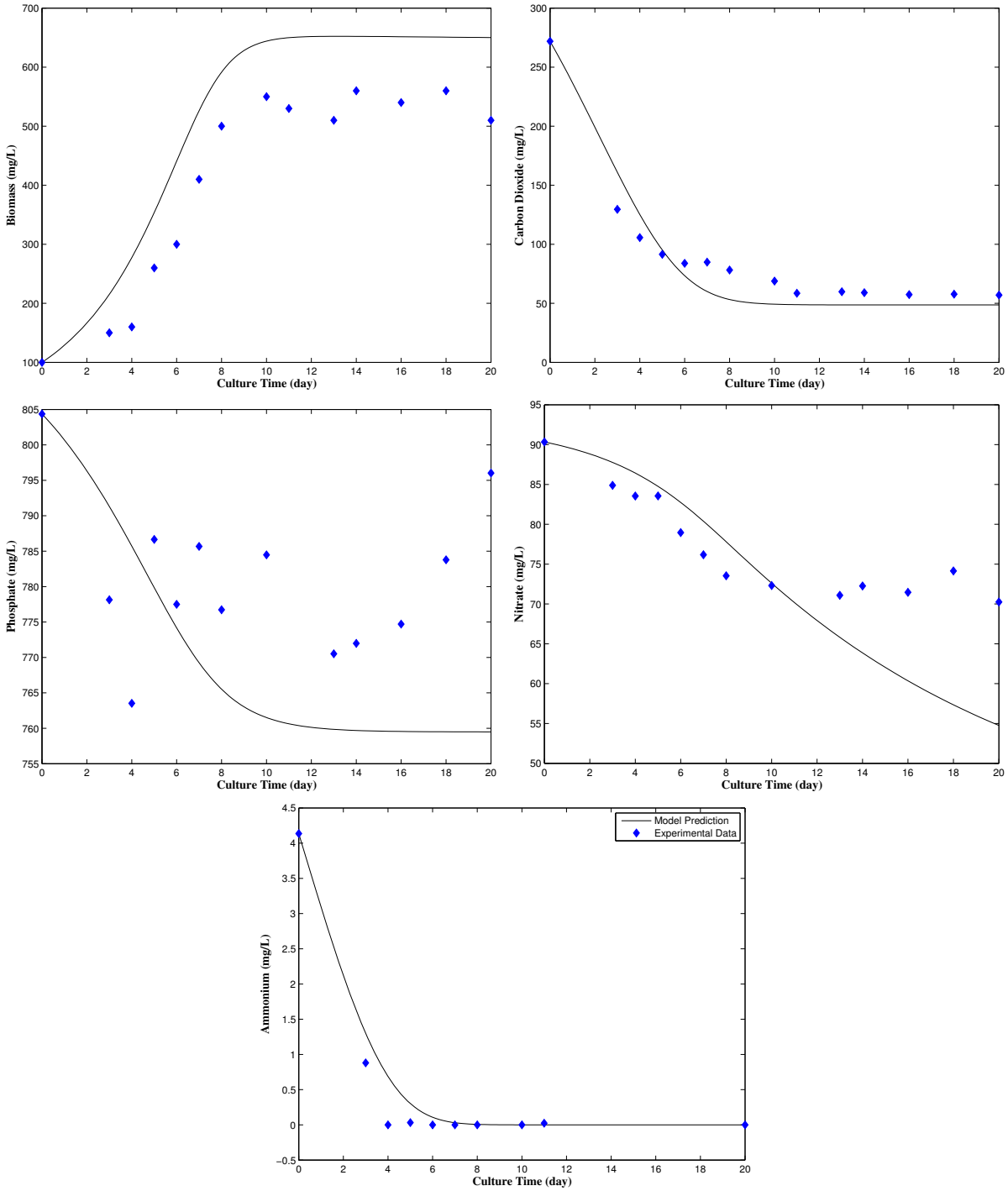

Figure 4.2: Validation of the model in flask 5 (conditions of low CO_2 concentration, low phosphate concentration and high light intensity)

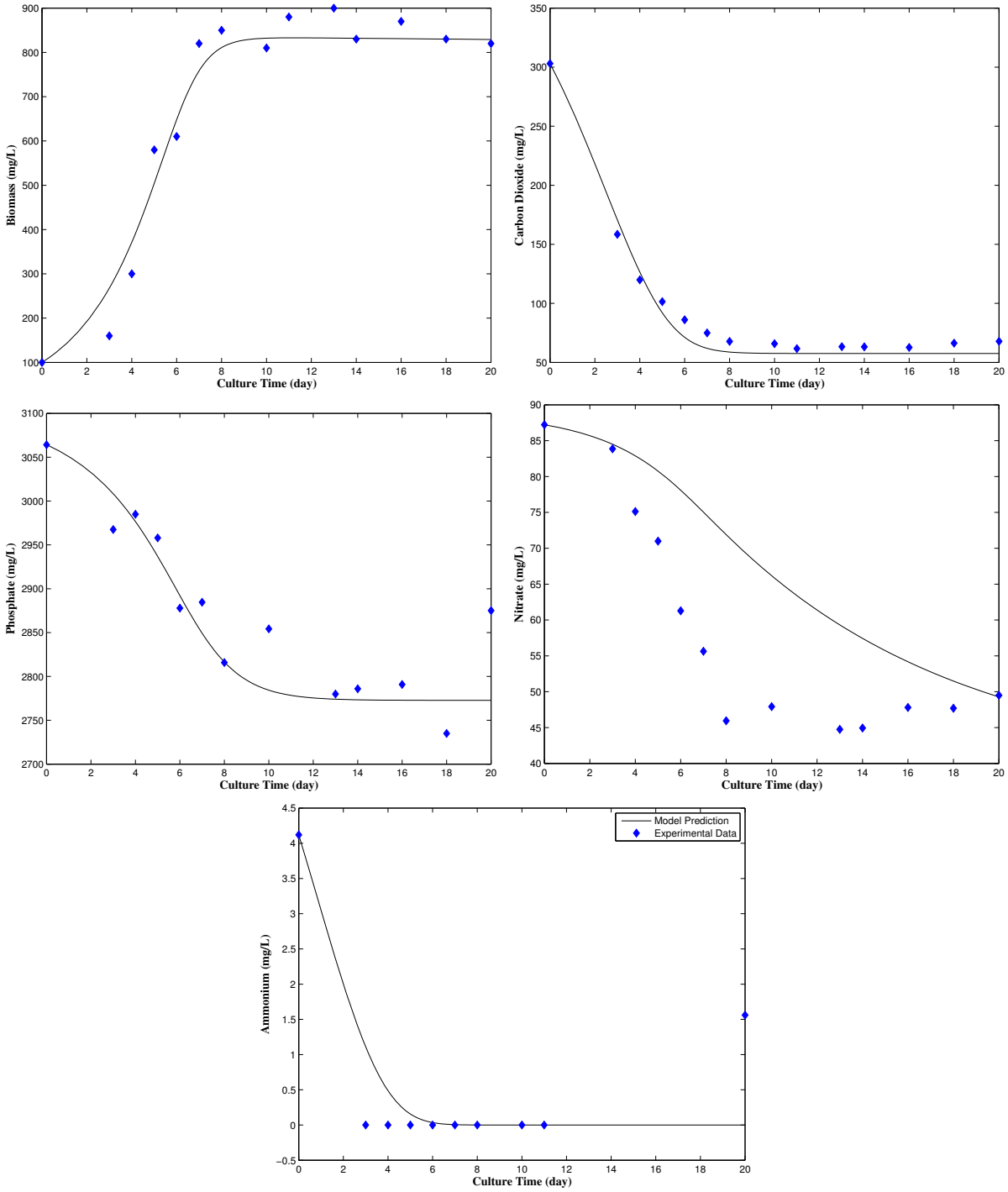

Figure 4.3: Validation of the model in flask 7 (conditions of low CO_2 concentration, high phosphate concentration and high light intensity)

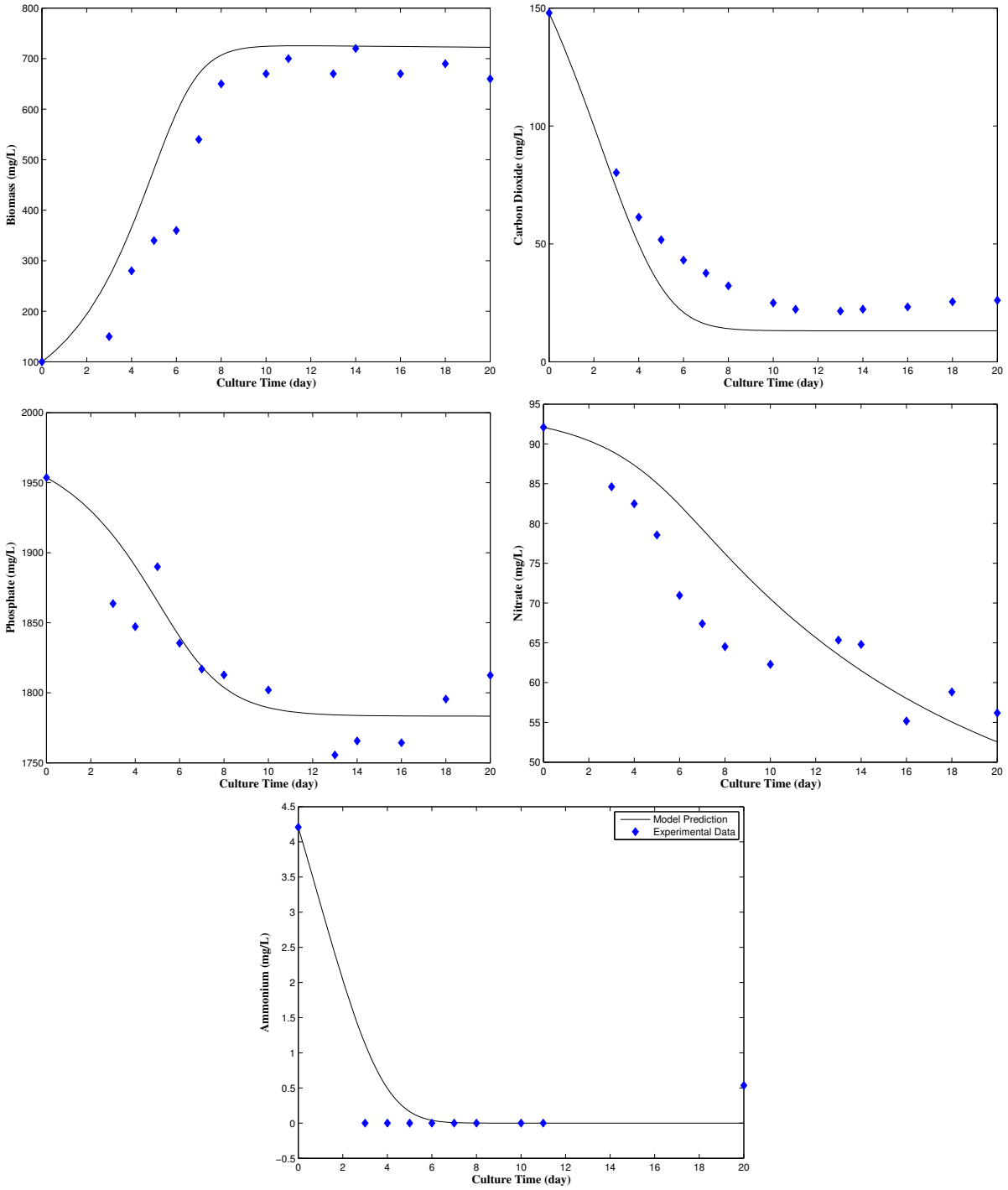

Figure 4.4: Validation of the model in flask 9 (conditions of very low CO_2 concentration, intermediate phosphate concentration and intermediate light intensity)

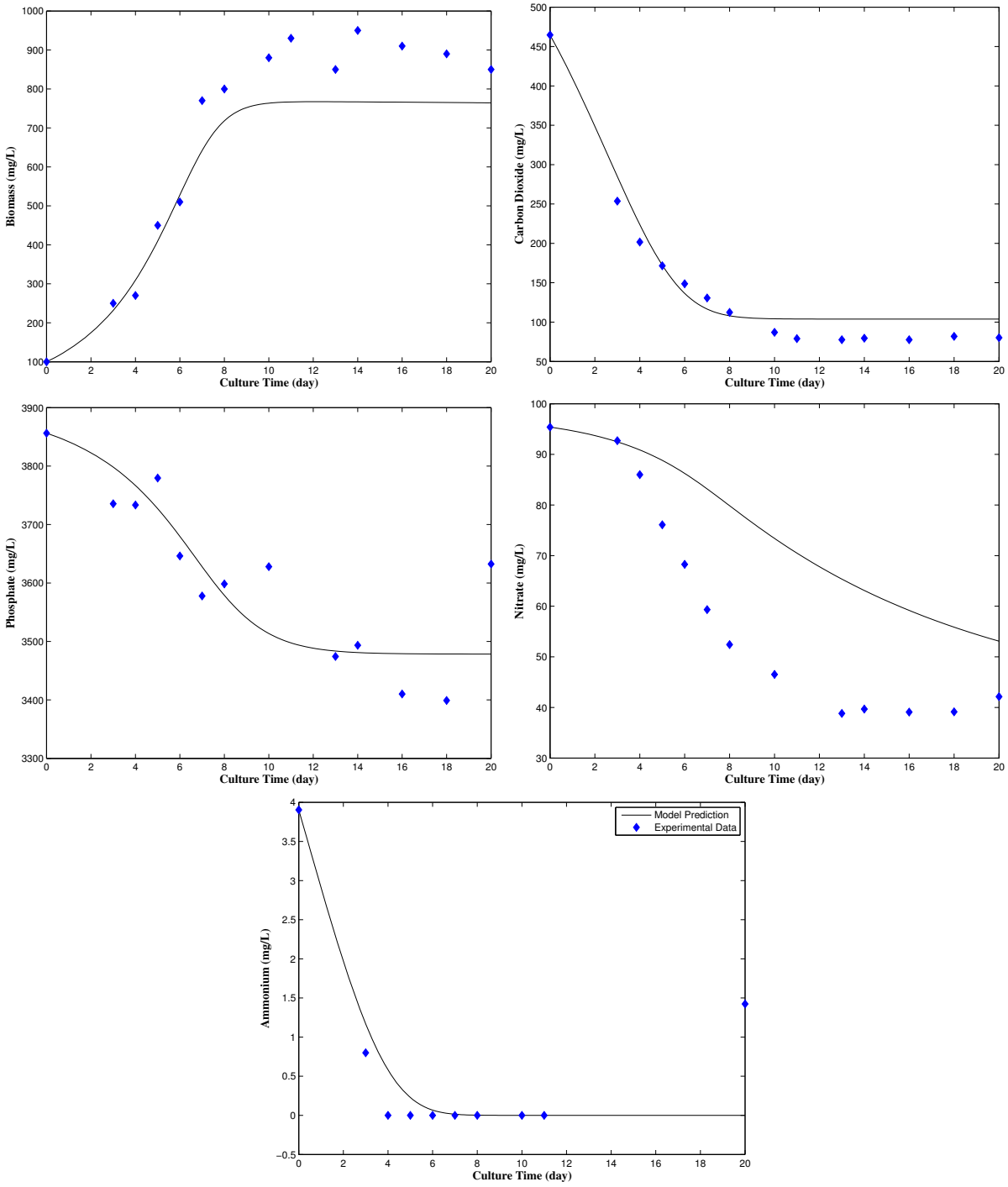

Figure 4.5: Validation of the model in flask 12 (conditions of intermediate CO_2 concentration, very high phosphate concentration and intermediate light intensity)

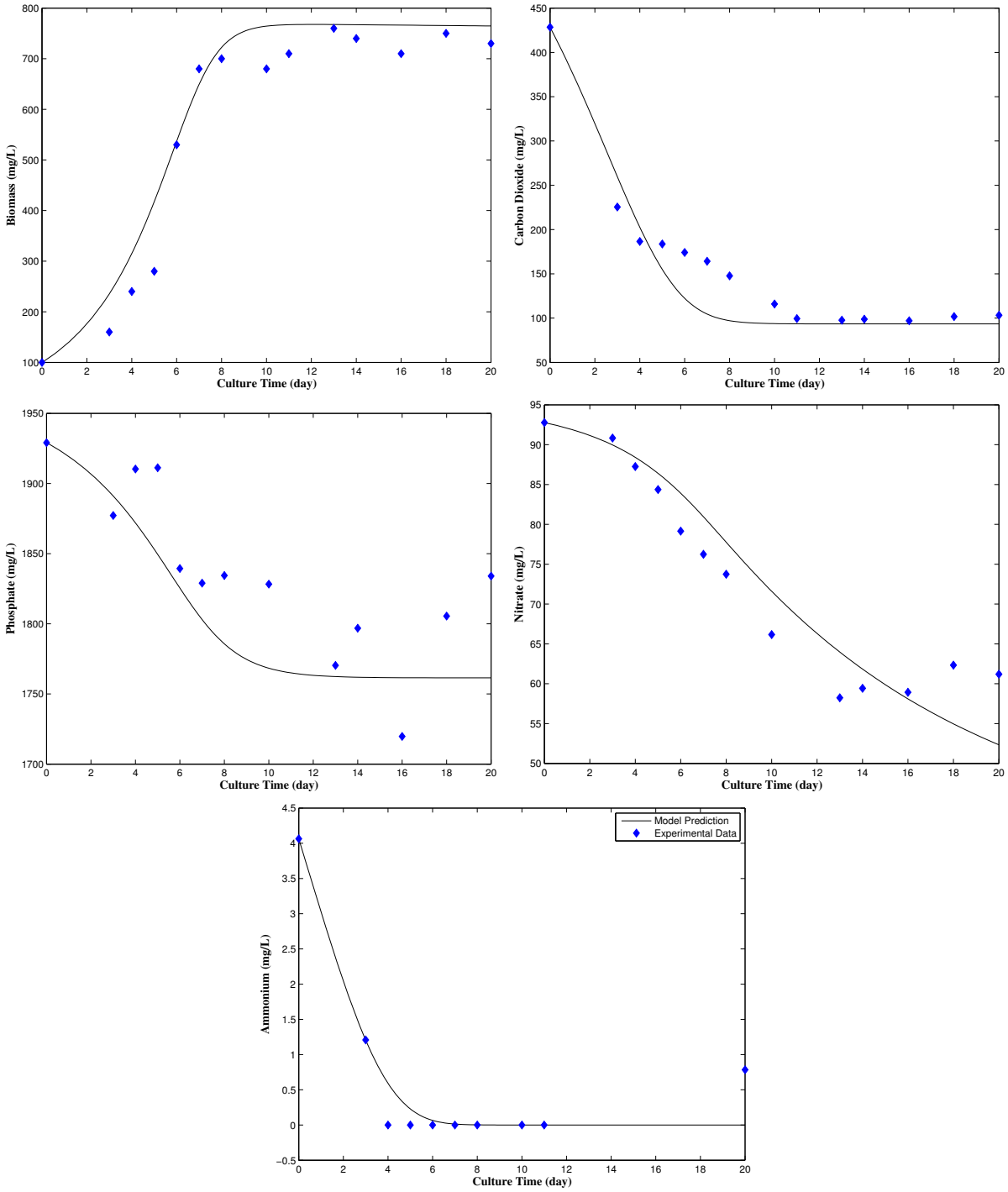

Figure 4.6: Validation of the model in flask 18 (conditions of intermediate CO_2 concentration, intermediate phosphate concentration and intermediate light intensity)

where ξ is a vector of manipulated variables including CO_2 concentration, phosphate concentration and light intensity. J is the objective function defined as:

$$J = [CO_2]_{t_0} - \frac{1}{t_f - t_0} \int_{t_0}^{t_f} [CO_2]_t \, dt \tag{4.41}$$

or

$$J = \frac{1}{t_f - t_0} \int_{t_0}^{t_f} X_t dt \tag{4.42}$$

where $[CO_2]_{t_0}$ is the initial concentration of CO_2, $[CO_2]_t$ is the concentration of CO_2 at each time step, X_t is the biomass concentration at each time step and t_f is a given culture time (21 days).

Note that *Chlorella kessleri* exhibited no growth at CO_2 concentrations above 42%. Also, due to limitations of our experimental apparatus, providing light intensity greater than 81 μmol photons.m^{-2}.s^{-1} was not possible. Therefore, beside the lower boundary constraints (ξ>0), there is an upper boundary constraint for CO_2 concentration and light intensity which can be handled by Eq. 4.12.

CO_2 Fixation

Considering CO_2 uptake as the objective function subjected to optimization results in optimal initial conditions of 42% CO_2, 29 mM phosphate and 81 μmol photons.m^{-2}.s^{-1} light intensity to achieve average CO_2 fixation of 477 mg/L over 21 days.

Algal Growth

The maximum biomass production is estimated to be 676 mg/L over 21 days. Also, the optimal CO_2, phosphate concentration and light intensity are found to be 16%, 30 mM

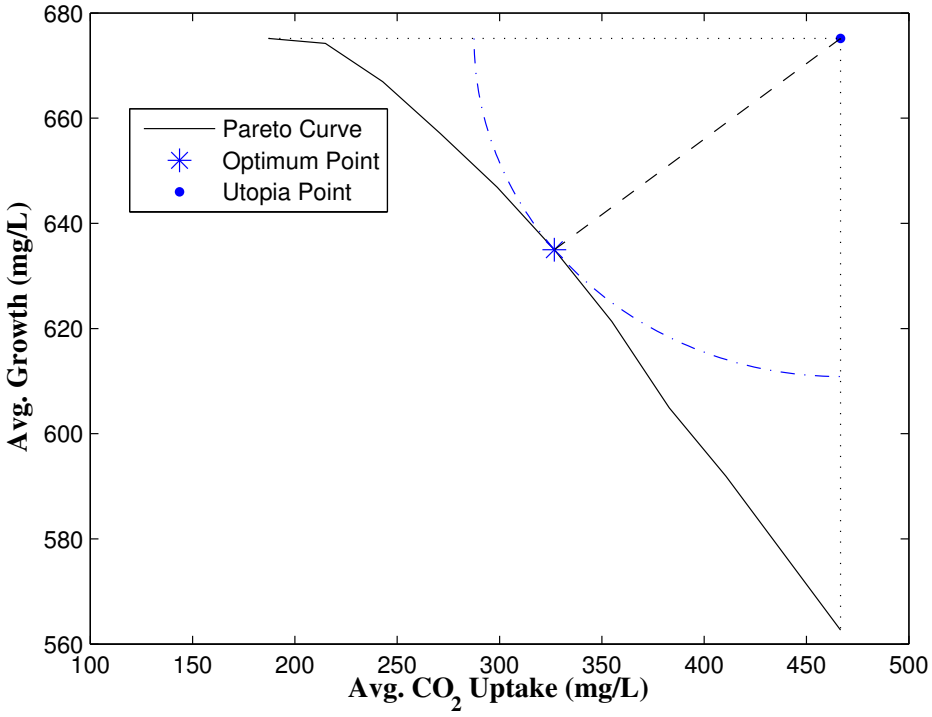

Figure 4.7: Pareto curve for CO_2 uptake and growth rate, the Pareto optimal set and the utopia point.

and 81 μmol photons.m^{-2}.s^{-1}, respectively.

Multi-objective Optimization

The ϵ-constraints method described in Section 4.2.7 was used to maximize CO_2 fixation and algal growth simultaneously.

A dynamic penalty function method proposed by Parsopoulos and Vrahatis (2002) was used to deal with the inequality constraints. In this study, the objective function is the algal growth that is subjected to an inequality constraint of CO_2 fixation ($g(x) \leq \epsilon$). Details of the penalty function used in this study based on the range of CO_2 fixation and ϵ and the problem requirements, are: 1) the function $h(.)$ is set to $h(k) = \sqrt{k}$ in

Eq. 4.14, where k is the algorithm's current iteration number; 2) In Eq. 4.15, $q(x) = max\{0; g(x)\}$. If $q(x)$<100, then $\gamma\,(q(x)) = 1$; if 100$\leq$ $q(x)$<500, then $\gamma\,(q(x)) = 5$; otherwise $\gamma\,(q(x)) = 10$. Further, if $q(x)$<100, then $\theta\,(q(x)) = 1$; if $q(x) \leq 200$, then $\theta\,(q(x)) = 100$; if $q(x) \leq 300$, then $\theta\,(q(x)) = 1000$, otherwise $\theta\,(q(x)) = 10000$.

The Pareto curve, the utopia point and the optimal Pareto set (*) are shown in Figure 4.7. To emphasize that this is, indeed, the closest point, a circle centered on the utopia point with a radius equal to length of the vector between the utopia point and the optimal Pareto set is drawn. Since no other points in the Pareto set appear within this circle, this point is the closest to the utopia point.

The optimal Pareto set is found to have an average CO_2 fixation of 327 mg/L and algal growth of 635 mg/L over 21 days. The $\xi(t_0)^*$ is estimated to be 28% initial CO_2, 32 mM phosphate concentration and 81 μmol photons.m^{-2}.s^{-1} light intensity.

It can be concluded that high phosphate concentrations and very high light intensities are required in order to maximize each of mentioned objective functions and the concentration of CO_2 plays an important role to maximize each individual objective function.

A normalized sensitivity analysis ($\frac{(\partial Y/Y)}{(\partial P/P)}$) has been performed on the model parameters to determine the effect of parameter values (P) on the average CO_2 fixation and algal growth (Y) at $\xi(t_0)^*$ (the initial condition). The significance of the effects of parameters on CO_2 fixation at this condition can be ordered as $\rho_{m_{CO_2}}$>μ_m>$K_{\rho_{CO_2}}$>$K_{I_{CO_2}}$>$K_{I_{PO_4^{-3}}}$> $K_{S_{PO_4^{-3}}}$>K_{S_I}>$K_{S_{CO_2}}$>k_d>$\rho_{m_{PO_4^{-3}}}$>$K_{\rho_{PO_4^{-3}}}$>$\rho_{m_{NH_4^+}}$>$K_{\rho_{NH_4^+}}$. Also, $\rho_{m_{NO_3^-}}$ and $K_{\rho_{NO_3^-}}$ have almost no effect on CO_2 fixation at these conditions. Similarly, the significance of the effects of parameters on algal growth can be written as μ_m>$\rho_{m_{CO_2}}$>$K_{\rho_{CO_2}}$>$K_{I_{CO_2}}$>$K_{I_{PO_4^{-3}}}$ >$K_{S_{PO_4^{-3}}}$>$K_{S_{CO_2}}$>K_{S_I}>k_d>$\rho_{m_{PO_4^{-3}}}$>$K_{\rho_{PO_4^{-3}}}$>$\rho_{m_{NH_4^+}}$>$K_{\rho_{NH_4^+}}$. $\rho_{m_{NO_3^-}}$ and $K_{\rho_{NO_3^-}}$ seem to have no effect on algal growth as well. Since nitrate concentration showed no significant effect on CO_2 uptake and algal growth, it has not been considered in our future investigations.

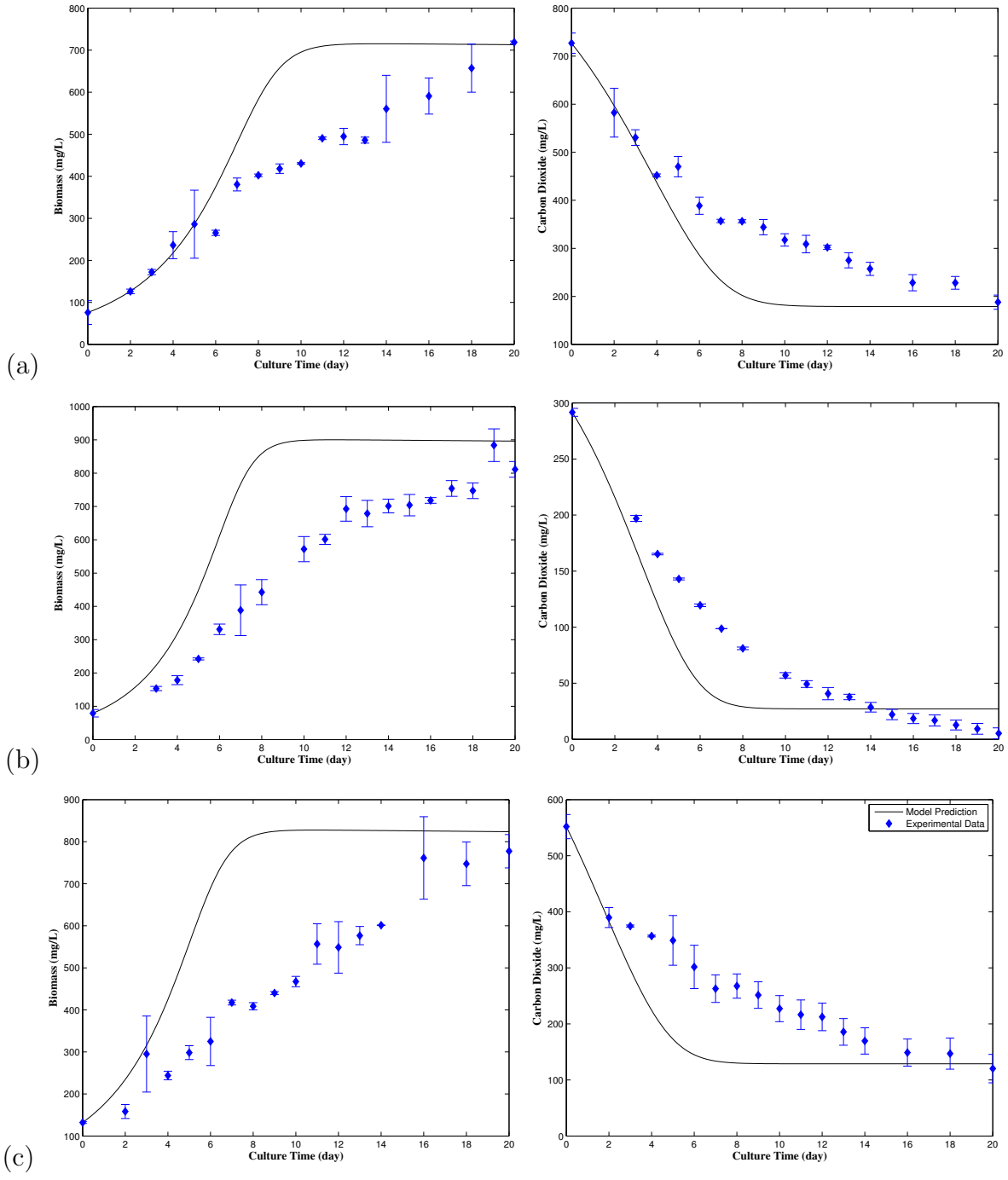

Figure 4.8: Model predictions and experimental data at (a) 42% CO_2, 29 mM phosphate and 81 μmol photons.m^{-2}.s^{-1} light intensity to maximize the CO_2 uptake; (b) 16% CO_2, 30 mM phosphate and 81 μmol photons.m^{-2}.s^{-1} light intensity to maximize the biomass ; (c) 28% CO_2, 32 mM phosphate and 81 μmol photons.m^{-2}.s^{-1} light intensity to simultaneously maximize the CO_2 uptake and algal growth over 21 days. Data are means $\pm$ one standard deviation of duplicate runs.

Validation of Optimal Points

A set of experiments with duplicate runs including three sets of initial conditions: 1) 42% CO_2, 29 mM phosphate and 81 μmol photons.m^{-2}.s^{-1} light intensity, 2) 16% CO_2, 30 mM phosphate and 81 μmol photons.m^{-2}.s^{-1} light intensity, and 3) 28% CO_2, 32 mM phosphate and 81 μmol photons.m^{-2}.s^{-1} light intensity, was performed to validate the optimal model predictions of CO_2 uptake, algal growth and the Pareto optimal set.

The model predictions and experimental data at these three initial conditions are presented in Figure 4.8. It can be concluded that the dynamics of CO_2 concentration can be adequately explained by the model; however, the experimental algal growth is slower than that predicted by the model at these conditions, although the final biomass concentration is very close to the model predictions in each condition. A number of factors could have contributed to this, including the fact that 1) OSPW is from the same pond but it was taken in a different year than the one used for the previous experiments; 2) The inoculation culture for *Chlorella kessleri* was different from the previous experiments; and 3) Providing exactly the same conditions as the base experiment is impossible.

4.4 Conclusions

The proposed mathematical model adequately described the algal growth, CO_2 uptake, phosphate uptake, nitrate uptake and ammonium uptake rate of *Chlorella kessleri* cultivated in oil sands process water (OSPW). The optimal initial CO_2 concentration, phosphate concentration and light intensity was determined using this nonlinear time varying model to maximize algal growth and CO_2 uptake over a period of 21 days. Moreover, a multi-objective optimization technique was used to maximize the CO_2 fixation and algal growth simultaneously. The maximum average CO_2 uptake of 477 mg/L was obtained at very high CO_2 concentration and light intensity and at high phosphate concentration.

Also, low CO_2 concentrations, high phosphate concentrations and very high light intensity maximized algal growth to 676 mg/L. Finally, the Pareto optimization resulted in CO_2 uptake of 327 mg/L and algal growth of 635 mg/L at intermediate CO_2 concentration, high phosphate concentration and very high light intensity. In the next chapter, a raceway photobioreactor (as it is the most feasible and the foremost reactor configuration for large-scale cultivation of microalgal biomass (Mata et al., 2010)) is designed and built to calculate the optimal feeding strategy for fed-batch operation at larger scales.

4.5 References

Bastin, G., Dochain, D., 1990. On-line estimation and adaptive control of bioreactors. Elsevier, Amsterdam.

Bechet, Q., Shilton, A., Guieysse, B., 2013. Modeling the effects of light and temperature on algae growth: State of the art and critical assessment for productivity prediction during outdoor cultivation. Biotechnology Advances 31, 1648–1663.

Bernard, O., 2011. Hurdles and challenges for modelling and control of microalgae for CO_2 mitigation and biofuel production. Journal of Process Control 21, 1378–1389.

Bordel, S., Guieysse, B., Munoz, R., 2009. Mechanistic model for the reclamation of industrial wastewaters using algal-bacterial photobioreactors. Environmental Science and Technology 43, 3200–3207.

Cabrera, J.C.F., Coello, C.A.C., 2007. Handling constraints in particle swarm optimization using a small population size. Lecture Notes in Computer Science (including subseries Lecture Notes in Artificial Intelligence and Lecture Notes in Bioinformatics) 4827 LNAI, 41–51.

Caperon, J., Meyer, J., 1972. Nitrogen-limited growth of marine phytoplankton-II. uptake kinetics and their role in nutrient limited growth of phytoplankton. Deep-Sea Research and Oceanographic Abstracts 19, 619–632.

Cheng, J., Huang, Y., Feng, J., Sun, J., Zhou, J., Cen, K., 2013. Improving CO_2 fixation efficiency by optimizing *Chlorella* PY-ZU1 culture conditions in sequential bioreactors. Bioresource Technology 144, 321–327.

Chu, W., Gao, X., Sorooshian, S., 2011. Handling boundary constraints for particle swarm optimization in high-dimensional search space. Information Sciences 181, 4569–4581.

Droop, M.R., 1973. Some thoughts on nutrient limitation in algae. Journal of Phycology 9, 264–272.

Eaton, A.D., Greenberg, A.E., Clesceri, L.S., 1999. Standard methods for the examination of water and wastewater. American Public Health Association Publications. 20^{th} edition.

Flynn, K.J., 2001. A mechanistic model for describing dynamic multi-nutrient, light, temperature interactions in phytoplankton. Journal of Plankton Research 23, 977–997.

Geider, R.J., MacIntyre, H.L., Kana, T.M., 1996. A dynamic model of photoadaptation in phytoplankton. Limnology and Oceanography 41, 1–15.

Geider, R.J., MacIntyre, H.L., Kana, T.M., 1997. Dynamic model of phytoplankton growth and acclimation: Responses of the balanced growth rate and the chlorophyll a:carbon ratio to light, nutrient-limitation and temperature. Marine Ecology Progress Series 148, 187–200.

Geider, R.J., MacIntyre, H.L., Kana, T.M., 1998. A dynamic regulatory model of phytoplanktonic acclimation to light, nutrients, and temperature. Limnology and Oceanography 43, 679–694.

Haario, H., Kalachev, L., Laine, M., 2009. Reduced models of algae growth. Bulletin of Mathematical Biology 71, 1626–1648.

Ho, S.H., Chen, C.Y., Chang, J.S., 2012. Effect of light intensity and nitrogen starvation on CO_2 fixation and lipid/carbohydrate production of an indigenous microalga *Scenedesmus obliquus* cnw-n. Bioresource Technology 113, 244–252.

de la Hoz Siegler, H., Ben-Zvi, A., Burrell, R.E., McCaffrey, W.C., 2011. The dynamics of heterotrophic algal cultures. Bioresource Technology 102, 5764–5774.

Jassby, A.D., Platt, T., 1976. Mathematical formulation of the relationships between photosynthesis and light for phytoplankton. Limnology and Oceanography 21, 540–547.

Kasiri, S., Abdulsalam, S., Ulrich, A., Prasad, V., 2014a. Optimization of CO_2 fixation by *Chlorella kessleri* using response surface methodology (submitted) .

Kasiri, S., Prasad, V., Ulrich, A., 2014b. Strain and factor selection for carbon dioxide fixation using microalgae cultivated in oil sands process water. Canadian Journal of Chemical Engineering, *in press* (DOI: 10.1002/cjce.22055) .

Kasprzak, E.M., Lewis, K.E., 2000. Pareto analysis in multiobjective optimization using the colinearity theorem and scaling method. Structural and Multidisciplinary Optimization 22, 208–218.

Kennedy, J., Eberhart, R., 1995. Particle swarm optimization. IEEE International Conference on Neural Networks - Conference Proceedings 4, 1942–1948.

Kern, D.M., 1960. The hydration of carbon dioxide. Journal of Chemical Education 37, 14–23.

Mahdavi, H., Ulrich, A.C., Liu, Y., 2012. Metal removal from oil sands tailings pond water by indigenous micro-alga. Chemosphere 89, 350–354.

Mata, T.M., Martins, A.A., Caetano, N.S., 2010. Microalgae for biodiesel production and other applications: A review. Renewable and Sustainable Energy Reviews 14, 217–232.

Myers, R., Montgomery, D., 2002. Response surface methodology: Product and process optimization using designed experiments. John Wiley and Sons, New York. 2^{nd} edition.

Niu, B., Wang, H., Wang, J., Tan, L., 2013. Multi-objective bacterial foraging optimization. Neurocomputing 116, 336–345.

Packer, A., Li, Y., Andersen, T., Hu, Q., Kuang, Y., Sommerfeld, M., 2011. Growth and neutral lipid synthesis in green microalgae: A mathematical model. Bioresource Technology 102, 111–117.

Parsopoulos, K., Vrahatis, M., 2002. Particle swarm optimization method for constrained optimization problems. Proceedings of the 2nd Euro-International Symposium on Computational Intelligence, Kosice, Slovakia , 214–220.

Pic-Marco, E., Navarro, J.L., Bruno-Barcena, J.M., 2006. A closed loop exponential feeding law: Invariance and global stability analysis. Journal of Process Control 16, 395–402.

Post, A.F., De Wit, R., Mur, L.R., 1985. Interactions between temperature and light intensity on growth and photosynthesis of the cyanobacterium *Oscillatoria agardhii*. Journal of Plankton Research 7, 487–495.

Wang, L., 2006. Recommendations for Design Parameters for Central Composite Designs with Restricted Randomization. Ph.D. thesis. Virginia Polytechnic Institute and State University, USA.

Zhang, W., Xie, X.F., Bi, D.C., 2004. Handling boundary constraints for numerical optimization by particle swarm flying in periodic search space. Proceedings of the 2004 Congress on Evolutionary Computation, CEC2004 2, 2307–2311.

Chapter 5

Optimization of CO_2 Fixation by *Chlorella kessleri* in a Closed Raceway Photo-bioreactor

5.1 Introduction

The optimization of CO_2 fixation by microalgae is difficult due to the lack of appropriate mathematical models describing the dynamics of CO_2 in microalgal cultures. Most of the modeling studies carried out so far have focused on the influence of culture conditions and nutrient avalability on biomass growth (Geider et al., 1998; Flynn, 2001; Packer et al., 2011; Costache et al., 2013; Pruvost et al., 2011; Sforza et al., 2014). For example, Costache et al. (2013) developed an overall model that allows the simulation of the photosynthesis rate under different culture conditions (irradiance, temperature, pH, and dissolved oxygen). The model has then been validated against experimental data obtained at different culture conditions. Sforza et al. (2014) developed a mathematical model to explain the biomass concentration and irradiation in a photobioreactor. Bernard and Remond (2012) also developed a model to describe the effect of temperature and light on microalgal growth, and predict productivity in outdoor photobioreactors or raceways. Using the bioprocess model, the evolution of states and inputs can be deter-

mined and used for optimization. He et al. (2012) developed a kinetic model for algal CO_2 utilization to describe the CO_2 uptake and algal growth as a function of CO_2 and light intensity in a fed-batch culture, and then determined the dynamic CO_2 inlet partial pressure using control vector parameterization to optimize the growth of algae fed by flue gases. A more complex model containing a set of six differential equations was proposed by de la Hoz Siegler et al. (2011) to model growth and oil production rates as a function of carbon and nitrogen sources in a photobioreactor. Later, de la Hoz Siegler et al. (2012) determined the optimal feeding strategies that maximize algal growth and experimentally compared the performance of the model-based optimization strategies against the performance of non-optimal fed-batch and batch cultures. Also, Abdollahi and Dubljevic (2012) established an optimal feeding strategy for lipid production using a state-of-the-art interior point optimizer (IPOPT) solver for the model developed by de la Hoz Siegler et al. (2011).

Reactor configuration and cultivation techniques to improve biomass growth with flue gas have also received attention in the literature (Kumar et al., 2010; Schenk et al., 2008; Zhao et al., 2011). Generally, there are two environments used for the cultivation of microalgae: open raceway ponds and closed photobioreactors. Open ponds are easy and inexpensive to construct and operate, although they are limited in the ability to control culture conditions and have a high risk of culture contamination. On the other hand, closed photobioreactors allow for better control of the cultivation conditions than open systems (Sanchez et al., 2011). For example, Zhao et al. (2011) reported that the specific growth rate and CO_2 fixation rate of *Chlorella* sp. in aerated closed cultivation were 1.78 and 5.39 times of those in the open cultivation, respectively. For that reason, we have designed and built a closed raceway photobioreactor aerated with different concentrations of CO_2 for *Chlorella kessleri* cultivation in OSPW; this allowed us to have better control on culture conditions and also be able to monitor CO_2 dynamics in the photobioreactor.

In addition, the raceway bioreactor operates under conditions that are directly scalable to large-scale installation (Brennan and Owende, 2010; James and Boriah, 2010; Sanchez et al., 2011; Schenk et al., 2008; Singh and Dhar, 2011). The changes in algal growth, medium composition (phosphate, ammonium, dissolved CO_2, dissolved O_2, pH and alkalinity) and gas content (CO_2 concentration) at the inlet and outlet were monitored in fed-batch cultures over a period of 18 days (432 h). The experimental data generated was used to modify a nonlinear kinetic model developed by us for batch cultures of *Chlorella kessleri* in OSPW, include mass transfer and flow considerations, and develop a model for the closed bench-scale raceway photobioreactor. The model considers the dilution rate due to inlet streams and includes the effect of outlet flow (sampling). It also considers CO_2 mass transfer between liquid and gas phase. A model-based optimization method was then applied to calculate the optimal feeding strategies for CO_2 and phosphate and light intensity to maximize biomass growth and CO_2 fixation.

To the best of our knowledge, this is the first study that optimizes CO_2 fixation by microalgae grown in OSPW under scalable fed-batch conditions.

5.2 Materials and Methods

5.2.1 Strain and Media Composition

Chlorella kessleri was obtained from our laboratory culture collection (Mahdavi et al., 2012). Since *Chlorella kessleri* is indigenous to OSPW, it is maintained in this environment and no other media is used. The OSPW medium was made of 100% OSPW, phosphate (KH_2PO_4, 1mM) and ammonium (NH_4Cl, 1mM). Phosphate and ammonium were added to provide phosphorus and nitrogen, the most important nutrients required for microalgal growth.

5.2.2 Equipment Design and Process Condition

Raceway Photobioreactor

The bench-scale raceway photobioreactor was fabricated out of plexiglass (poly methyl methacrylate) with the thickness of 0.5 cm. The size of the photobioreactor and the central partition is shown in Figure 5.1. The bioreactor set up shown in Figure 5.2 consists of:

Paddlewheel: A paddlewheel made of plexiglass is used to recirculate the biomass and the growth media (nutrients and OSPW) to avoid concentration gradients and the shadowing effect of the microalgae cells (Sanchez et al., 2011). The movement is produced by a US425-401U2/4GN25RAA speed control AC motor (Oriental Motor, Tokyo, Japan). The speed can be controlled from 3.6 to 64 rpm. Mixing is obtained by a combination of the motion of the paddlewheel and the interaction of the flow with the bottom and sides of the raceway.

Sensors: There are five sensors located inside the photobioreactor; each is immersed in the culture. A Mettler Toledo Ingold 5000i dissolved CO_2 probe (Mississauga, Ontario, Canada) is used to measure the concentration of dissolved CO_2 in the culture, a Mettler Toledo Ingold 6850i dissolved O_2 probe (Mississauga, Ontario, Canada) is used to monitor the concentration of dissolved O_2, a Mettler Toledo Ingold 3253i pH/Temp probe (Mississauga, Ontario, Canada) is used to measure the pH and temperature of the culture, and Gems ELS-900 high and low level sensors (Plainville, Connecticut, USA) are used to monitor the level of the algal culture and prevent any overflow or low level in the bioreactor.

Heater: A Marina mini 50 W submersible aquarium heater (Montreal, Quebec, Canada) is used to control the temperature of the algal culture based on the temperature indicated by pH/Temp probe.

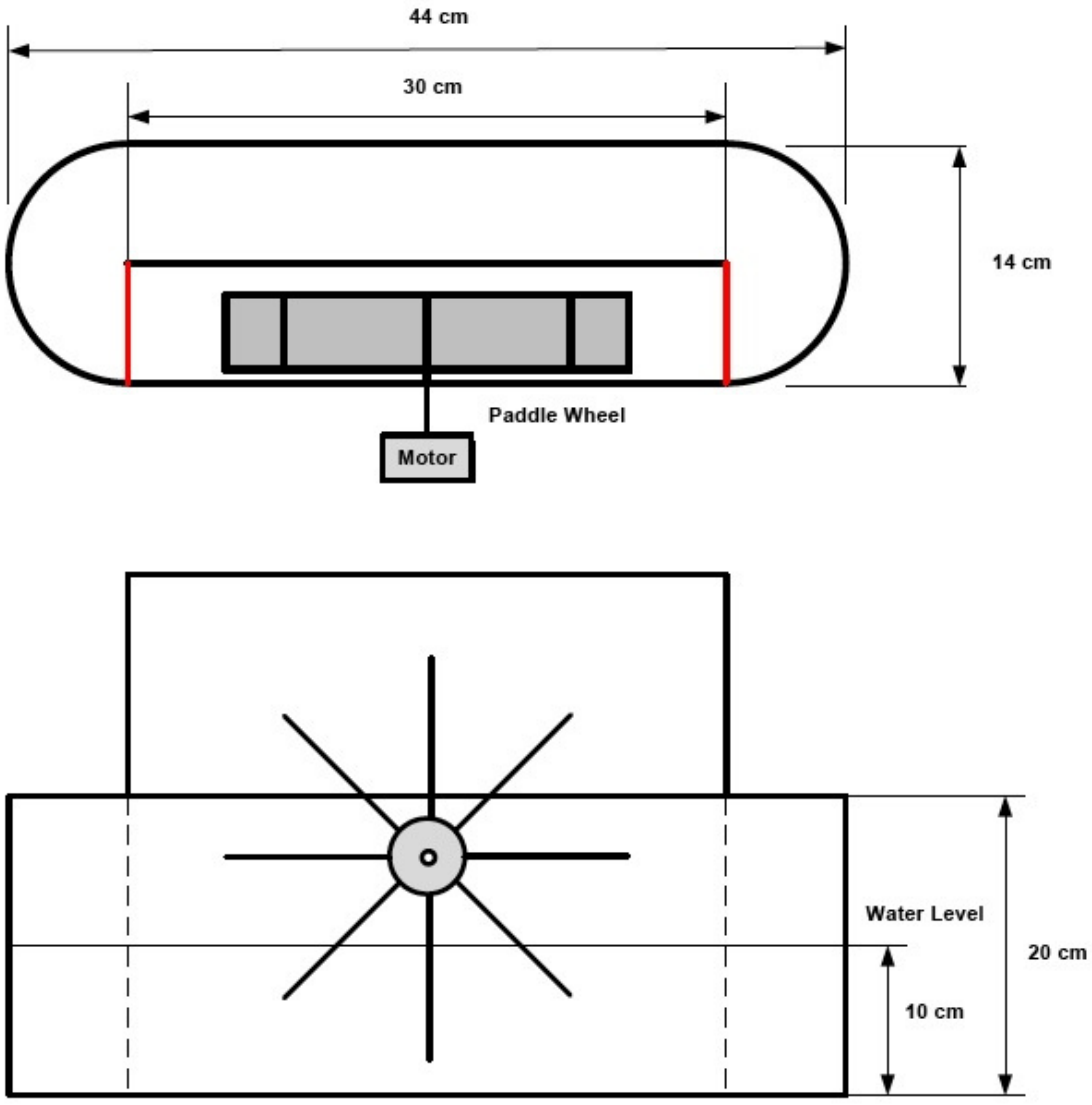

Figure 5.1: Top and side views of the closed raceway photobioreactor

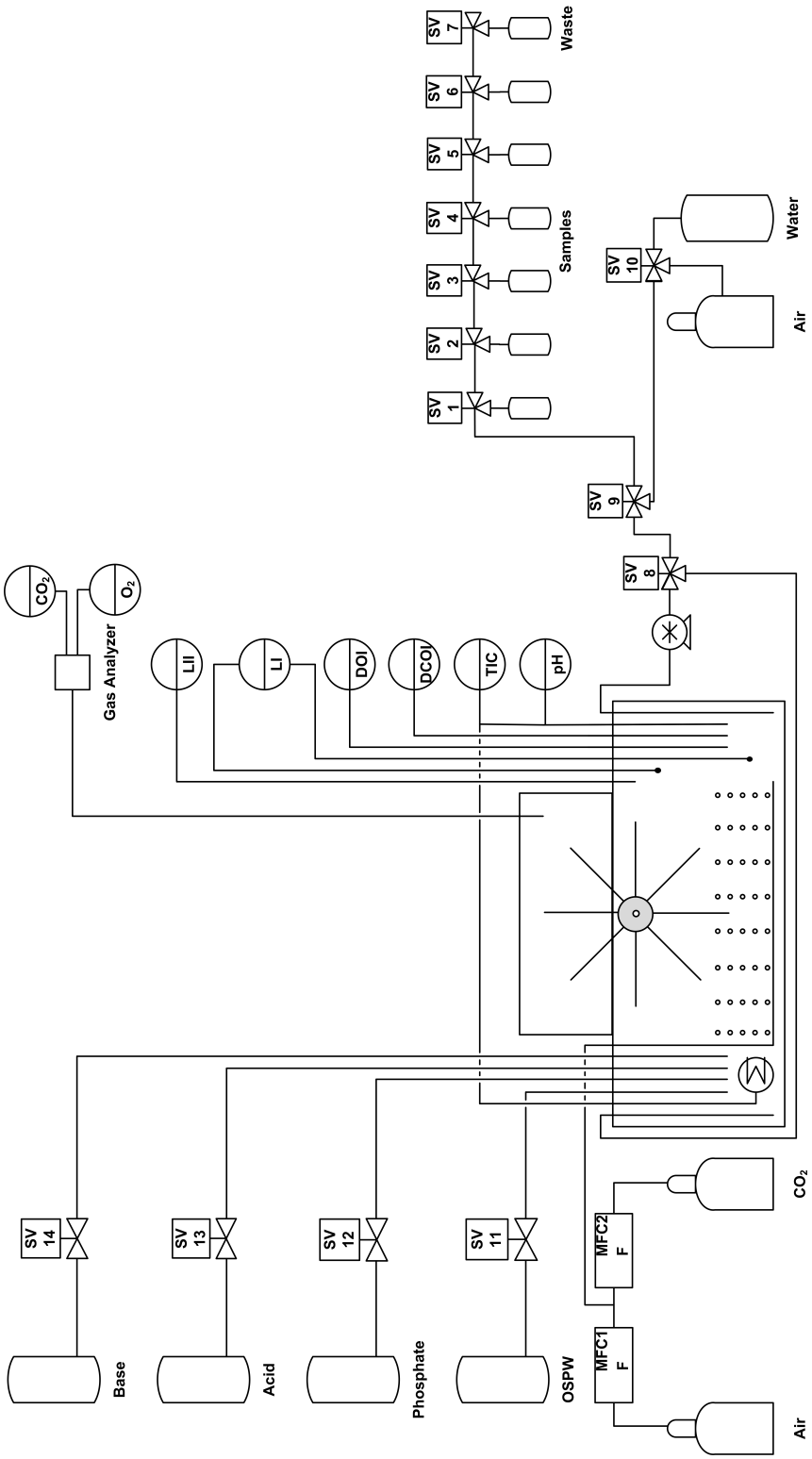

Figure 5.2: Process and instrumentation diagram for the closed raceway photobioreactor

Lighting System: The lighting system is located over the pond. This system consists of two high power LED strips (LED Supply, Randolph, Vermont, USA) with controllable dimmers to change the light intensity between 0 and 140 μmol photons.m^{-2}.s^{-1}. The light intensity is measured using a Sper Scientific Light Meter LUX/FC model 840020 (Scottsdale, Arizona, USA).

Inlet Streams: There are four liquid inlet streams and one gas inlet. The liquid streams are controlled by four two-way normally closed solenoid pinch valves (Cole-Parmer, Montreal, Quebec, Canada). The first stream contains OSPW to feed a fresh medium to the culture and also compensate for the amount taken for sampling; the second stream contains phosphate to be able to manipulate the concentration of phosphate in the culture; the third and fourth streams contain acid and base to control the pH of the culture. As shown in Figure 5.2, a mixture of air and CO_2 with a flowrate of 500 mL/min is sparged from the bottom of the pond to create bubbles. The gas mixture is regulated by two Brooks Instrument SLA 5800 series thermal mass flow controllers (Hatfield, Pennsylvania, USA) to provide different concentrations of CO_2 varying from 0.03 to 10%.

Outlet Stream: The gas outlet stream from the top of the photobioreactor is pumped (500 mL/min) to the Rapidox 3100ZA CO_2 and O_2 gas analyzer (Cambridge Sensotec Ltd., Cambridgeshire, United Kingdom) to monitor the composition of the outlet gas.

Auto-Sampling Line: An auto-sampler was built using a Masterflex peristaltic pump (C/L variable-speed pump, Cole-Parmer, Montreal, Quebec, Canada), six two-way normally closed, one two-way normally open solenoid pinch valves (Cole-Parmer, Montreal, Quebec, Canada) and three three-way solenoid pinch valves (Cole-Parmer, Montreal, Quebec, Canada) to take 15 mL of sample every 4 h and store it in a refrigerator at 4°C for further analysis. Recycling starts 5 min before each sampling to pump a part of the algal culture from tank to tank and after 5 min pump to the sampling tube. The culture

usually is fed ahead of the paddlewheel and is sampled behind the paddlewheel (James and Boriah, 2010). The full sample tubes are then replaced by empty tubes every day.

Data Acquisition and Control System: A National Instrument data acquisition system (Austin, Texas, USA) was used to log the output from all sensors, analyzers, and mass flow controllers every 5 min and to manipulate the inputs. National Instrument LabView programming (Austin, Texas, USA) was used to interface the computer to the experimental apparatus and manipulate and regulate variables and conditions.

5.2.3 Fed-Batch Experiment

Fed-batch experiments were conducted in the raceway photobioreactor. OSPW medium was used as the start-up medium; also every 1 h, 6 mL of fresh medium was added to the raceway photobioreactor to replenish the culture and replace the amount withdrawn during sampling. CO_2 and phosphate were added in two different streams as nutrients. The first stream contained air enriched with stepwise changes in concentration of CO_2. The second stream contained KH_2PO_4 at a concentration of 1 mM. Also, light, which is another important component for algal photosynthesis, was provided to the culture at regular intervals. The periodic feeding profiles of CO_2 and phosphate along with light intensity are presented in Figure 5.3. As shown in this figure, the concentration of CO_2 at the inlet was changed in very short time intervals. The first section of this periodic feeding (day 3-4) indicates 30 min injection of air enriched with 15% CO_2 and then 90 min injection of air. The second section (day 4-5) indicates shorter time intervals of 5 min injection of air enriched with 15% CO_2 and then 15 min injection of air. A 12 mL dose of phosphate feed was added at once every 100 min on day 12 and can be considered to be an impulse excitation. Also, light intensity profile exhibits light/dark cycle of 16/8 h from day 7 to day 10.

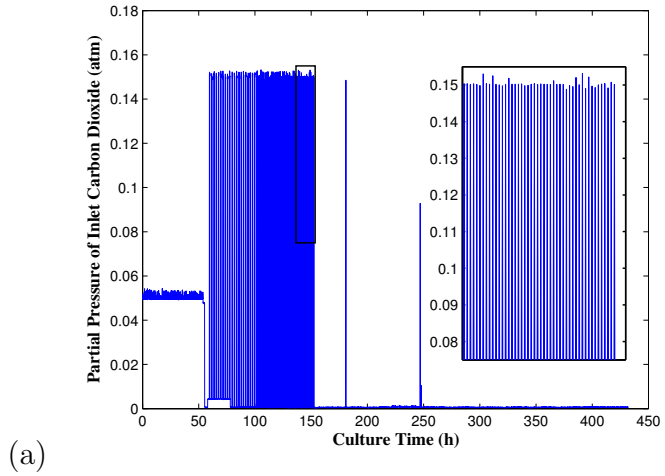

(a)

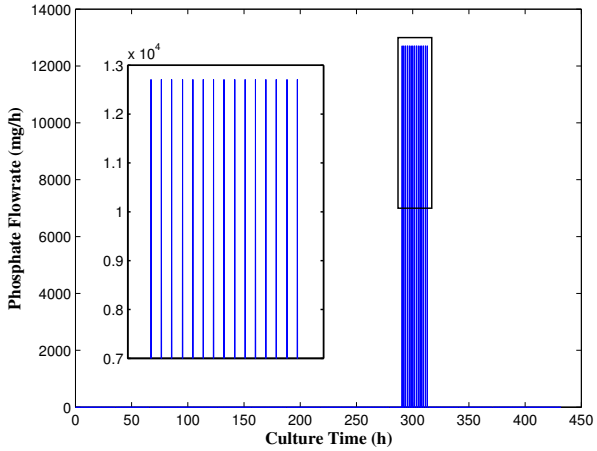

(b)

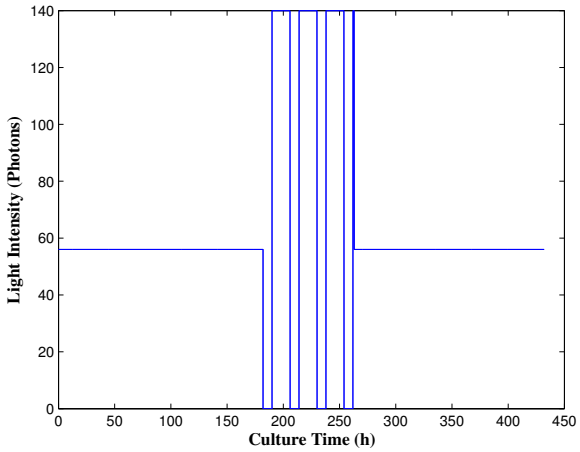

(c)

Figure 5.3: Periodic feeding profiles, (a) CO_2; (b) phosphate; (c) light intensity

The level of the medium in the bioreactor was set to 10 cm to provide the light more homogeneously to the microalgae, and the temperature of the bioreactor was controlled at 23±0.5°C; the speed of the electric motor was kept constant at 20 rpm.

5.2.4 Analytical Methods

Growth Analysis: Biomass concentration was determined as total suspended solids (TSS) by centrifuging 12 mL of cell suspension with a relative centrifugal force (RCF) of 2500g for 15 min. The pellets were washed with autoclaved Milli-Q water and recentrifuged. The final precipitate was dried at 105°C for 24 hours and then weighed by a Mettler Toledo XP205 microbalance (Mississauga, Ontario, Canada).

Water Chemistry: A 500μL sample of clear supernatant from the centrifugation was used to determine the amount of phosphate and nitrate using Dionex ICS-2100 Ion Chromatography with an IonPac AS18 hydroxide-selective anion-exchange column (Dionex, Sunnyvale, CA, USA). The amount of ammonium was measured using the colorimetric methods of 4500-NH_3 and 4500-NO_3 (Eaton et al., 1999) in the Biogeochemical Analytical Service Laboratory (BASL) at the University of Alberta. The alkalinity of the cell-free supernatant was measured by titration with a 0.02 N H_2SO_4 solution using a Mettler Toledo DL53 titrator (Mississauga, Ontario, Canada).

5.3 Results and Discussion

5.3.1 Model Formulation

The data obtained from the experiment with the periodic feeding strategy was used to develop a mathematical model that can describe the dynamics of biomass, dissolved CO_2, phosphate and ammonium in a fed-batch photobioreactor.

Kinetics

As mentioned before, a nonlinear kinetic model was developed by us in a previous study based on data from batch cultures (Chapter 4) (Kasiri et al., 2014c). In this study, the same kinetic expressions were used for describing the algal growth rate and CO_2, phosphate and ammonium uptake rates since they have already been validated. The important details of the expressions are reported here for clarity of exposition:

Specific Growth Rate:

$$\mu = \mu_m \frac{[dCO_2] - [dCO_2]_0}{K_{S_{dCO_2}} + [dCO_2] - [dCO_2]_0 + [dCO_2]^2 / K_{I_{dCO_2}}} \frac{\left[PO_4^{-3}\right]}{K_{S_{PO_4^{-3}}} + \left[PO_4^{-3}\right] + \left[PO_4^{-3}\right]^2 / K_{I_{PO_4^{-3}}}} \frac{I}{K_{S_I} + I} \tag{5.1}$$

where μ is the specific growth rate, μ_m is the maximum growth rate, $[dCO_2]$ is the concentration of dissolved CO_2 (mg/L), $[dCO_2]_0$ is the dissolved CO_2 concentration at which the uptake rate is zero, $K_{S_{dCO_2}}$ is the half-substrate saturation constant, $K_{I_{CO_2}}$ is an inhibition parameter, $\left[PO_4^{-3}\right]$ is the concentration of PO_4^{-3} (mg/L), $K_{S_{PO_4^{-3}}}$ is the half-substrate saturation constant, $K_{I_{PO_4^{-3}}}$ is the inhibition parameter, I is the light intensity (μmol photons.m^{-2}.s^{-1}) and K_{S_I} is the half-light saturation constant.

CO_2 Uptake Rate:

$$\rho_{dCO_2} = -\rho_{m_{dCO_2}} \frac{[dCO_2] - [dCO_2]_0}{K_{\rho_{dCO_2}} + [dCO_2] - [dCO_2]_0} \tag{5.2}$$

where ρ_{dCO_2} is the uptake rate of dissolved CO_2, $\rho_{m_{dCO_2}}$ is the maximum uptake rate of dissolved CO_2, $K_{\rho_{dCO_2}}$ is the uptake half-saturation constant of dissolved CO_2.

Phosphate Uptake Rate:

$$\rho_{PO_4^{-3}} = -\rho_{m_{PO_4^{-3}}} \frac{\left[PO_4^{-3}\right] - \left[PO_4^{-3}\right]_0}{K_{\rho_{PO_4^{-3}}} + \left[PO_4^{-3}\right] - \left[PO_4^{-3}\right]_0} \tag{5.3}$$

where $\rho_{PO_4^{-3}}$ is the uptake rate of phosphate, $\rho_{m_{PO_4^{-3}}}$ is the maximum uptake rate of phosphate and $K_{\rho_{PO_4^{-3}}}$ is the uptake half-saturation constant of phosphate and $\left[PO_4^{-3}\right]_0$ is the phosphate concentration at which the uptake rate is zero.

Ammonium Uptake Rate:

$$\rho_{NH_4^+} = -\rho_{m_{NH_4^+}} \frac{\left[NH_4^+\right]}{K_{\rho_{NH_4^+}} + \left[NH_4^+\right]} X \tag{5.4}$$

where $\rho_{NH_4^+}$ is the uptake rate of ammonium, $\rho_{m_{NH_4^+}}$ is the maximum uptake rate of ammonium and $K_{\rho_{NH_4^+}}$ is the uptake half-saturation constant of ammonium.

Fed-Batch Culture Considerations

Liquid Inlet Streams: OSPW medium and phosphate feeds were added to the photobioreactor and diluted the culture. This dilution rate was considered in formulating the model and is defined as:

$$D = \frac{Q_1^{In} + Q_2^{In}}{V} \tag{5.5}$$

where Q_1^{In} is the volumetric flow rate of the OSPW, Q_2^{In} is the volumetric flow rate of the phosphate stream and V is the working volume of the photobioreactor.

CO_2 Inlet Stream: CO_2 significantly affects the algal growth in the photobioreactors and it is dynamically exchanged between different phases and chemical forms. In order to explain the dynamics of CO_2 exchange between the liquid and gas phases and its

hydration, we have modified a model developed by Nedbal et al. (2010). This is coupled with our expression for the uptake of CO_2 by microalgae to explain fully the behavior of CO_2 in the photobioreactor. The model considers mass transfer from a stream of bubbles of air enriched with CO_2 and the photobioreactor headspace to the algal culture. It also includes the hydration of dissolved CO_2 to bicarbonate ions. In this study the above model was modified to become:

$$\begin{aligned}\frac{d\left[dCO_2\right]}{dt} = &- \rho_{dCO_2} X + \frac{J}{RT}\frac{h}{V}\left(\frac{P_{CO_2}^{In}}{h} - \left[dCO_2\right]\right)\left\{1 - exp\left[-\left(\frac{k_L a_B RT}{h}\tau\right)\right]\right\} \\ &+ k_L \frac{S_H}{V}\left(\frac{P_{CO_2}^{Out}}{h} - \left[dCO_2\right]\right) + l\left[HCO_3^-\right]\left[H^+\right] - k\left[dCO_2\right] \\ &+ \frac{Q_1^{In}}{V}\left[dCO_2\right]^{In} - D\left[dCO_2\right] \end{aligned} \tag{5.6}$$

where X is the biomass concentration, J is the aeration rate (L/min), R is the universal gas constant (L.atm/K.mol), T is the temperature (K), h is the Henry's constant (L.atm/mg), $P_{CO_2}^{In}$ is the partial pressure of CO_2 in the gas entering the bioreactor (atm), $P_{CO_2}^{Out}$ is the partial pressure of CO_2 in the gas leaving the bioreactor (atm), k_L is the liquid-phase mass transfer coefficient (m/min), a_B is the specific gas-liquid interfacial bubble area (m^{-1}), τ is the bubble lifetime (min), S_H is the interfacial surface between the liquid and the headspace (m^2), k is the rate of CO_2 hydration, l is the rate of HCO_3^- dehydration, $\left[HCO_3^-\right]$ is the concentration of HCO_3^- ions, $[H^+]$ is the concentration of H^+ ions, Q_1^{In} is the volumetric flow rate of OSPW and $[dCO_2]^{In}$ is the concentration of dissolved CO_2 in the OSPW medium.

Overall Model

Overall, the dynamics of the system can be described by the following set of differential equations:

$$\frac{dX}{dt} = \mu X - k_d X - DX \tag{5.7}$$

$$\frac{d\left[dCO_2\right]}{dt} = -\rho_{dCO_2} X + \frac{J}{RT}\frac{h}{V}\left(\frac{P_{CO_2}^{In}}{h} - \left[dCO_2\right]\right)\left\{1 - exp\left[-\left(\frac{k_L a_B RT}{h}\tau\right)\right]\right\}$$
$$+ k_L \frac{S_H}{V}\left(\frac{P_{CO_2}^{Out}}{h} - \left[dCO_2\right]\right) + l\left[HCO_3^-\right]\left[H^+\right] - k\left[dCO_2\right]$$
$$+ \frac{Q_1^{In}}{V}\left[dCO_2\right]^{In} - D\left[dCO_2\right] \tag{5.8}$$

$$\frac{d\left[PO_4^{-3}\right]}{dt} = -\rho_{PO_4^{-3}} X + \frac{Q_1^{In}}{V}\left[PO_4^{-3}\right]_1^{In} + \frac{Q_2^{In}}{V}\left[PO_4^{-3}\right]_2^{In} - D\left[PO_4^{-3}\right] \tag{5.9}$$

$$\frac{d\left[NH_4^+\right]}{dt} = -\rho_{NH_4^+} X + \frac{Q_1^{In}}{V}\left[NH_4^+\right]_1^{In} - D\left[NH_4^+\right] \tag{5.10}$$

$$\frac{dV}{dt} = VD - Q^{Out} \tag{5.11}$$

where k_d is the decay coefficient of biomass, $\left[PO_4^{-3}\right]_1^{In}$ is the concentration of phosphate in the OSPW feed, $\left[PO_4^{-3}\right]_2^{In}$ is the concentration of phosphate in the phosphate feed, $\left[NH_4^+\right]_1^{In}$ is the concentration of ammonium in the OSPW feed and Q^{Out} is the flow rate of the outlet stream (which is only non-zero when samples are being drawn).

5.3.2 Parameter Estimation and Model Validation

The parameters involved in the model were estimated by minimizing the weighted sum of squared errors (WSSE). The WSSE for a set of model parameters (P) can be calculated

as (de la Hoz Siegler et al., 2011):

$$WSSE(P) = \sum_{i=1}^{M} \sum_{j=1}^{N} \left(Y_{ij} - \hat{Y}_{ij}\right)^T W_i^{-1} \left(Y_{ij} - \hat{Y}_{ij}\right) \tag{5.12}$$

where N is the number of experimental data points used to estimate the model, M is the number of measurable states, Y_{ij} is the measured value of state i at time j and $\hat{Y}_{ij}$ is the value of the state i at time j as predicted by the model and W_i is the weight factor of the state i.

Particle swarm optimization (PSO) algorithm with 20 particles was used to minimize the WSSE. The estimated model parameters are presented in Table 5.1. It should be noted that all the parameters were subjected to a lower boundary constraint (P>0) which was handled by the method developed in Chapter 4 (Kasiri et al., 2014c).

Table 5.1: The estimated parameters for the model described in Section 5.3.1, Eqs. 5.7-5.11

Parameter	Estimated Value	Unit	Parameter	Estimated Value	Unit
μ_m	4.01×10^{-2}	1/h	k_d	1.09×10^{-5}	1/h
$K_{S_{dCO_2}}$	4.84	mg_{dCO_2}/L	$K_{I_{dCO_2}}$	1.25×10^{3}	mg_{dCO_2}/L
$K_{S_{PO_4^{-3}}}$	155	$\text{mg}_{PO_4^{-3}}$/L	$K_{I_{PO_4^{-3}}}$	1.25×10^{3}	$\text{mg}_{PO_4^{-3}}$/L
K_{S_I}	28.2	μmol photons.m^{-2}.s^{-1}			
$\rho_{m_{dCO_2}}$	6.29×10^{-5}	mg_{dCO_2}/(mg$_{Biomass}$.h)	$K_{\rho_{dCO_2}}$	1.88	mg_{dCO_2}/L
$\rho_{m_{PO_4^{-3}}}$	1.50×10^{-3}	$\text{mg}_{PO_4^{-3}}$/(mg$_{Biomass}$.h)	$K_{\rho_{PO_4^{-3}}}$	1410	$\text{mg}_{PO_4^{-3}}$/L
$\rho_{m_{NH_4^+}}$	0.273	$\text{mg}_{NH_4^+}$/(mg$_{Biomass}$.h)	$K_{\rho_{NH_4^+}}$	2.75×10^{3}	$\text{mg}_{NH_4^+}$/L
k_L	0.200	m/h	$a_B\tau$	1.11	h/m
k	0.330	1/h	l	2.40×10^{4}	L/(mol.h)

Normalized sensitivity analysis ($\frac{(\partial Y/Y)}{(\partial P/P)}$) was performed on all model parameters to determine the parameters (P) with significant effect on the average CO_2 uptake rate and algal growth (Y). The results are obtained by changing each parameters value by 10% (5% higher and lower) from the estimated value. Table 5.2 summarizes the significance of the eight model parameters that may be considered to be important. As expected the CO_2

uptake rate is very sensitive to its maximum uptake rate and the uptake half-saturation constant of dissolved CO_2. Also, the rate of HCO_3^- dehydration and CO_2 hydration, specific gas-liquid interfacial bubble area and bubble lifetime play a significant role in the CO_2 uptake rate. However, algal growth showed the most sensitivity toward the maximum growth rate and the half-saturation constant of phosphate, light intensity and dissolved CO_2.

Table 5.2: Normalized sensitivity of CO_2 uptake rate and algal growth to model parameters obtained based on the periodic feeding strategy

CO_2 uptake rate (ρ_{dCO_2})	$\rho_{m_{dCO_2}}$	$K_{\rho_{dCO_2}}$	l	k	$a_B\tau$	μ_m	$K_{S_{PO_4^{-3}}}$	K_{S_I}
	0.999	0.239	0.132	0.116	0.039	0.002	0.001	0.001
Algal growth (X)	μ_m	$K_{S_{PO_4^{-3}}}$	K_{S_I}	$K_{S_{dCO_2}}$	$K_{I_{PO_4^{-3}}}$	k	$K_{I_{dCO_2}}$	$a_B\tau$
	2.04	0.710	0.668	0.401	0.256	0.094	0.061	0.011

The model predictions were then compared with the measured experimental data. The adequacy of the model is shown in Figures 5.4-5.7, which show reasonably good agreement between the model predictions and the corresponding experimental data. Figure 5.4 indicates that the model can adequately explain a downtrend followed by an increment in the microalgal growth due to the effects of light/ dark cycle and phosphate feed, respectively. It can be seen that the intermittent phosphate feeding increases the microalgal growth. This is in agreement with Jin et al. (2006), who reported that intermittent nitrate feeding increases microalgal growth and can be used to prolong the duration of exponential growth phase in a given photobioreactor system. The results also indicate that the model can capture the dynamics of dissolved CO_2 perfectly in short time intervals (Figure 5.5). As shown in Figure 5.6, the dynamics of phosphate have been captured adequately by the model. However, the model shows a slight weakness in capturing ammonium dynamics (Figure 5.7). Based on these results, we concluded that the accuracy of the model was adequate for use in optimization studies.

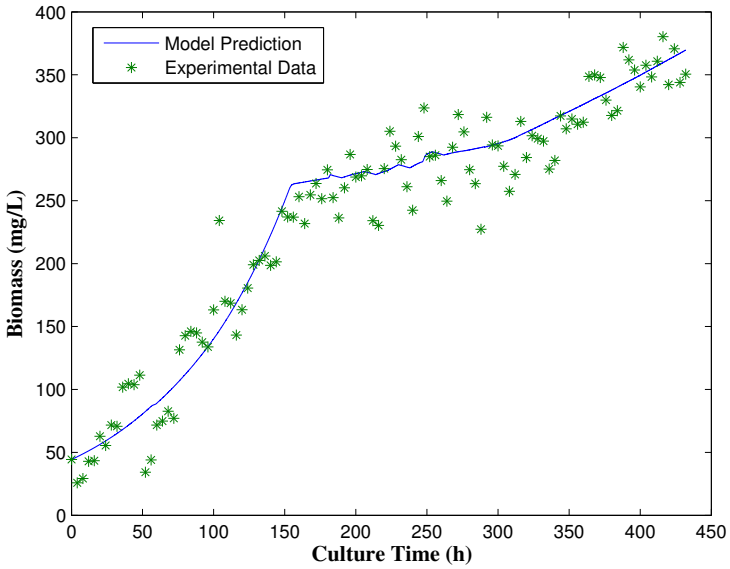

Figure 5.4: Fed-batch model predictions and biomass data achieved based on the periodic feeding strategy

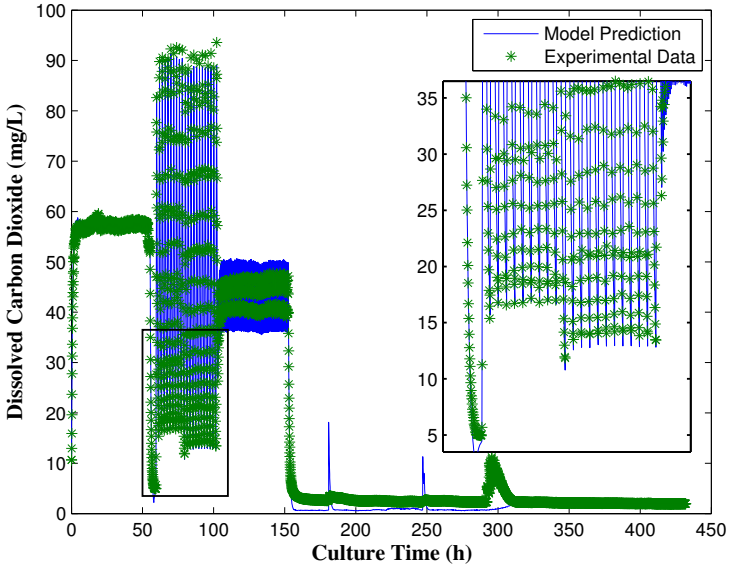

Figure 5.5: Fed-batch model predictions and dissolved CO_2 data achieved based on the periodic feeding strategy

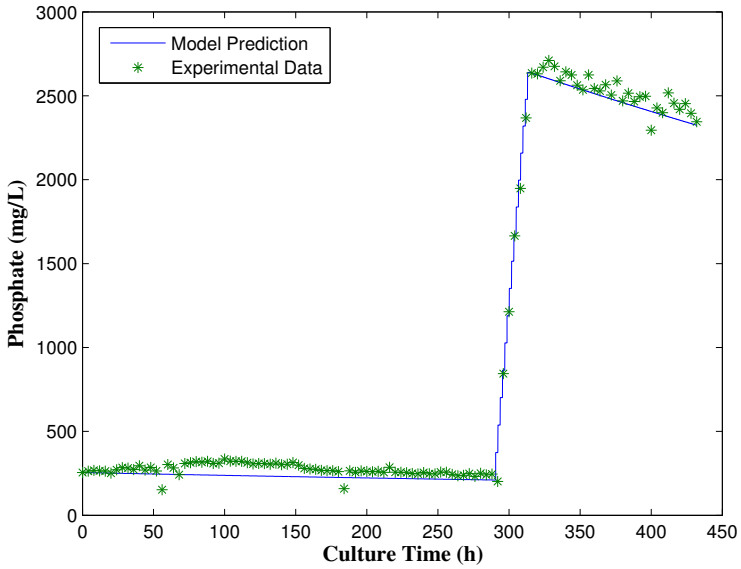

Figure 5.6: Fed-batch model predictions and phosphate data achieved based on the periodic feeding strategy

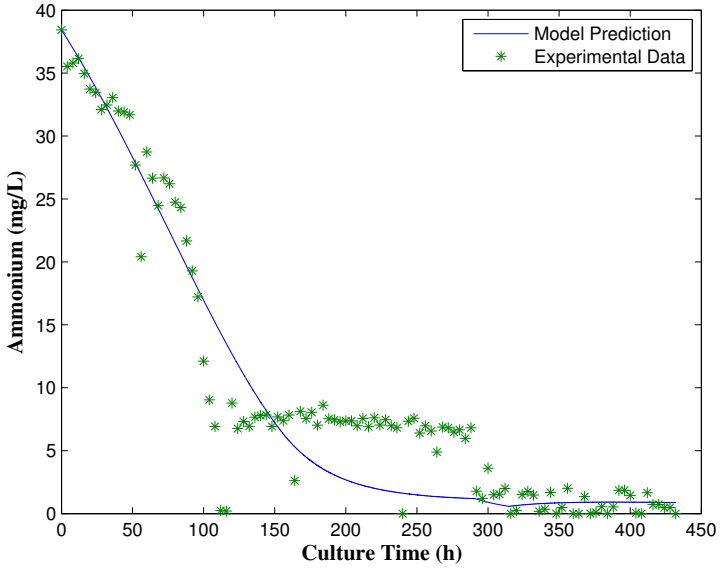

Figure 5.7: Fed-batch model predictions and ammonium data achieved based on the periodic feeding strategy

It should be noted that the mathematical model describing the algal growth rate and CO_2, phosphate and ammonium uptake rates of *Chlorella kessleri* cultivated in the raceway photobioreactor is identified experimentally. The model parameters were estimated using data generated by the photobioreactor working under a certain operating condition and cultivation mode (fed-batch). Therefore, different cultivation mode and operating conditions resulted in different model parameters for fed-batch and batch cultures, although the same kinetic expressions were used for both cultivation modes (Chapter 4) (Kasiri et al., 2014c) . For example, the maximum specific growth rate μ_m is found to be higher for the fed-batch culture than for the batch cultures. This increase in μ_m could be the result of better mixing of the culture which facilitates better light distribution between microalgal cells. Also, there are feed streams containing highly concentrated nutrient solutions and fresh medium into the photobioreactor that increase algal growth (Coelho et al., 2014; Yadala and Cremaschi, 2014). It is concluded that the model parameters require to be tuned when the cultivation mode or operating range/conditions are different to obtain the accurate models.

5.3.3 Feeding Strategy Optimization

Bioprocess optimization is usually performed by calculating the optimal feeding profile for the duration of the culture. In this study, there are two possible scenarios: maximum algal biomass or maximum CO_2 fixation rate. Algal growth and the CO_2 fixation rate can be manipulated by varying the CO_2 and phosphate feed rates as well as the light intensity profiles. The optimal feeding strategy u^* is given by:

$$u^* = \underset{u}{\operatorname{argmax}}\, J_{avg.}\left(u; \xi(t_0); t_f\right) \tag{5.13}$$

where t_0 is the initial time, t_f is a given culture time and $J_{avg.}$ is the objective function defined as:

$$J_{avg.} = \frac{1}{t_f - t_0} \int_{t_0}^{t_f} J_t dt \tag{5.14}$$

where J can be defined either as algal growth or CO_2 uptake rate. The model developed can be used to calculated the optimal feeding strategy u^*. The dynamic model of photobioreactor can be represented as:

$$\frac{d\xi}{dt} = f(\xi, u) \tag{5.15}$$

and can be discretized using Euler's method to:

$$\xi^{t+1} = \xi^t + \Delta t f\left(\xi^t, u^t\right) \tag{5.16}$$

where $\xi = [X\ [dCO_2]\ \left[PO_4^{-3}\right]\ \left[NH_4^+\right]\ V]$ is the state vector, ξ^t is the state vector at time t and Δt is the time interval of discretization.

The dynamics of the photobioreactor are highly nonlinear and there are constraints on the process inputs and final bioreactor volume which are given by:

$$\begin{aligned} 0 \leq u^t \leq u_{max} \\ V_{min} \leq V^{t_f} \leq V_{max} \end{aligned} \tag{5.17}$$

Table 5.3 shows the constraints used in the optimization of algal growth and CO_2 uptake rate, which are taken into account by the PSO algorithm during optimization. It is worthwhile to mention that an explicit constraint on the pH is not imposed in this experiment because it has been proven in our laboratory that even the injection of pure

CO_2 (99.99%) into the OSPW causes the pH to settle around a value of 6 and *Chlorella kessleri* maintains its growth in such conditions.

Table 5.3: List of constraints imposed using Eq. 5.17

Variable	Lower Bound	Upper Bound	Unit
Phosphate Feed rate (Q_2^{In})	0	50	mL
CO_2 Concentration ($P_{CO_2}^{In}$)	0.03	15	%
Light Intensity (I)	0	140	μmol photons.m^{-2}.s^{-1}
Reaction Volume (V)	4	8	L

The PSO algorithm with 20 particles was used to determine $u^* = [u_{t_0} \dots u_{t_f-1}]$ such that the objective function, Eq. (5.14), is maximized. The total cultivation time was assumed to be 432 h (18 days) with a time interval of 24 h for input manipulation. Thus, 54 parameters (3 manipulating inputs $\times$ 18 days) were estimated using the PSO algorithm to maximize each objective function. Note that a light/dark cycle of 16/8 h is considered and consequently it is assumed that only air (0.03% CO_2) is sparged into the bioreactor during the dark cycle since the algal growth rate is zero during this cycle.

CO_2 Fixation

Considering the CO_2 uptake rate as the objective function results in an increase in the average CO_2 uptake rate to 5.60$\times$ 10^{-5} $mg_{dCO_2}/(mg_{Biomass}.h)$; a 1.7-fold increase with respect to the initial fed-batch experiment 3.28$\times$ 10^{-5} $mg_{dCO_2}/(mg_{Biomass}.h)$ as a result of the optimal feeding strategy shown in Figure 5.8. As shown in Figure 5.8, due to luxury cosumption of CO_2 in high CO_2 concentration, a high concentration of CO_2 is required in all injection periods. Also, a relatively high phosphate concentration is required to achieve the maximum CO_2 uptake rate. That is in agreement with Xu et al. (2010) who reported that elevated CO_2 at high P_i levels improved the photosynthetic capability of *Gracilaria lemaneiformis*. However, in order to maximize the CO_2 uptake rate, high light

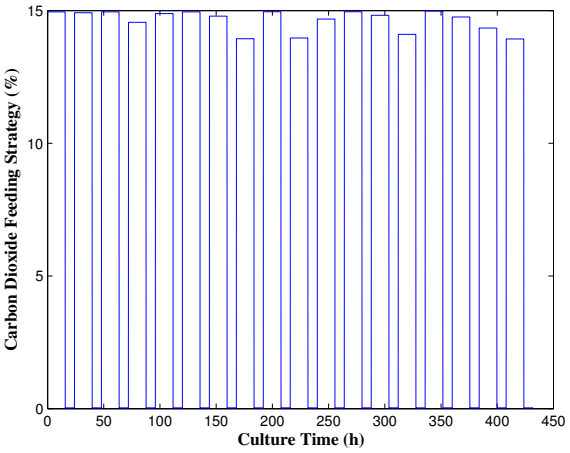

(a)

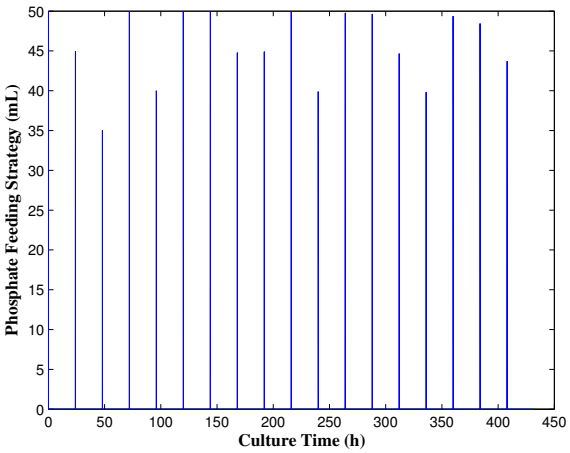

(b)

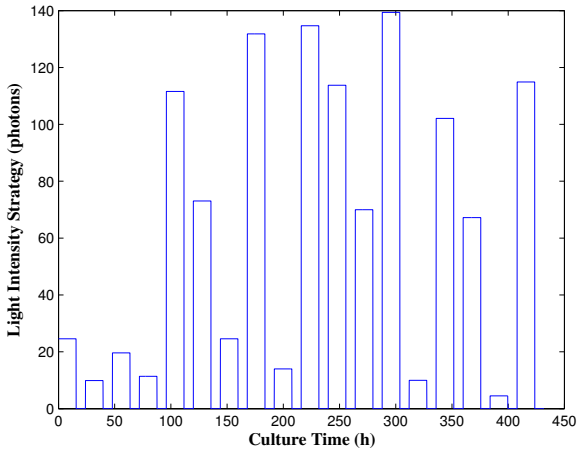

(c)

Figure 5.8: Optimal feeding strategy to maximize average CO_2 uptake rate, (a) CO_2; (b) phosphate; (c) light intensity

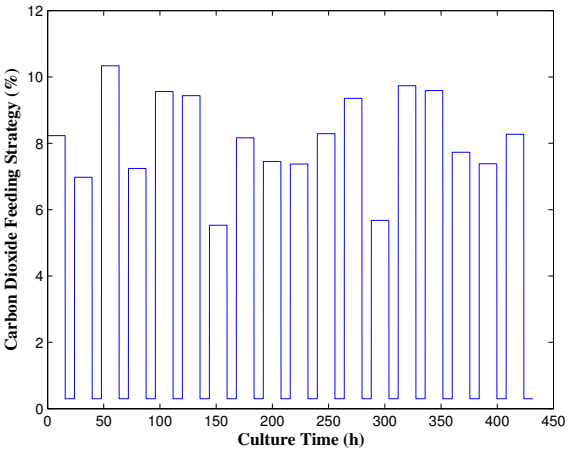

(a)

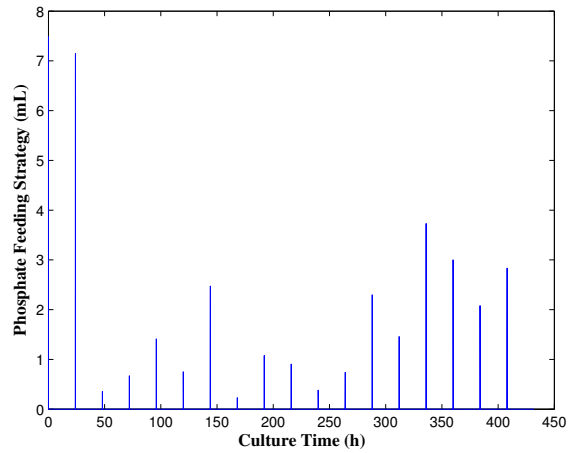

(b)

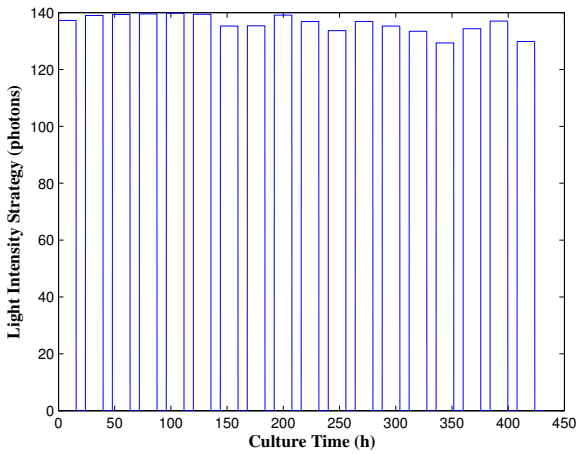

(c)

Figure 5.9: Optimal feeding strategy to maximize average algal growth, (a) CO_2; (b) phosphate; (c) light intensity

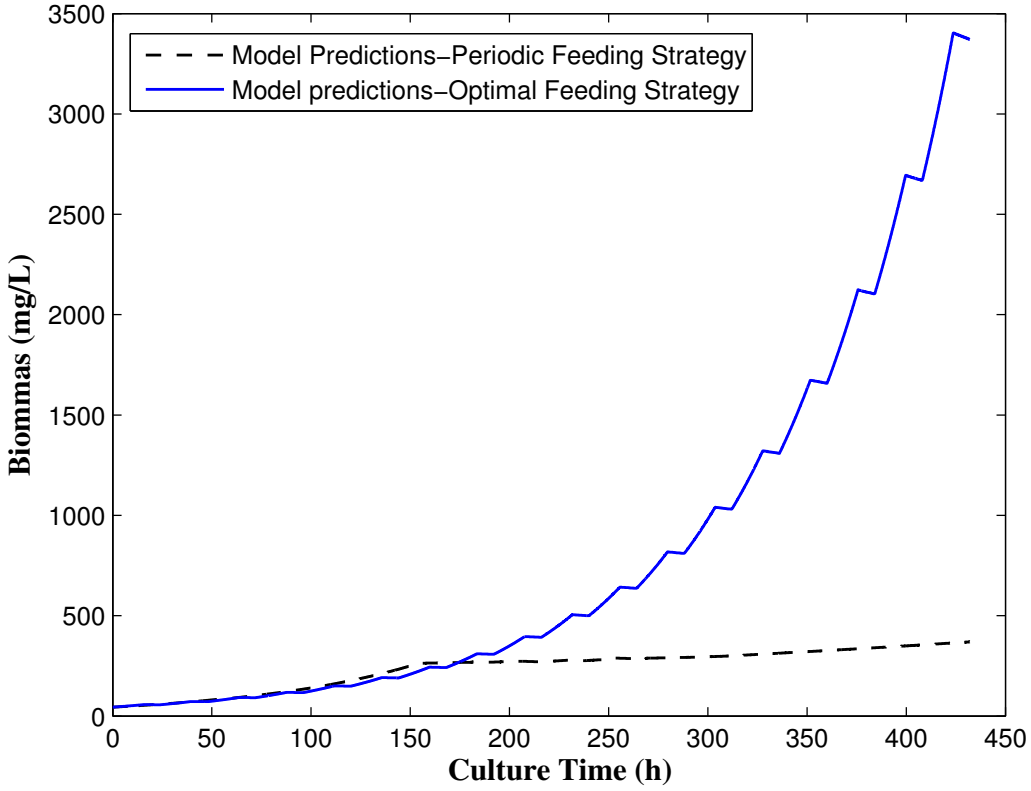

Figure 5.10: Algal growth as a result of optimal feeding strategy and periodic feeding strategy

intensity is not required. The average light intensity in the profile is approximately 60 μmol photons.m^{-2}.s^{-1}.

Algal Growth

Similarly, considering algal growth as the objective to be maximized results in average algal growth of 816 mg/L; this is a 3.5-fold increase in the biomass production with respect to the original fed-batch experiment 238 mg/L as a result of the optimal feeding strategy shown in Figure 5.9. Also, the final concentration of biomass is calculated to be 3410 mg/L; this is a 9.2-fold increase in final biomass concentration with respect to the

initial fed-batch experiment 370 mg/L (Figure 5.10). As shown in Figure 5.9, high light intensity as well as relatively high concentration of CO_2 are required to optimize algal growth. However, in order to maximize the algal growth, high phosphate concentration is not required. Generally, increasing CO_2 levels increase algal growth because more CO_2 from the external bulk medium diffuses to the active site of Rubisco (Xu et al., 2010; Spalding, 2008); also, an increase in the light intensity corresponds to an increase in algal photosynthesis (Chisti, 2007; Fan et al., 2007).

5.4 Conclusions

The dynamics of *Chlorella kessleri* cultivated in OSPW in the closed raceway photobioreactor (fed-batch) was adequately described by a dynamic mathematical model developed based on batch kinetics identified from a previous study of ours explained in Chapter 4. The proposed model then was used to calculate the optimal levels for CO_2, phosphate and light intensity to maximize CO_2 uptake and algal growth. The estimated optimal feeding strategy resulted in a 1.7-fold increase in the average CO_2 uptake rate, a 3.5-fold increase in the average algal growth when each of these objectives was maximized. In our future studies, Pareto optimization as a multi-objective optimization method will be used to calculate the optimal feeding strategy to maximize CO_2 uptake rate and algal growth simultaneously. The optimal feeding strategies then will be experimentally validated in the raceway photobioreactor. Subsequently, the obtained results from the experiment can be used for tuning the parameters to achieve a more accurate model. Moreover, algal cultivation can be perfomed in continuous mode to provide a basis for the design and scale-up of industrial algal cultivation. Industrial algal cultivation can be integrated with CO_2 fixation and wastewater treatment by exploiting CO_2 from flue gas, along with phosphate and ammonium from agricultural run-off.

5.5 References

Abdollahi, J., Dubljevic, S., 2012. Lipid production optimization and optimal control of heterotrophic microalgae fed-batch bioreactor. Chemical Engineering Science 84, 619–627.

Bernard, O., Remond, B., 2012. Validation of a simple model accounting for light and temperature effect on microalgal growth. Bioresource Technology 123, 520–527.

Brennan, L., Owende, P., 2010. Biofuels from microalgae-A review of technologies for production, processing, and extractions of biofuels and co-products. Renewable and Sustainable Energy Reviews 14, 557–577.

Chisti, Y., 2007. Biodiesel from microalgae. Biotechnology Advances 25, 294–306.

Coelho, R.S., Vidotti, A.D.S., Reis, E.M., Franco, T.T., 2014. High cell density cultures of microalgae under fed-batch and continuous growth. Chemical Engineering Transactions 38, 313–318.

Costache, T.A., Gabriel Acien Fernandez, F., Morales, M.M., Fernandez-Sevilla, J.M., Stamatin, I., Molina, E., 2013. Comprehensive model of microalgae photosynthesis rate as a function of culture conditions in photobioreactors. Applied Microbiology and Biotechnology 97, 7627–7637.

de la Hoz Siegler, H., Ben-Zvi, A., Burrell, R.E., McCaffrey, W.C., 2011. The dynamics of heterotrophic algal cultures. Bioresource Technology 102, 5764–5774.

de la Hoz Siegler, H., McCaffrey, W.C., Burrell, R.E., Ben-Zvi, A., 2012. Optimization of microalgal productivity using an adaptive, non-linear model based strategy. Bioresource Technology 104, 537–546.

Eaton, A.D., Greenberg, A.E., Clesceri, L.S., 1999. Standard methods for the examination of water and wastewater. American Public Health Association Publications. 20^{th} edition.

Fan, L., Zhang, Y., Cheng, L., Zhang, L., Tang, D., Chen, H., 2007. Optimization of carbon dioxide fixation by *Chlorella vulgaris* cultivated in a membrane-photobioreactor. Chemical Engineering and Technology 30, 1094–1099.

Flynn, K.J., 2001. A mechanistic model for describing dynamic multi-nutrient, light, temperature interactions in phytoplankton. Journal of Plankton Research 23, 977–997.

Geider, R.J., MacIntyre, H.L., Kana, T.M., 1998. A dynamic regulatory model of phytoplanktonic acclimation to light, nutrients, and temperature. Limnology and Oceanography 43, 679–694.

He, L., Subramanian, V.R., Tang, Y.J., 2012. Experimental analysis and model-based optimization of microalgae growth in photo-bioreactors using flue gas. Biomass and Bioenergy 41, 131–138.

James, S.C., Boriah, V., 2010. Modeling algae growth in an open-channel raceway. Journal of Computational Biology 17, 895–906.

Jin, H.F., Lim, B.R., Lee, K., 2006. Influence of nitrate feeding on carbon dioxide fixation by microalgae. Journal of Environmental Science and Health - Part A Toxic/Hazardous Substances and Environmental Engineering 41, 2813–2824.

Kasiri, S., Ulrich, A., Prasad, V., 2014c. Kinetic modeling and optimization of carbon dioxide fixation using microalgae cultivated in oil sands process water (submitted) .

Kumar, A., Ergas, S., Yuan, X., Sahu, A., Zhang, Q., Dewulf, J., Malcata, F.X., van Langenhove, H., 2010. Enhanced CO_2 fixation and biofuel production via microalgae: Recent developments and future directions. Trends in Biotechnology 28, 371–380.

Lee, C.G., 1999. Calculation of light penetration depth in photobioreactors. Biotechnology and Bioprocess Engineering 4, 78–81.

Mahdavi, H., Ulrich, A.C., Liu, Y., 2012. Metal removal from oil sands tailings pond water by indigenous micro-alga. Chemosphere 89, 350–354.

Nedbal, L., Cerveny, J., Keren, N., Kaplan, A., 2010. Experimental validation of a nonequilibrium model of CO_2 fluxes between gas, liquid medium, and algae in a flat-panel photobioreactor. Journal of Industrial Microbiology and Biotechnology 37, 1319–1326.

Packer, A., Li, Y., Andersen, T., Hu, Q., Kuang, Y., Sommerfeld, M., 2011. Growth and neutral lipid synthesis in green microalgae: A mathematical model. Bioresource Technology 102, 111–117.

Pruvost, J., Van Vooren, G., Le Gouic, B., Couzinet-Mossion, A., Legrand, J., 2011. Systematic investigation of biomass and lipid productivity by microalgae in photobioreactors for biodiesel application. Bioresource Technology 102, 150–158.

Sanchez, A., Gonzalez, A., Maceiras, R., Cancela, A., Urrejola, S., 2011. Raceway pond design for microalgae culture for biodiesel. Chemical Engineering Transactions 25, 845–850.

Schenk, P., Thomas-Hall, S., Stephens, E., Marx, U., Mussgnug, J., Posten, C., Kruse, O., Hankamer, B., 2008. Second generation biofuels: High-efficiency microalgae for biodiesel production. Bioenergy Research 1, 20–43.

Sforza, E., Enzo, M., Bertucco, A., 2014. Design of microalgal biomass production in a continuous photobioreactor: An integrated experimental and modeling approach. Chemical Engineering Research and Design 92, 1153–1162.

Singh, N.K., Dhar, D.W., 2011. Microalgae as second generation biofuel. A review. Agronomy for Sustainable Development 31, 605–629.

Spalding, M.H., 2008. Microalgal carbon-dioxide-concentrating mechanisms: Chlamydomonas inorganic carbon transporters. Journal of Experimental Botany 59, 1463–1473.

Wang, B., Li, Y., Wu, N., Lan, C.Q., 2008. CO_2 bio-mitigation using microalgae. Applied Microbiology and Biotechnology 79, 707–718.

Xu, Z., Zou, D., Gao, K., 2010. Effects of elevated CO_2 and phosphorus supply on growth, photosynthesis and nutrient uptake in the marine macroalga *Gracilaria lemaneiformis* (rhodophyta). Botanica Marina 53, 123–129.

Yadala, S., Cremaschi, S., 2014. Design and optimization of artificial cultivation units for algae production. Energy, (*in press*) .

Zhao, B., Zhang, Y., Xiong, K., Zhang, Z., Hao, X., Liu, T., 2011. Effect of cultivation mode on microalgal growth and CO_2 fixation. Chemical Engineering Research and Design 89, 1758–1762.

Chapter 6

Conclusions and Future work

6.1 CONCLUSIONS

Biological fixation of CO_2 using microalgae is an environmentally sustainable option for CO_2 capture. To make this option economically competitive compared to other CO_2 capture techniques, it is necessary to reduce the cost of cultivation and optimize the CO_2 fixation rate and operate the algal culture at the optimal process conditions. Since oil sands process water (OSPW) contains a variety of inorganic compounds necessary for microalgal growth it can be used as a growth medium to reduce the cost of water and chemicals required for the growth medium. Moreover, the biomass growth and CO_2 uptake rate of phototrophic microalgal cultures can be optimized by manipulating the effective factors such as light intensity, nutrient availability, temperature and pH. However, optimization of algal cultures is difficult because of their complex dynamic behaviour and the lack of appropriate models of microalgal growth and CO_2 dynamics. The purpose of this research was to further identify the best microalgal strain that can grow in OSPW with high capacity of CO_2 fixation, develop a model of the algal system by applying statistical and mathematical approaches and subsequently determine the operating conditions that maximize algal growth and CO_2 uptake rate in batch and fed-batch cultures. Development of such an accurate model and calculating the optimal

operation condition was the underlying goal throughout the thesis. Concluding remarks about the materials discussed in the thesis are summarized as follows:

Chapter 2

Botryococcus braunii, *Chlorella pyrenoidosa* and *Chlorella kessleri* were cultivated in OSPW to identify microalgal strains that can grow in OSPW. The results indicated that *Botryococcus braunii* was unable to grow in OSPW; therefore, only *Chlorella pyrenoidosa* and *Chlorella kessleri* were evaluated further based on their specific growth rate and ability to uptake CO_2 in different conditions with varying CO_2, phosphate, nitrate levels, and light intensity. The results indicated that *Chlorella kessleri* exhibited higher CO_2 uptake and specific growth rate compared to *Chlorella pyrenoidosa* at the same conditions. Also, the results revealed that CO_2 concentration, light intensity and phosphate concentration (in that order) had the strongest effect on growth and CO_2 uptake rate.

Chapter 3

At first, a statistical approach was used to develop two quadratic models to describe the CO_2 uptake rate and specific growth rate of *Chlorella kessleri* in batch cultures. The models were then validated against experimental data and used to determine the optimal sets of CO_2 concentration, phosphate concentration and light intensity for CO_2 uptake rate and specific growth rate. 35% CO_2 concentration, 29 mM phosphate concentration and 70 μmol photons.m^{-2}.s^{-1} light intensity maximized CO_2 uptake rate to 65.03 mg/L/day. Also, the maximum specific growth rate of 0.310 per day was obtained at 22% CO_2 concentration, 29 mM phosphate concentration and 70 μmol photons.m^{-2}.s^{-1} light intensity. Moreover, a multi-objective Pareto optimization method was applied and resulted in a CO_2 uptake rate of 62.98 mg/L/day and a specific growth rate of 0.309 per day at 28% CO_2 concentration, 29 mM phosphate concentration and 70 μmol photons.m^{-2}.s^{-1} light

intensity.

Chapter 4

A kinetic model was developed to achieve a better understanding of the behavior of microalgae cultivated in batch cultures and eventually to find the optimal operation conditions. The proposed mathematical model adequately described the algal growth, CO_2 uptake, phosphate uptake, nitrate uptake and ammonium uptake rate of *Chlorella kessleri* cultivated in OSPW. The results of a single-objective optimization revealed that initial conditions of 42% CO_2, 29 mM phosphate and 81 μmol photons.m^{-2}.s^{-1} light intensity maximized average CO_2 uptake to 477 mg/L. Also, initial conditions of 16% CO_2, 30 mM phosphate and 81 μmol photons.m^{-2}.s^{-1} light intensity maximized algal growth to 676 mg/L. Finally, the results of multi-objective Pareto optimization indicated that initial conditions of 28% CO_2, 32 mM phosphate and 81 μmol photons.m^{-2}.s^{-1} light intensity resulted in CO_2 uptake of 327 mg/L and algal growth of 635 mg/L.

Chapter 5

Since the cultivation mode significantly affects the efficiency and effectiveness of a microalgal production process, an automated lab-scale raceway photobioreactor was used to develop a model based on modification of batch kinetics determined in Chapter 4 and the inclusion of mass transfer and other transport effects. The dynamics of *Chlorella kessleri* cultivated in OSPW in the closed raceway photobioreactor (fed-batch) was adequately captured by the developed dynamic mathematical model. The estimated optimal feeding strategy resulted in a 1.7-fold increase in the average CO_2 uptake rate, and a 3.5-fold increase in the average algal growth when each of these objectives was maximized.

Summary of Findings

To summarize, *Chlorella kessleri* which is indigenous to OSPW exhibited higher CO_2 uptake and specific growth rate compared to other selected candidates. In order to maximize CO_2 uptake and growth of *Chlorella kessleri*, appropriate models of microalgal cultures were developed using data generated by manipulating CO_2 concentration, light intensity and phosphate concentration which exhibited significant effects on CO_2 uptake and specific growth rate. The results showed that CO_2 uptake rate and algal growth can be maximized successfully by applying optimal initial conditions in batch cultures or applying optimal feeding strategy in fed-batch culture. These findings and results have the potential to be used in the design and scale-up of industrial algal cultivation in OSPW with the aim of CO_2 fixation.

6.2 FUTURE WORK

- Pareto optimization as a multi-objective optimization method can be used to calculate the optimal feeding strategy to maximize CO_2 uptake rate and algal growth simultaneously in fed-batch and continuous systems.

- The mathematical model of *Chlorella kessleri* cultivated in OSPW in the closed raceway photobioreactor is an experimentally identified model. The model parameters are identified using experimental data which is obtained over a certain range. The optimal feeding strategies can be experimentally validated. The obtained results from these experiments then can be used for tuning the parameters in the model to obtain a more accurate model for the range of data collected.

- The algal cultivation can be perfomed in the raceway photobioreactor in a continuous mode to provide a basis for the design and scale-up of industrial algal

cultivation with the aim of CO_2 fixation.

- The industrial algal cultivation can be performed at a larger scale in an integrated fashion by exploiting CO_2 from flue gas, medium from OSPW and phosphate and ammonium from agricultural run-off.

- The direct injection of CO_2 into the tailing ponds water can be investigated, since algal growth and CO_2 fixation can provide oxygen for aerobic micro-organisms and improve the biodegradation of unwanted dissolved compounds in the ponds.

Bibliography

Abdollahi, J., Dubljevic, S., 2012. Lipid production optimization and optimal control of heterotrophic microalgae fed-batch bioreactor. Chemical Engineering Science 84, 619–627.

Allen, E.W., 2008. Process water treatment in Canada's oil sands industry: I. Target pollutants and treatment objectives. Journal of Environmental Engineering and Science 7, 123–138.

Anjos, M., Fernandes, B.D., Vicente, A.A., Teixeira, J.A., Dragone, G., 2013. Optimization of CO_2 bio-mitigation by *Chlorella vulgaris*. Bioresource Technology 139, 149–154.

Aslan, N., Cebeci, Y., 2007. Application of Box-Behnken design and response surface methodology for modeling of some Turkish coals. Fuel 86, 90–97.

Bastin, G., Dochain, D., 1990. On-line estimation and adaptive control of bioreactors. Elsevier, Amsterdam.

Bechet, Q., Shilton, A., Guieysse, B., 2013. Modeling the effects of light and temperature on algae growth: State of the art and critical assessment for productivity prediction during outdoor cultivation. Biotechnology Advances 31, 1648–1663.

Bender, D., Diaz-Pulido, G., Dove, S., 2014. The impact of CO_2 emission scenarios and nutrient enrichment on a common coral reef macroalga is modified by temporal effects. Journal of Phycology 50, 203–215.

Bernard, O., 2011. Hurdles and challenges for modelling and control of microalgae for CO_2 mitigation and biofuel production. Journal of Process Control 21, 1378–1389.

Bernard, O., Remond, B., 2012. Validation of a simple model accounting for light and temperature effect on microalgal growth. Bioresource Technology 123, 520–527.

Bordel, S., Guieysse, B., Munoz, R., 2009. Mechanistic model for the reclamation of industrial wastewaters using algal-bacterial photobioreactors. Environmental Science and Technology 43, 3200–3207.

Brennan, L., Owende, P., 2010. Biofuels from microalgae-A review of technologies for production, processing, and extractions of biofuels and co-products. Renewable and Sustainable Energy Reviews 14, 557–577.

Cabrera, J.C.F., Coello, C.A.C., 2007. Handling constraints in particle swarm optimization using a small population size. Lecture Notes in Computer Science (including subseries Lecture Notes in Artificial Intelligence and Lecture Notes in Bioinformatics) 4827 LNAI, 41–51.

Camacho, F.R., Camacho, F.G., Sevilla, J.M.F., Chisti, Y., Grima, E.M., 2003. A mechanistic model of photosynthesis in microalgae. Biotechnology and Bioengineering 81, 459–473.

Caperon, J., Meyer, J., 1972. Nitrogen-limited growth of marine phytoplankton-II. uptake kinetics and their role in nutrient limited growth of phytoplankton. Deep-Sea Research and Oceanographic Abstracts 19, 619–632.

Carvalho, A.P., Silva, S.O., Baptista, J.M., Malcata, F.X., 2011. Light requirements in microalgal photobioreactors: An overview of biophotonic aspects. Applied Microbiology and Biotechnology 89, 1275–1288.

Chefurka, W., Kashi, K.P., Bond, E.J., 1976. The effect of phosphine on electron transport in mitochondria. Pesticide Biochemistry and Physiology 6, 65–84.

Cheng, J., Huang, Y., Feng, J., Sun, J., Zhou, J., Cen, K., 2013. Improving CO_2 fixation efficiency by optimizing *Chlorella* PY-ZU1 culture conditions in sequential bioreactors. Bioresource Technology 144, 321–327.

Chisti, Y., 2000. Marine biotechnology - A neglected resource. Biotechnology Advances 18, 547–548.

Chisti, Y., 2007. Biodiesel from microalgae. Biotechnology Advances 25, 294–306.

Chisti, Y., 2008. Biodiesel from microalgae beats bioethanol. Trends in Biotechnology 26, 126–131.

Chu, W., Gao, X., Sorooshian, S., 2011. Handling boundary constraints for particle swarm optimization in high-dimensional search space. Information Sciences 181, 4569–4581.

CK-12 Foundation, 2014. Photosynthesis: Sugar as food (http://www.ck12.org/book/ck-12-biology/r23/section/4.2).

Coelho, R.S., Vidotti, A.D.S., Reis, E.M., Franco, T.T., 2014. High cell density cultures of microalgae under fed-batch and continuous growth. Chemical Engineering Transactions 38, 313–318.

Collos, Y., 1998. Nitrate uptake, nitrite release and uptake, and new production estimates. Marine Ecology Progress Series 171, 293–301.

Colman, B., Huertas, I.E., Bhatti, S., Dason, J.S., 2002. The diversity of inorganic carbon acquisition mechanisms in eukaryotic microalgae. Functional Plant Biology 29, 261–270.

Costache, T.A., Gabriel Acien Fernandez, F., Morales, M.M., Fernandez-Sevilla, J.M., Stamatin, I., Molina, E., 2013. Comprehensive model of microalgae photosynthesis rate as a function of culture conditions in photobioreactors. Applied Microbiology and Biotechnology 97, 7627–7637.

de la Hoz Siegler, H., 2012. Optimization of biomass and lipid production in heterotrophic microalgal cultures. Ph.D. thesis. University of Alberta, Canada.

de la Hoz Siegler, H., Ben-Zvi, A., Burrell, R.E., McCaffrey, W.C., 2011. The dynamics of heterotrophic algal cultures. Bioresource Technology 102, 5764–5774.

de la Hoz Siegler, H., McCaffrey, W.C., Burrell, R.E., Ben-Zvi, A., 2012. Optimization of microalgal productivity using an adaptive, non-linear model based strategy. Bioresource Technology 104, 537–546.

de Morais, M.G., Costa, J.A.V., 2007b. Isolation and selection of microalgae from coal fired thermoelectric power plant for biofixation of carbon dioxide. Energy Conversion and Management 48, 2169–2173.

de Morais, M.G., Costa, J.A.V., 2007c. Carbon dioxide fixation by *Chlorella kessleri*, *C. vulgaris*, *Scenedesmus obliquus* and *Spirulina* sp. cultivated in flasks and vertical tubular photobioreactors. Biotechnology Letters 29, 1349–1352.

Droop, M.R., 1973. Some thoughts on nutrient limitation in algae. Journal of Phycology 9, 264–272.

Eaton, A.D., Greenberg, A.E., Clesceri, L.S., 1999. Standard methods for the examination of water and wastewater. American Public Health Association Publications. 20^{th} edition.

Encarnacao, T., Burrows, H., Pais, A., Campos, M., Kremer, A., 2012. Effect of N and P on the uptake of magnesium and iron and on the production of carotenoids and chlorophyll by the microalgae *Nannochloropsis* sp. Journal of Agricultural Science and Technology 2, 824–832.

Erifi, I.R., Turpin, D.H., 1985. Steady state luxury consumption and the concept of optimum nutrient ratios: a study with phosphate and nitrate limited *Selenastrum minutum* (chlorophyta). Journal of Phycology 21, 592–602.

Fan, L., Zhang, Y., Cheng, L., Zhang, L., Tang, D., Chen, H., 2007. Optimization of carbon dioxide fixation by *Chlorella vulgaris* cultivated in a membrane-photobioreactor. Chemical Engineering and Technology 30, 1094–1099.

Flynn, K.J., 2001. A mechanistic model for describing dynamic multi-nutrient, light, temperature interactions in phytoplankton. Journal of Plankton Research 23, 977–997.

Flynn, K.J., 2003. Modelling multi-nutrient interactions in phytoplankton; balancing simplicity and realism. Progress in Oceanography 56, 249–279.

Freeman, B., Rhudy, R., 2007. Assessment of post-combustion capture technology developments. Technical Report. Electric Power Research Institute, Palo Alto, CA, USA.

Fried, S., Mackie, B., Nothwehr, E., 2003. Nitrate and phosphate levels positively affect the growth of algae species found in perry pond. Tillers 4, 21–24.

Fu, M., Song, X., Yu, Z., Liu, Y., 2013. Responses of phosphate transporter gene and alkaline phosphatase in *Thalassiosira pseudonana* to phosphine. PLoS ONE 8.

Geider, R.J., Macintyre, H.L., Graziano, L.M., McKay, R.M.L., 1998a. Responses of the photosynthetic apparatus of *Dunaliella tertiolecta* (Chlorophyceae) to nitrogen and phosphorus limitation. European Journal of Phycology 33, 315–332.

Geider, R.J., MacIntyre, H.L., Kana, T.M., 1996. A dynamic model of photoadaptation in phytoplankton. Limnology and Oceanography 41, 1–15.

Geider, R.J., MacIntyre, H.L., Kana, T.M., 1997. Dynamic model of phytoplankton growth and acclimation: Responses of the balanced growth rate and the chlorophyll a:carbon ratio to light, nutrient-limitation and temperature. Marine Ecology Progress Series 148, 187–200.

Geider, R.J., MacIntyre, H.L., Kana, T.M., 1998b. A dynamic regulatory model of phytoplanktonic acclimation to light, nutrients, and temperature. Limnology and Oceanography 43, 679–694.

Haario, H., Kalachev, L., Laine, M., 2009. Reduced models of algae growth. Bulletin of Mathematical Biology 71, 1626–1648.

He, L., Subramanian, V.R., Tang, Y.J., 2012. Experimental analysis and model-based optimization of microalgae growth in photo-bioreactors using flue gas. Biomass and Bioenergy 41, 131–138.

Ho, S.H., Chen, C.Y., Chang, J.S., 2012. Effect of light intensity and nitrogen starvation on CO_2 fixation and lipid/carbohydrate production of an indigenous microalga *Scenedesmus obliquus* cnw-n. Bioresource Technology 113, 244–252.

Hu, H., Gao, K., 2006. Response of growth and fatty acid compositions of *Nannochloropsis* sp. to environmental factors under elevated CO_2 concentration. Biotechnology Letters 28, 987–992.

Jacob-Lopes, E., Scoparo, C.H.G., Lacerda, L.M.C.F., Franco, T.T., 2009. Effect of light cycles (night/day) on CO_2 fixation and biomass production by microalgae in photobioreactors. Chemical Engineering and Processing: Process Intensification 48, 306–310.

James, S.C., Boriah, V., 2010. Modeling algae growth in an open-channel raceway. Journal of Computational Biology 17, 895–906.

Jassby, A.D., Platt, T., 1976. Mathematical formulation of the relationships between photosynthesis and light for phytoplankton. Limnology and Oceanography 21, 540–547.

Jin, H.F., Lim, B.R., Lee, K., 2006. Influence of nitrate feeding on carbon dioxide fixation by microalgae. Journal of Environmental Science and Health - Part A Toxic/Hazardous Substances and Environmental Engineering 41, 2813–2824.

Kane, B., Houghton, J., Reichle, D., Ekmann, J., Benson, S., Clarke, J., R., D., Hendrey, G., Herzog, H., Hunter-Cevera, J., Jacobs, G., Judkins, R., J., O., A., P., Socolow, R., Stringer, J., Surles, T., Wolsky, A., Woodward, N., York, M., 1999. Carbon sequestration: State of the science. Technical Report. Department of Energy, Washington, DC, USA: Office of Fossil Energy.

Kasiri, S., Abdulsalam, S., Ulrich, A., Prasad, V., 2014b. Optimization of CO_2 fixation by *Chlorella kessleri* using response surface methodology (submitted) .

Kasiri, S., Prasad, V., Ulrich, A., 2014a. Strain and factor selection for carbon dioxide fixation using microalgae cultivated in oil sands process water. Canadian Journal of Chemical Engineering, *in press* (DOI: 10.1002/cjce.22055) .

Kasiri, S., Ulrich, A., Prasad, V., 2014c. Kinetic modeling and optimization of carbon dioxide fixation using microalgae cultivated in oil sands process water (submitted) .

Kasprzak, E.M., Lewis, K.E., 2001. Pareto analysis in multiobjective optimization using the colinearity theorem and scaling method. Structural and Multidisciplinary Optimization 22, 208–218.

Kennedy, J., Eberhart, R., 1995. Particle swarm optimization. IEEE International Conference on Neural Networks - Conference Proceedings 4, 1942–1948.

Kern, D.M., 1960. The hydration of carbon dioxide. Journal of Chemical Education 37, 14–23.

Khoeyi, Z.A., Seyfabadi, J., Ramezanpour, Z., 2011. Effect of light intensity and photoperiod on biomass and fatty acid composition of the microalgae, *Chlorella vulgaris*. Aquaculture International , 1–9.

Kishimoto, M., Okakura, T., Nagashima, H., Minowa, T., Yokoyama, S.Y., Yamaberi, K., 1994. CO_2 fixation and oil production using micro-algae. Journal of Fermentation and Bioengineering 78, 479–482.

Kumar, A., Ergas, S., Yuan, X., Sahu, A., Zhang, Q., Dewulf, J., Malcata, F.X., van Langenhove, H., 2010. Enhanced CO_2 fixation and biofuel production via microalgae: Recent developments and future directions. Trends in Biotechnology 28, 371–380.

Lai, J., Yu, Z., Song, X., Cao, X., Han, X., 2011. Responses of the growth and biochemical composition of *Prorocentrum donghaiense* to different nitrogen and phosphorus concentrations. Journal of Experimental Marine Biology and Ecology 405, 6–17.

Lee, C.G., 1999. Calculation of light penetration depth in photobioreactors. Biotechnology and Bioprocess Engineering 4, 78–81.

Lee, K., Lee, C.G., 2002. Nitrogen removal from wastewater by microalgae without consuming organic carbon sources. Journal of Microbiology and Biotechnology 12, 979–985.

Leung, S.S.C., MacKinnon, M.D., Smith, R.E.H., 2001. Aquatic reclamation in the Athabasca, Canada, oil sands: Naphthenate and salt effects on phytoplankton communities. Environmental Toxicology and Chemistry 20, 1532–1543.

Li, Y., Zhou, W., Hu, B., Min, M., Chen, P., Ruan, R.R., 2012. Effect of light intensity on algal biomass accumulation and biodiesel production for mixotrophic strains *Chlorella kessleri* and *Chlorella protothecoide* cultivated in highly concentrated municipal wastewater. Biotechnology and Bioengineering 109, 2222–2229.

Lipinsky, E.S., 1992. R&D status of technologies for utilization of carbon dioxide. Energy Conversion and Management 33, 505–512.

Mahdavi, H., Ulrich, A.C., Liu, Y., 2012. Metal removal from oil sands tailings pond water by indigenous micro-alga. Chemosphere 89, 350–354.

Mata, T.M., Martins, A.A., Caetano, N.S., 2010. Microalgae for biodiesel production and other applications: A review. Renewable and Sustainable Energy Reviews 14, 217–232.

Molloy, C.J., Syrett, P.J., 1988. Effect of light and N deprivation on inhibition of nitrate uptake by urea in microalgae. Journal of Experimental Marine Biology and Ecology 118, 97–101.

Morel, F.M.M., 1987. Kinetics of uptake and growth in phytoplankton. Journal of Phycology 23, 137–150.

Moroney, J.V., Somanchi, A., 1999. How do algae concentrate CO_2 to increase the efficiency of photosynthetic carbon fixation? Plant Physiology 119, 9–16.

Murakami, M., Ikenouchi, M., 1997. The biological CO_2 fixation and utilization project by RITE (2): Screening and breeding of microalgae with high capability in fixing CO_2. Energy Conversion and Management 38, S493–S497.

Myers, R., Montgomery, D., 2002. Response surface methodology: Product and process optimization using designed experiments. John Wiley and Sons, New York. 2^{nd} edition.

Nedbal, L., Cerveny, J., Keren, N., Kaplan, A., 2010. Experimental validation of a nonequilibrium model of CO_2 fluxes between gas, liquid medium, and algae in a flat-panel photobioreactor. Journal of Industrial Microbiology and Biotechnology 37, 1319–1326.

Niu, B., Wang, H., Wang, J., Tan, L., 2013. Multi-objective bacterial foraging optimization. Neurocomputing 116, 336–345.

Noctor, G., Foyer, C.H., 1998. Ascorbate and glutathione: Keeping active oxygen under control. Annual Review of Plant Physiology and Plant Molecular Biology 49, 249–279.

Ogunnaike, B.A., 2010. Random phenomena: Fundamentals of probability and statistics for engineers. CRC Press.

Packer, A., Li, Y., Andersen, T., Hu, Q., Kuang, Y., Sommerfeld, M., 2011. Growth and neutral lipid synthesis in green microalgae: A mathematical model. Bioresource Technology 102, 111–117.

Parsopoulos, K., Vrahatis, M., 2002. Particle swarm optimization method for constrained optimization problems. Proceedings of the 2nd Euro-International Symposium on Computational Intelligence, Kosice, Slovakia , 214–220.

Pic-Marco, E., Navarro, J.L., Bruno-Barcena, J.M., 2006. A closed loop exponential feeding law: Invariance and global stability analysis. Journal of Process Control 16, 395–402.

Post, A.F., De Wit, R., Mur, L.R., 1985. Interactions between temperature and light intensity on growth and photosynthesis of the cyanobacterium *Oscillatoria agardhii*. Journal of Plankton Research 7, 487–495.

Pruvost, J., Van Vooren, G., Le Gouic, B., Couzinet-Mossion, A., Legrand, J., 2011. Systematic investigation of biomass and lipid productivity by microalgae in photobioreactors for biodiesel application. Bioresource Technology 102, 150–158.

Purba, E., Taharuddin, 2010. CO_2 reduction and production of algal oil using microalgae *Nannochloropsis oculata* and *Tetraselmis chuii*. Chemical Engineering Transactions 21, 397–402.

Richmond, A., 1996. Efficient utilization of high irradiance for production of photoautotropic cell mass: A survey. Journal of Applied Phycology 8, 381–387.

Rosenberg, J.N., Mathias, A., Korth, K., Betenbaugh, M.J., Oyler, G.A., 2011. Microalgal biomass production and carbon dioxide sequestration from an integrated ethanol biorefinery in Iowa: A technical appraisal and economic feasibility evaluation. Biomass and Bioenergy 35, 3865–3876.

Ruan, M., Li, Y., Cheng, Y., 2012. Effect of exogenous CO_2 on algae growth and wastewater treatment under simulated natural light/dark cycle using municipal wastewater as feedstock. International Agricultural Engineering Journal 21, 1–8.

Sanchez, A., Gonzalez, A., Maceiras, R., Cancela, A., Urrejola, S., 2011. Raceway pond design for microalgae culture for biodiesel. Chemical Engineering Transactions 25, 845–850.

Sato, N., Tsuzuki, M., Kawaguchi, A., 2003. Glycerolipid synthesis in *Chlorella kessleri* 11 h - II. effect of the CO_2 concentration during growth. Biochimica et Biophysica Acta - Molecular and Cell Biology of Lipids 1633, 35–42.

Sawayama, S., Inoue, S., Dote, Y., Yokoyama, S.Y., 1995. CO_2 fixation and oil production through microalga. Energy Conversion and Management 36, 729–731.

Schenk, P., Thomas-Hall, S., Stephens, E., Marx, U., Mussgnug, J., Posten, C., Kruse, O., Hankamer, B., 2008. Second generation biofuels: High-efficiency microalgae for biodiesel production. Bioenergy Research 1, 20–43.

Scragg, A.H., Illman, A.M., Carden, A., Shales, S.W., 2002. Growth of microalgae with increased calorific values in a tubular bioreactor. Biomass and Bioenergy 23, 67–73.

Sforza, E., Enzo, M., Bertucco, A., 2014. Design of microalgal biomass production in a continuous photobioreactor: An integrated experimental and modeling approach. Chemical Engineering Research and Design 92, 1153–1162.

Singh, N.K., Dhar, D.W., 2011. Microalgae as second generation biofuel. A review. Agronomy for Sustainable Development 31, 605–629.

Spalding, M.H., 2008. Microalgal carbon-dioxide-concentrating mechanisms: Chlamydomonas inorganic carbon transporters. Journal of Experimental Botany 59, 1463–1473.

Stepan, D., Shockey, R., Moe, T., Dorn, R., 2002. Subtask 2.3 - Carbon dioxide sequestering using microalgal systems. Technical Report. Department of Energy, Pittsburgh, PA, USA.

Sydney, E.B., Sturm, W., de Carvalho, J.C., Thomaz-Soccol, V., Larroche, C., Pandey, A., Soccol, C.R., 2010. Potential carbon dioxide fixation by industrially important microalgae. Bioresource Technology 101, 5892–5896.

Tang, D., Han, W., Li, P., Miao, X., Zhong, J., 2011. CO_2 biofixation and fatty acid composition of *Scenedesmus obliquus* and *Chlorella pyrenoidosa* in response to different CO_2 levels. Bioresource Technology 102, 3071–3076.

Tansey, M.R., Brock, T.D., 1972. The upper temperature limit for eukaryotic organisms. Proceedings of the National Academy of Sciences of the United States of America 69, 2426–2428.

Tubea, B., Hawxby, K., Mehta, R., 1981. The effects of nutrient, ph and herbicide levels on algal growth. Hydrobiologia 79, 221–227.

Wang, B., Lan, C.Q., 2011. Biomass production and nitrogen and phosphorus removal by the green alga *Neochloris oleoabundans* in simulated wastewater and secondary municipal wastewater effluent. Bioresource Technology 102, 5639–5644.

Wang, B., Li, Y., Wu, N., Lan, C.Q., 2008. CO_2 bio-mitigation using microalgae. Applied Microbiology and Biotechnology 79, 707–718.

Wang, L., 2006. Recommendations for Design Parameters for Central Composite Designs with Restricted Randomization. Ph.D. thesis. Virginia Polytechnic Institute and State University, USA.

Xu, Z., Zou, D., Gao, K., 2010. Effects of elevated CO_2 and phosphorus supply on growth, photosynthesis and nutrient uptake in the marine macroalga *Gracilaria lemaneiformis* (rhodophyta). Botanica Marina 53, 123–129.

Yadala, S., Cremaschi, S., 2014. Design and optimization of artificial cultivation units for algae production. Energy, (*in press*) .

Yewalkar, S., Li, B., Posarac, D., Duff, S., 2011. Potential for CO_2 fixation by *Chlorella pyrenoidosa* grown in oil sands tailings water. Energy and Fuels 25, 1900–1905.

Yun, Y.S., Park, J.M., 2003. Kinetic modeling of the light-dependent photosynthetic activity of the green microalga *Chlorella vulgaris*. Biotechnology and Bioengineering 83, 303–311.